ASoIL (8)

NASA
National Aeronautics and Space Administration

esa
european space agency
agence spatiale européenne

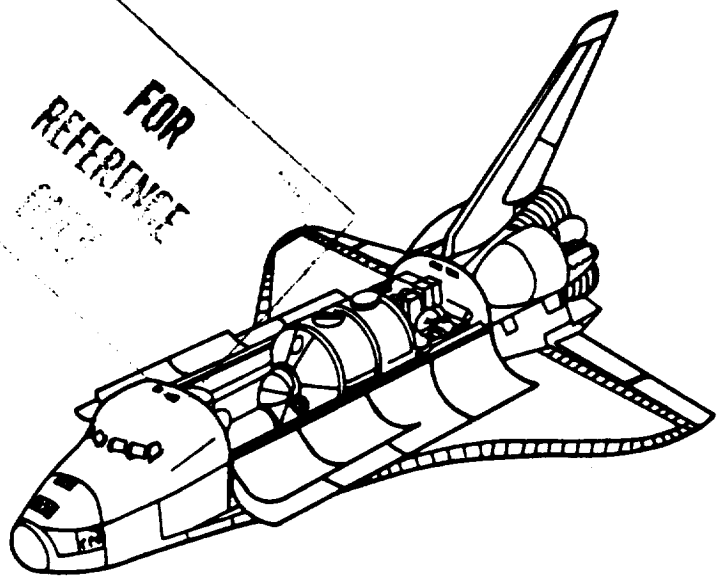
NASA TM - 78173

ESA/FSLP-EX-001

Superseded by TM-82448-

SPACELAB MISSION 1 EXPERIMENT DESCRIPTIONS

FOR REFERENCE



Edited by Paul D. Craven
Space Sciences Laboratory
May 1978

George C. Marshall Space Flight Center
Marshall Space Flight Center, Alabama 35812

(NASA-TM-78173) SPACELAB MISSION 1 EXPERIMENT DESCRIPTIONS (NASA) 152 p

N92-70895

Unclas

29/12 0110258

TECHNICAL REPORT STANDARD TITLE PAGE

1. REPORT NO.	2. GOVERNMENT ACCESSION NO.	3. RECIPIENT'S CATALOG NO.
NASA TM-78173		

4. TITLE AND SUBTITLE	5. REPORT DATE
Spacelab Mission 1 Experiment Descriptions	May 1978
	6. PERFORMING ORGANIZATION CODE
7. AUTHOR(S)	8. PERFORMING ORGANIZATION REPORT #
Edited by Paul D. Craven	
9. PERFORMING ORGANIZATION NAME AND ADDRESS	10. WORK UNIT NO.
George C. Marshall Space Flight Center Marshall Space Flight Center, Alabama 35812	11. CONTRACT OR GRANT NO.
	13. TYPE OF REPORT & PERIOD COVERED
12. SPONSORING AGENCY NAME AND ADDRESS	Technical Memorandum
National Aeronautics and Space Administration Washington, D.C. 20546	14. SPONSORING AGENCY CODE

15. SUPPLEMENTARY NOTES

Prepared by Space Sciences Laboratory, Science and Engineering

16. ABSTRACT

This document presents brief descriptions of experiments and facilities planned for Spacelab 1. These experiments and facilities were selected from the responses to the Announcement of Opportunity for the first Spacelab mission.

17. KEY WORDS	18. DISTRIBUTION STATEMENT
Spacelab Payloads Shuttle	Unclassified — Unlimited Paul D. Craven

19. SECURITY CLASSIF. (of this report)	20. SECURITY CLASSIF. (of this page)	21. NO. OF PAGES	22. PRICE
Unclassified	Unclassified	154	NTIS

For sale by National Technical Information Service, Springfield, Virginia 22151

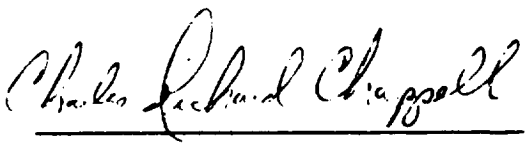
ACKNOWLEDGMENTS

The editor would like to thank all the Spacelab 1 investigators who wrote the original experiment descriptions and who then assisted and waited patiently while the report was being assembled, edited, and printed. He is also grateful to W. Taylor, B. Noblitt, and H. Glaser for their patience and their many helpful suggestions. Special thanks are due to C. R. Chappell, B. Feuerbacher, A. Gonfalone, and especially A. Tingle for their assistance.

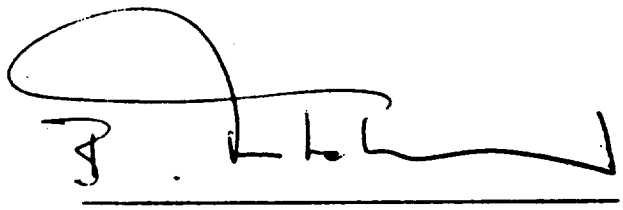
SPACELAB MISSION 1
EXPERIMENT DESCRIPTIONS

Edited by Paul D. Craven

May 1978



C. R. CHAPPELL
Mission Scientist, Spacelab 1



BERNDT FEUERBACHER
ESA Project Scientist, Spacelab 1

FOREWORD

Spacelab 1, known in Europe as the First Spacelab Payload (FSLP), is the first Shuttle flight of the European Spacelab system. The primary purpose of the mission will be to test and verify the operation of the Spacelab system, with a secondary goal being the demonstration of the ability of the Spacelab to conduct scientific investigations in a variety of discipline areas. The Spacelab consists of a pressurized laboratory or module and unpressurized pallets, all of which are carried in the payload bay of the Orbiter. The Spacelab 1 configuration which employs a long module and one pallet is shown in Figure 1.

Spacelab 1 will be the first Shuttle mission to carry passengers who are not career astronauts. These passengers, or payload specialists, will have been selected and trained by the scientists who are developing the instruments for this mission. There will be two payload specialists, one from Europe and one from the United States.

This mission is a cooperative effort between NASA and the European Space Agency (ESA). ESA will provide the Spacelab and NASA the Shuttle/Orbiter, with both agencies sharing in the sponsoring and coordinating of the experiments. The investigations originate from countries all over the world. The map in Figure 2 shows the number of principal investigators from each of the countries represented.

There are 40 different instruments on Spacelab 1, including four multiuser facilities which are supplied by ESA. These facilities are designed for continuous reuse by many different investigators in a given discipline (e.g., material sciences) and will be flown on many missions. At present there are 75 separate investigations, including 36 experiments in the materials science facility. Eighteen of the 40 instruments are located on the pallet and 19 in the module, with three having components both on the pallet and in the module. Many of the pallet-mounted instruments are controlled from within the pressurized module by the onboard crew. Three of the four facilities are located in the module and one on the pallet. The location (module or pallet) of each instrument is given in Table 1. The physical location of each instrument is shown in Figures 3 through 5. For the instruments on the pallet, the layout in Figure 3 can be correlated with Figure 1.

Spacelab 1 will be launched from the Kennedy Space Center (KSC). The mission duration is planned for 7 days at an orbital altitude of 250 kilometers and an inclination of 57 degrees. Following the flight, the Shuttle will land at KSC. Launch is presently planned for late 1980.

PRECEDING PAGE BLANK NOT FILMED

PAGE IV INTENTIONALLY BLANK

TABLE 1. INSTRUMENT LOCATION

On Pallet	In Module	Both Module and Pallet
NS001	NA009	NS006
ES013	EA033*	ES027
ES015	ES300*	ES020
ES014	NT011	
ES017	NT012	
EA034*	ES022	
NS002	ES201/ES200*	
NS003	NS102	
ES019	NS104	
ES019B	NS103	
NS004	ES026	
ES024	ES032	
NS005	NS105	
NA008	ES028	
ES021	ES030	
ES016	ES025	
ES023	ES031	
ES029	NS101	
	NS007	

* ESA Facilities

For organization purposes, the experiments have been categorized into five discipline groups: (1) Atmospheric Physics and Earth Observations, (2) Space Plasma Physics, (3) Material Sciences and Technology, (4) Astronomy and Solar Physics, and (5) Life Sciences.

The atmospheric physics investigators will be performing studies of the Earth's environment through surveys of temperature, composition, and motion of the Atmosphere. These investigations will employ a remote sensing technique

to study the emissions or absorptions from the atmospheric gases to determine their sources, flow patterns, and decay mechanisms. The Earth observations experiments will demonstrate advanced measuring systems (the metric camera and the microwave scatterometer) which will be used on future Spacelab missions.

Experiments in the Space Plasma Physics group will study the plasma envelope which surrounds the Earth. These experiments will investigate key cause-and-effect relationships that couple the Earth's magnetosphere and atmosphere. Two cosmic-ray experiments will measure the charge and number distribution of cosmic-ray nuclei and their isotopes.

The Material Sciences and Technology investigations will demonstrate and use the capability of Spacelab as a technological development and test facility. These experiments take advantage of the microgravity conditions to perform studies in such areas as tribology, fluid physics, crystal growth, and metallurgy.

The investigations in Astronomy and Solar Physics will study astronomical sources of radiation in the ultraviolet and X-ray wavelengths, performing both surveys and detailed studies of specific objects. The solar experiments will measure the energy output of the Sun using three different methods. These instruments will be cross-calibrated so that meaningful comparisons can be made. The goal of these experiments will be to determine quantitatively any variations in the solar energy output.

The Life Sciences investigations will be concerned with the effects of the space environment (microgravity and hard radiation) on human physiology and on the growth, development, and organization of biological systems. In this low-gravity environment a special category of vestibular function experiments will probe the interaction between man's vestibular system and brain, with a goal being the understanding of the causes of space motion sickness.

In demonstrating the capability of the Spacelab system to conduct scientific investigations across a broad range of disciplines, Spacelab 1 will acquire fundamentally important knowledge of the physical processes which control man's environment and will give insight into the functions which control human and biological systems on Earth.

The experiment descriptions in this report have been grouped into five sections, each section devoted to those experiments in a particular discipline group. The numbers assigned to each investigation are specific to Spacelab 1. An explanation of the symbols used is given in Table 2.

TABLE 2. EXPLANATION OF EXPERIMENT NUMBERS[1]

XYZNNN	
X	= Spacelab mission number (1 in this case)
Y	= Agency controlling the investigation:
	E = ESA
	N = NASA
Z	= Category of the investigation:
	S = Scientific
	T = Technology
	A = Application
NNN	= An identifying number, assigned arbitrarily

1. Units used in the descriptions are metric; however, no attempt has been made to impose a consistent system of units (e.g., mks) on all the experiments. In many cases the investigators in a given field use a particular set of units for traditional reasons. To keep the text in the language used in that field, the units, although metric, have been left as they were written by the principal investigators.

   A separate list of acronyms is not included, but an attempt has been made to define acronyms within each description so that individual descriptions or sections can stand alone.

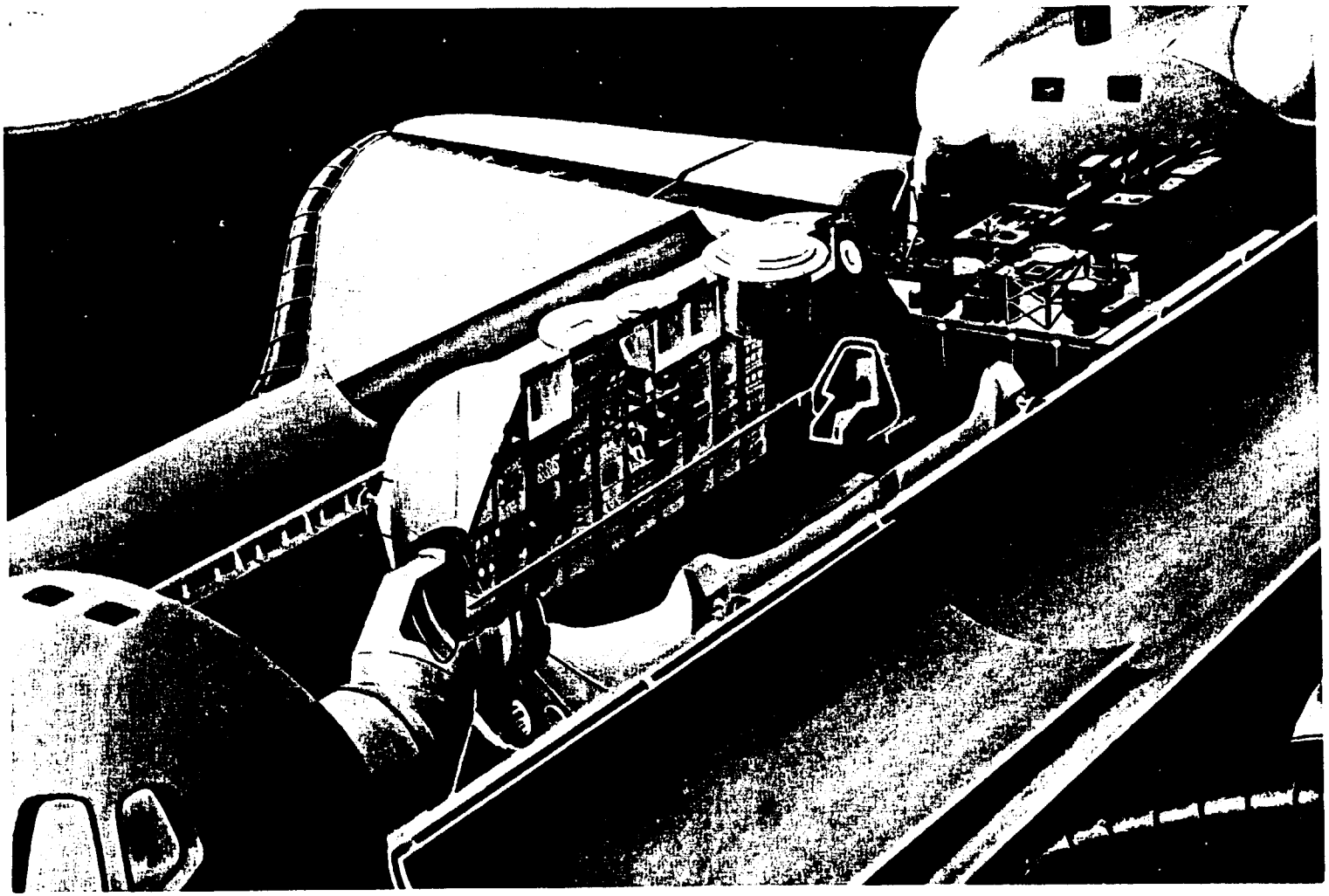


Figure 1. Spacelab 1 module and pallet with instruments.

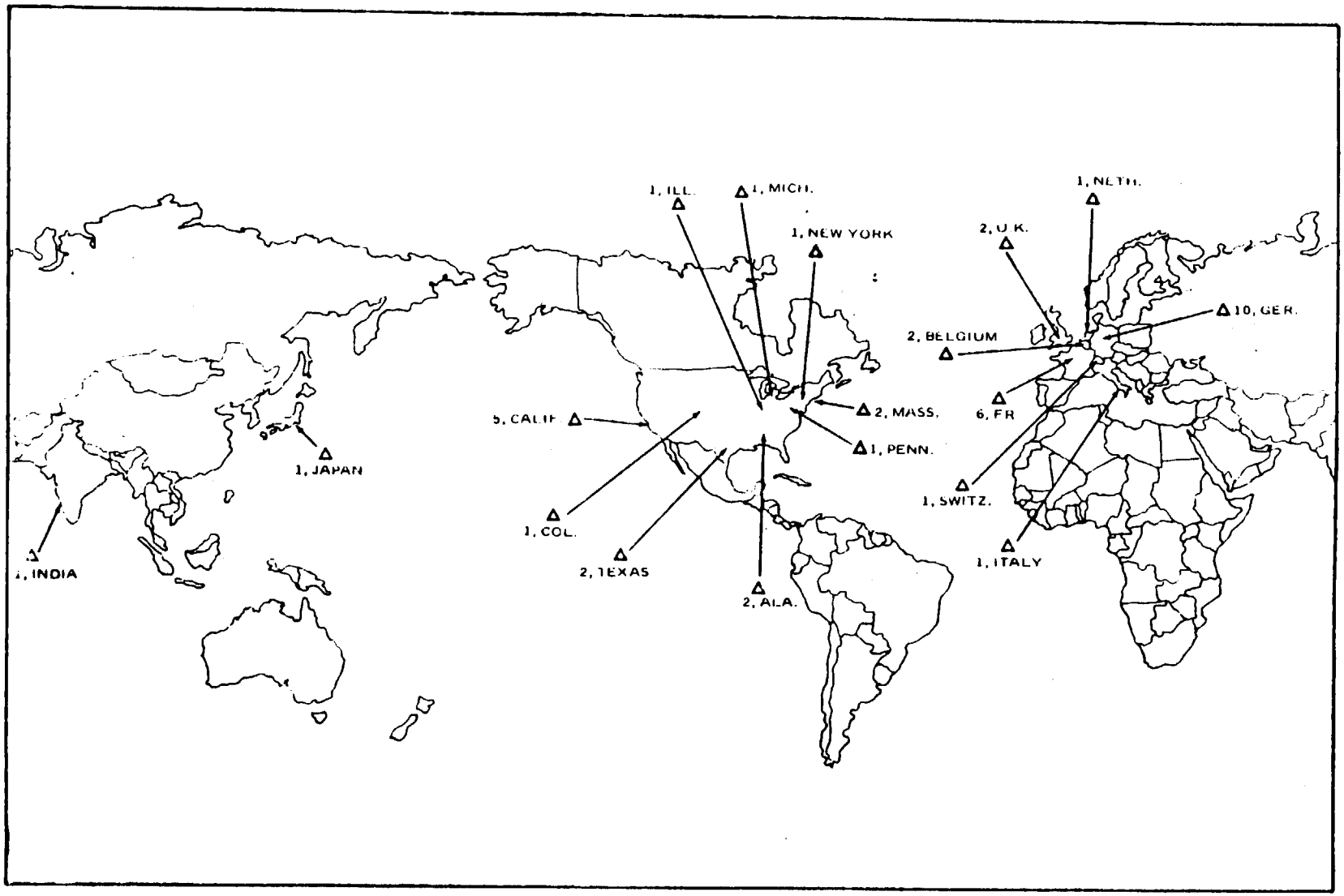
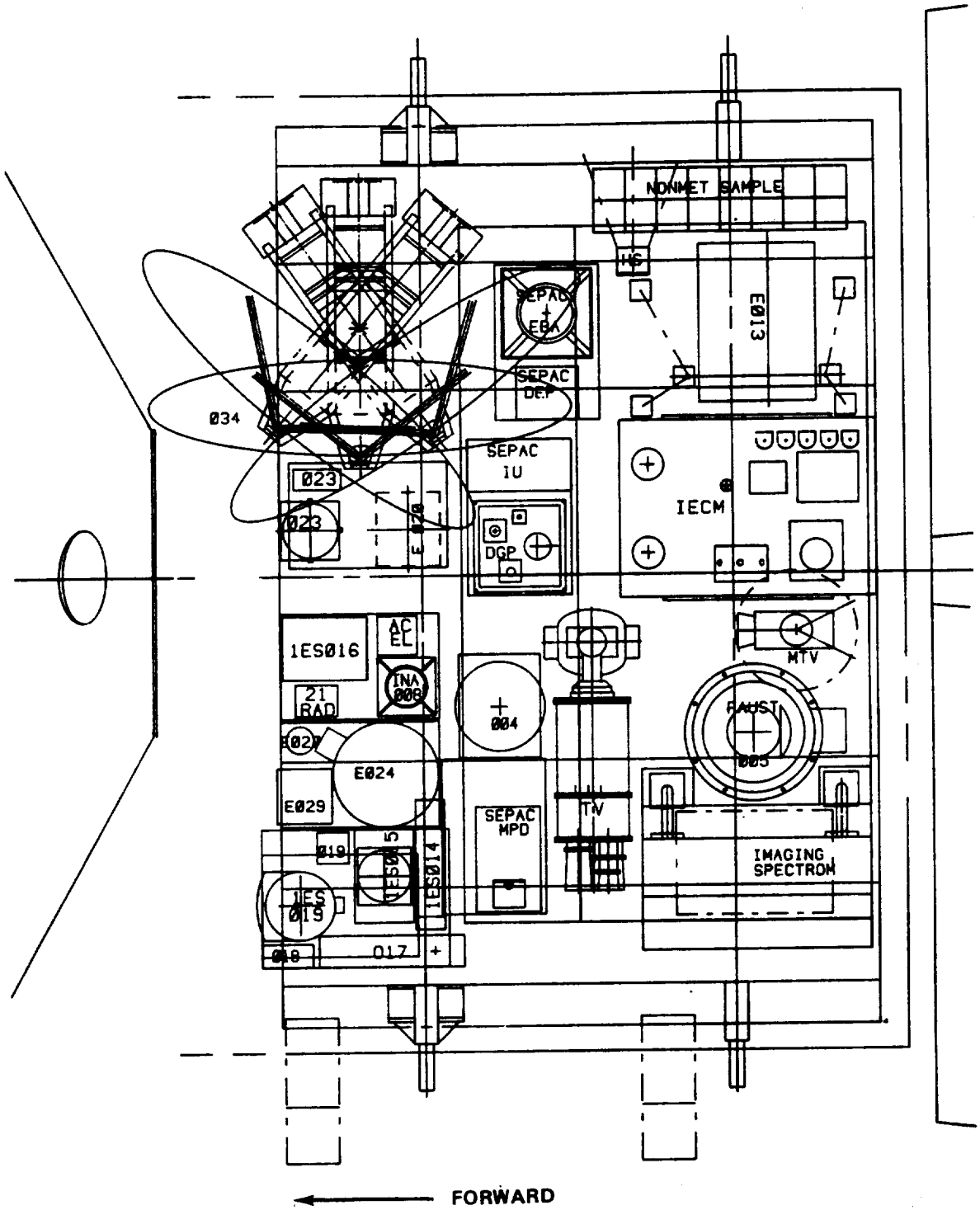


Figure 2. Spacelab 1 payload investigators.



NOTE: THE ITEMS LABELED IECM AND NONMET SAMPLES ARE PART OF THE VERIFICATION FLIGHT INSTRUMENTATION OF THE SHUTTLE AND ARE NOT A PART OF THE SCIENTIFIC PAYLOAD DESCRIBED IN THIS DOCUMENT.

Figure 3. Spacelab 1 pallet plan view.

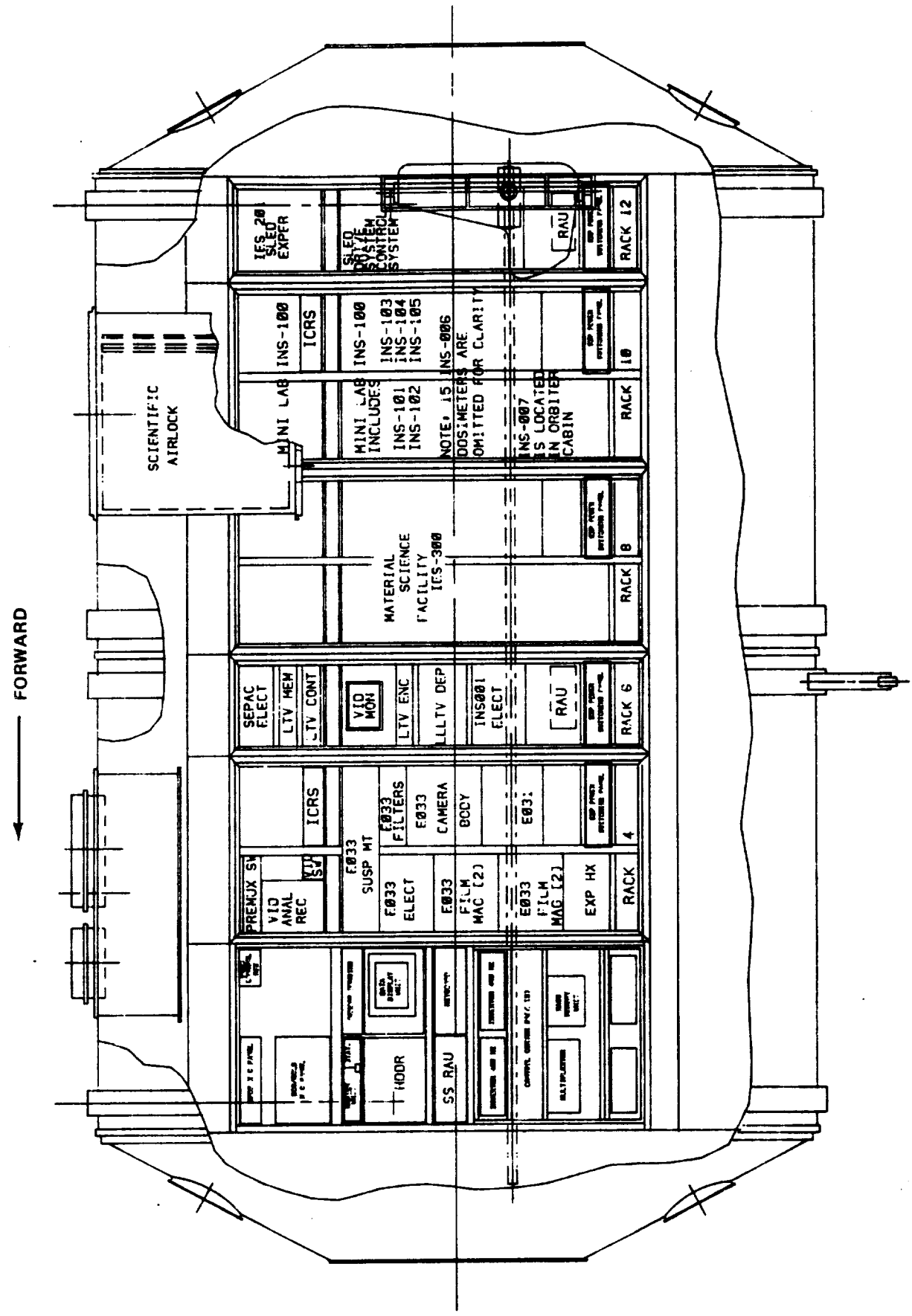


Figure 4. Spacelab 1 module starboard side.

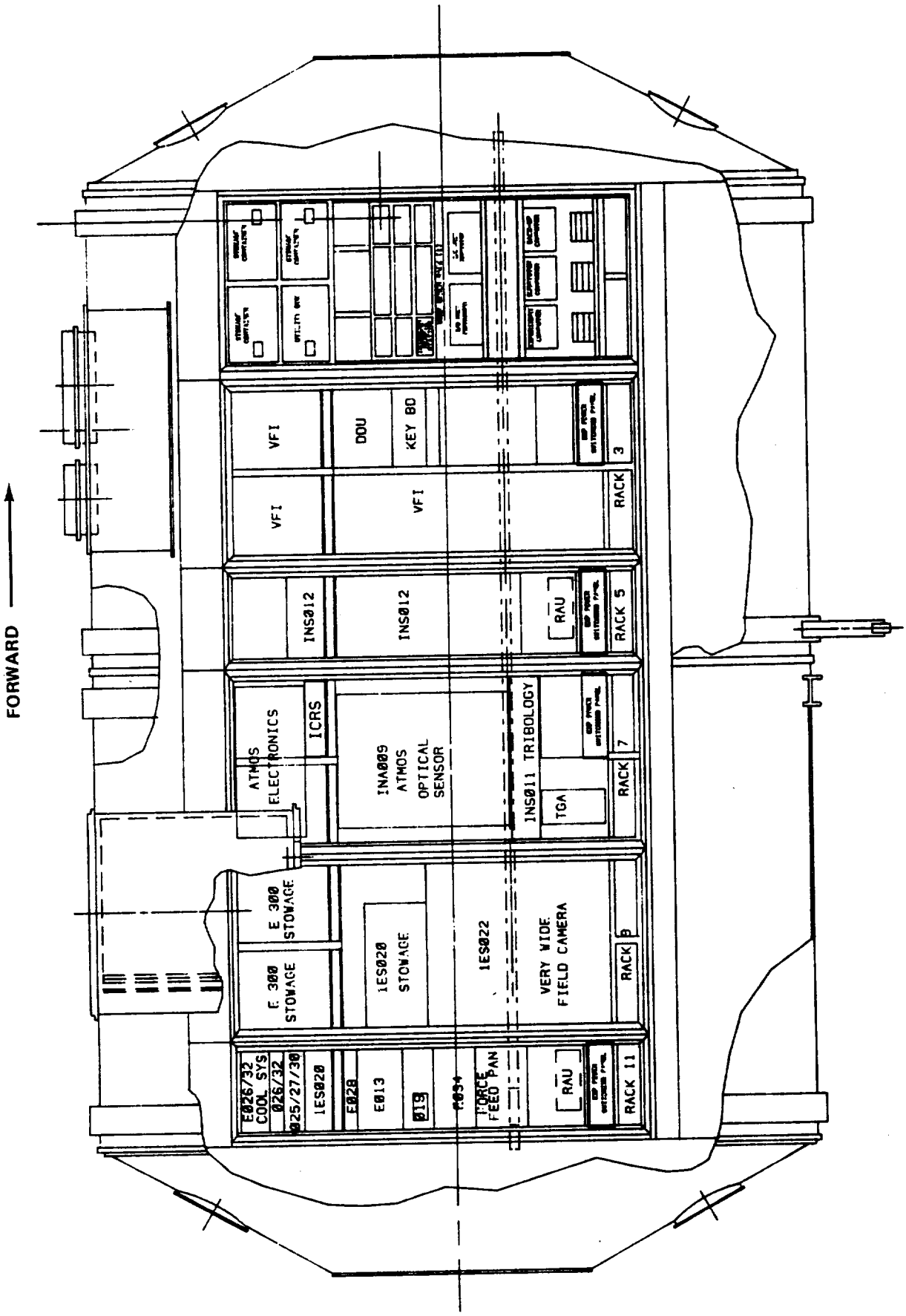


Figure 5. Spacelab 1 module port side.

TABLE OF CONTENTS

			Page
I.	ATMOSPHERIC PHYSICS AND EARTH OBSERVATIONS		
	An Imaging Spectrometric Observatory (M. R. Torr)	1NS001	I-1
	Atmospheric Trace Molecule Spectroscopy (C. B. Farmer)	1NA009	I-5
	Grille Spectrometer (M. Ackerman)	1ES013	I-9
	Temperature, Wind in Mesosphere and Thermosphere (G. Thuillier)	1ES015	I-12
	Waves in the OH Emissive Layer (M. Herse)	1ES014	I-15
	Investigation of Atmospheric H and D Through the Measurement of Their Lyman-α Emissions (J. L. Bertaux)	1ES017	I-17
	Metric Camera Experiment (M. Reynolds)	1EA033	I-20
	Microwave Remote Sensing Experiment (G. Dieterle)	1EA034	I-24
II.	SPACE PLASMA PHYSICS		
	Space Experiments with Particle Accelerators (Tatsuzo Obayashi)	1NS002	II-1
	Phenomena Induced by Charged Particle Beams (C. Beghin)	1ES020	II-5
	Atmospheric Emission Photometric Imaging (S. B. Mende)	1NS003	II-8
	Low-Energy Electron Flux and Its Reaction to Active Experimentation on Spacelab (K. Wilhelm)	1ES019	II-12
	DC-Magnetic Field Vector Measurement (R. Schmidt)	1ES019B	II-15

TABLE OF CONTENTS (Continued)

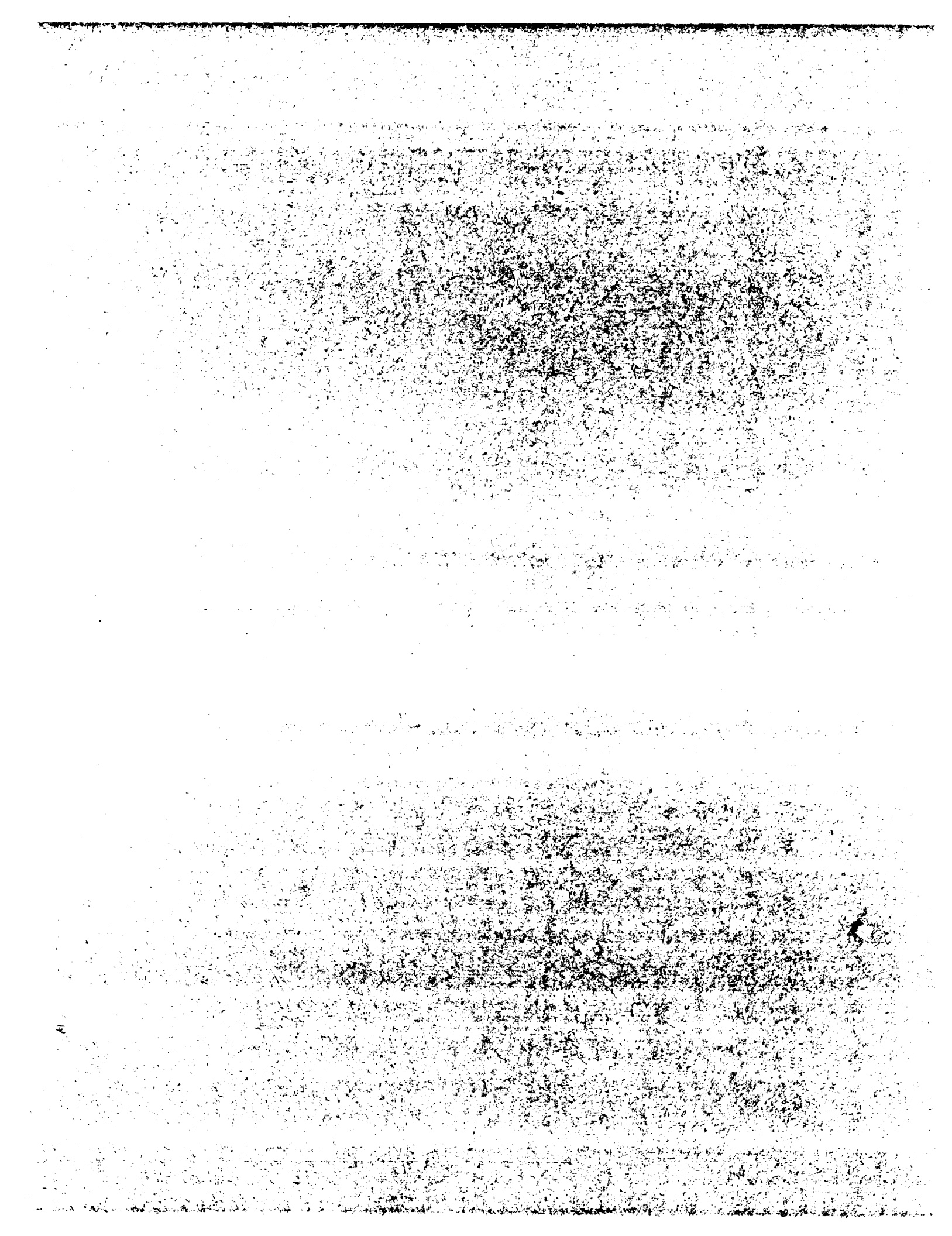
			Page
	Isotopic Stack — Measurement of Heavy Cosmic Ray Isotopes (R. Beaujean)	1ES024	II-17
	Studies of the Ionization States of Solar and Galactic Cosmic Ray Heavy Nuclei (S. Biswas)	1NS004	II-20
III.	MATERIAL SCIENCES AND TECHNOLOGY		
	Materials Science Facilities and Experiments (U. Huth)	1ES300	III-1
	Wetting, Spreading, and Operating Characteristics of Bearing Lubricants in a Zero-Gravity Environment (C. H. T. Pan)	1NT011	III-17
	Geophysical Fluid Flow Experiment (John E. Hart)	1NT012	III-21
IV.	ASTRONOMY AND SOLAR PHYSICS		
	Far Ultraviolet Astronomy Using the FAUST Telescope (C. S. Bowyer)	1NS005	IV-1
	Very Wide Field Camera (G. Courtes)	1ES022	IV-4
	Spectroscopy in X-Ray Astronomy (R. Andresen)	1ES023	IV-7
	Active Cavity Radiometer Irradiance Monitor (R. C. Wilson)	1NA008	IV-10
	Measurement of the Solar Constant (D. Crommelynck)	1ES021	IV-14
	Solar Spectrum from 170 to 3200 Nanometers (G. Thuiller)	1ES016	IV-17
V.	LIFE SCIENCES		
	Space Sled Vestibular Facility	1ES200	V-1

TABLE OF CONTENTS (Concluded)

		Page
Effects of Rectilinear Accelerations, Optokinetic, and Caloric Stimulations in Space (R. Von Baumgarten)	1ES201	V-2
Vestibular Experiments (L. R. Young)	1NS102	V-5
Vestibulo-Spinal Reflex Mechanisms (M. F. Reschke)	1NS104	V-8
The Influence of Space Flight on Erythrokinetics in Man (Stephen L. Kimzey)	1NS103	V-10
Measurement of Central Venous Pressure and Determination of Hormones in Blood Serum During Weightlessness (Otto H. Gauer)	1ES026 1ES032	V-13
Effects of Prolonged Weightlessness on the Humoral Immune Response of Humans (E. W. Voss, Jr.)	1NS105	V-15
Effect of Weightlessness on Lymphocyte Proliferation (Augusto Cogoli)	1ES031	V-17
Three-Dimensional Ballistocardiography in Weightlessness (A. Scano)	1ES028	V-20
Personal Miniature Electrophysiological Tape Recorder (H. Green)	1ES030	V-23
Mass Discrimination During Weightlessness (Helen Ross)	1ES025	V-25
Nutation of Helianthus Annuus in a Microgravity Environment (Allan H. Brown)	1NS101	V-28
Preliminary Characterization of Persisting Circadian Rhythms During Spaceflight: Neurospora as a Model System (Frank M. Sulzman)	1NS007	V-31
Microorganisms and Biomolecules in Hard Space Environment (G. Horneck)	1ES029	V-34
Advanced Biostack Experiment (H. Bucker)	1ES027	V-37
Radiation Environment Mapping (E. V. Benton)	1NS006	V-39

SECTION I

ATMOSPHERIC PHYSICS AND EARTH OBSERVATIONS



AN IMAGING SPECTROMETRIC OBSERVATORY
(1NS001)

M. R. Torr
University of Michigan, USA

Spacelab 1 offers the first opportunity to measure the airglow spectrum from the extreme ultraviolet (EUV) to the infrared (IR) (20 to 1200 nanometers); i.e., to measure the spectral signatures of a large range of minor constituents, metastable and excited species of both atomic and molecular ions, and neutrals in the atmosphere (ranging from the stratosphere to the upper thermosphere) for which no data or only incomplete empirical data are available. One of the more severe limitations on studies of middle and upper atmospheric processes based on optical observations has been the lack of complete spectral information acquired simultaneously from the same observational volume. Atmospheric reactions involve radiation through the entire optical spectrum, and the correlation of data over a broad wavelength region invariably becomes vital to an understanding of the origin of excitation.

The dayglow spectrum of the Earth's atmosphere contains a wealth of information relevant to the composition and energy budget of the thermosphere, the solar EUV flux and its influence on the production of photoelectrons, cross sections for photon and electron ionization and excitation, transport and energy loss of photoelectrons, precipitation of fast charged particles, and the production and loss of various metastable species. Despite this abundance of information, little has yet been learned about the spectrum because spectra obtained from the ground have been limited to the night and twilight visible, have had the nontrivial problems associated with scattering and extinction in the lower atmosphere, and have had to contend with the fact that the thermospheric emissions are measured through the underlying OH emission. The purpose of this experiment is to measure the optical emissions arising from the dayglow and nightglow and other emissions from the Earth's atmosphere, the spacecraft induced atmosphere, artificially induced aurorae, and the interplanetary and interstellar media. The objective is to study the composition of and the processes governing these targets.

The proposed instrument is designed for high-speed operation as an imaging device. The rate of production of equivalent spectra is estimated to be 100 times faster than existing ground-based equipment. The instrument is composed of five identical spectrometers (Fig. I-1), each of which is restricted to a given spectral range within the 20 to 1200 nanometer region. Each module

is an imaging scanning spectrometer with coincident 0.5 × 0.007 degree fields-of-view. Imaging capability is obtained along the length of the observational field by use of an area array detector comprising 190 × 244 elements. Thus, a single measurement produces adjacent spectra in a given module obtained from adjacent observational fields. Wavelength resolution varies between 0.2 and 0.6 nanometer over the spectral range. A single exposure at one scan position covers a 250 nanometer region. The telescope will be baffled to allow measurements to within 8 degrees of the Sun or the bright limb of the Earth with full sensitivity of the instrument. A microprocessor will control the mechanical scan mechanisms, the array detector readout, and the operations sequencing. The layout depicted in Figure I-2 will be used for all modules except the EUV module, which will be used as an objective grating spectrometer. The instrument will be constructed in a modular design so that gratings and detectors can be replaced readily with alternate selections and so that fewer than the full array of five modules can be flown if desired.

The experiment will serve as a precursor for a wide range of investigations to which the spectrometer can be applied in later missions. It is, therefore, an observatory for the study of problems related to the Spacelab environment; the terrestrial atmosphere; planetary, interplanetary, and interstellar media; and stellar sources.

For the Spacelab 1 mission, the instrument will have various operational modes to acquire data on both weak and strong sources at various altitudes in the day, night, and twilight atmosphere. The various functions of the instrument (such as grating scans, attenuation, exposure duration, gain control) are programmable and software controlled, giving great versatility. The instrument is capable of operating over a wide dynamic range and has the option of using pulse counting or analogue detection modes. Observational sequences can be run from predefined programs stored in the command and data management system or can be entered by an onboard payload specialist or by the investigator on the ground. The instrument views either along the +Z direction, or over a 30 degree range in the YZ plane using a scan mirror. Altitude profiles or other spatial scans can be obtained either by using the scan mirror or by using maneuvers of the vehicle.

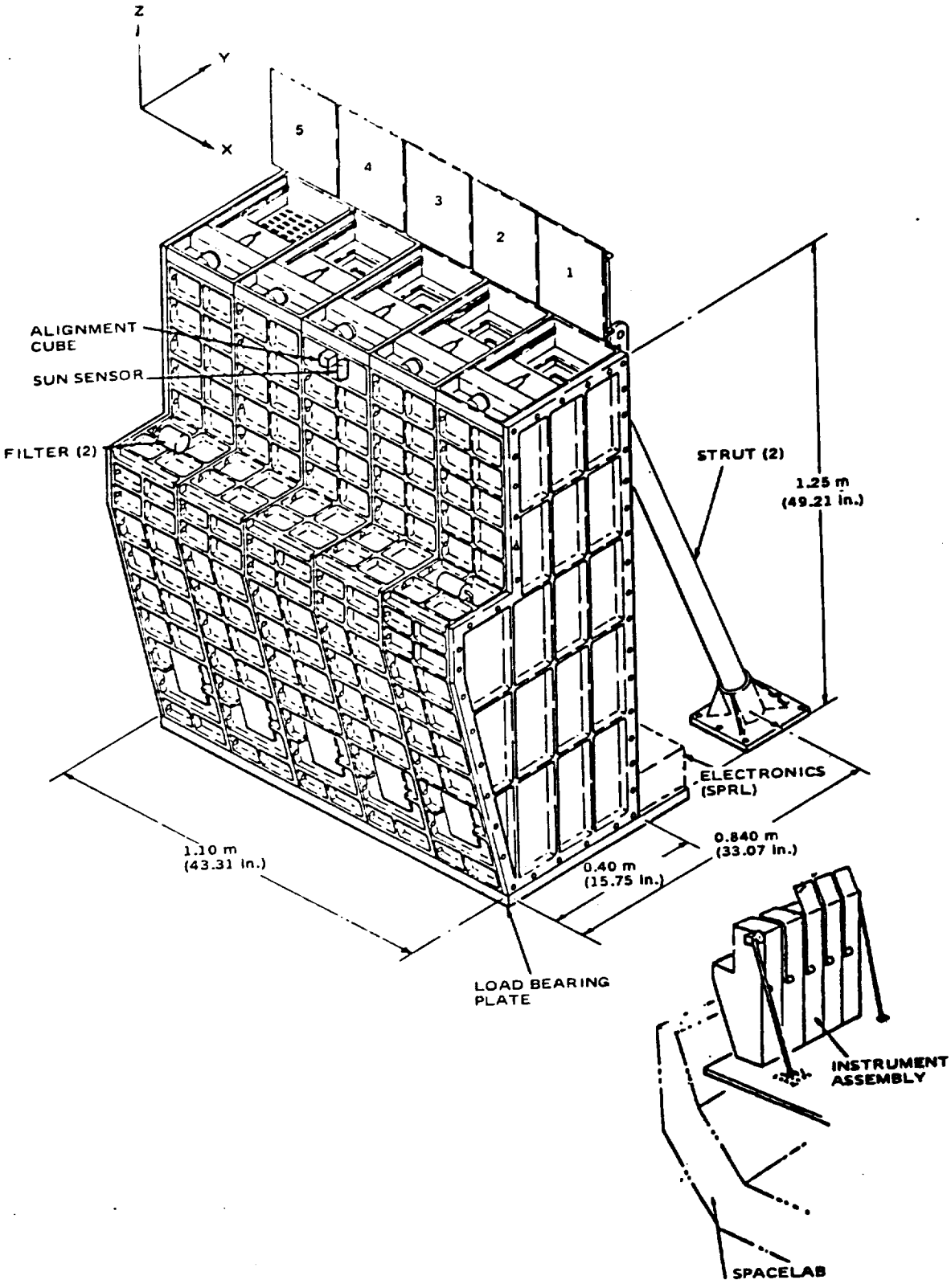


Figure I-1. Schematic of imaging spectrometer.

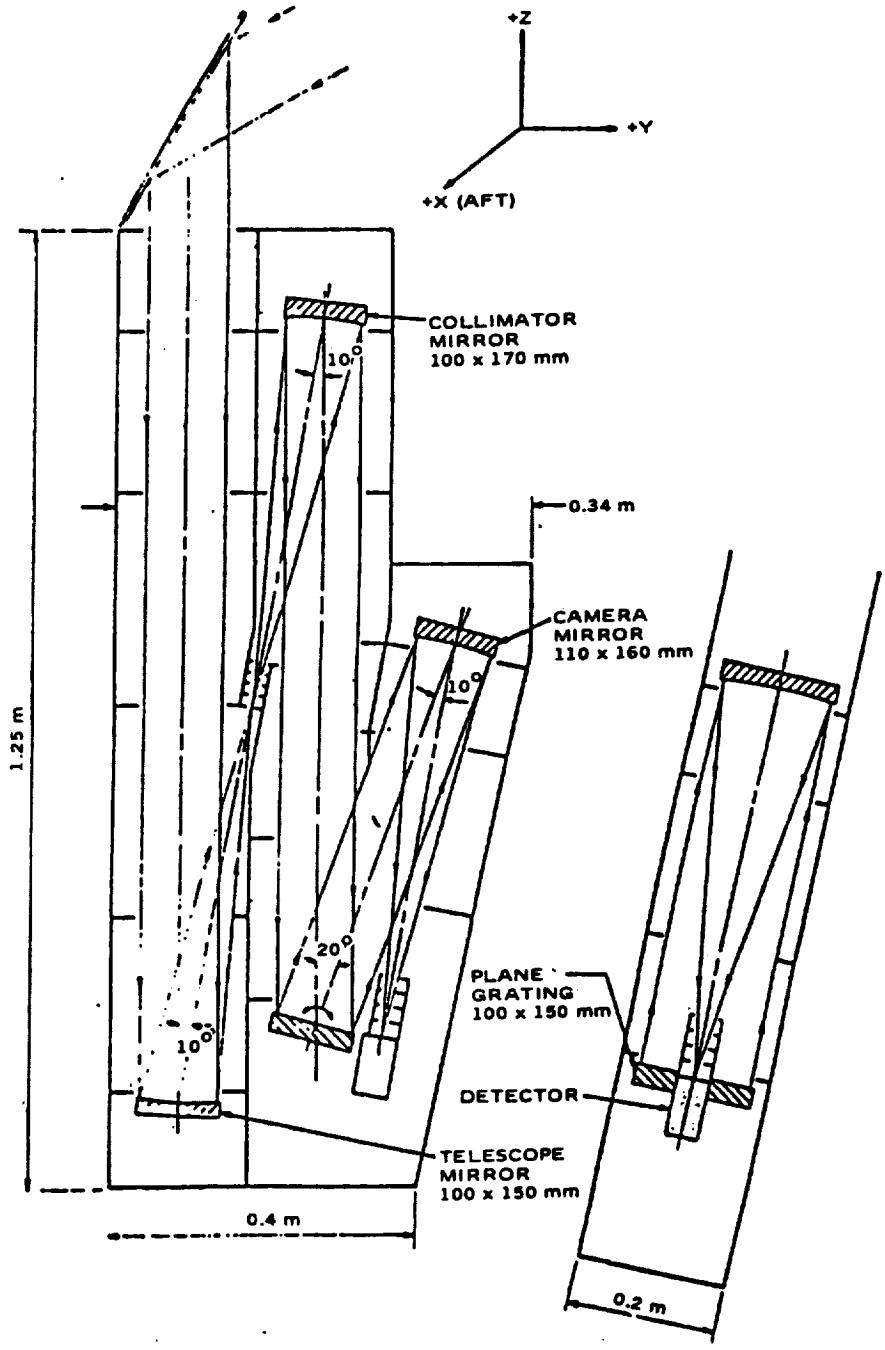


Figure I-2. Optical layout of imaging spectrometer module Nos. 1, 2, 3, and 4.

ATMOSPHERIC TRACE MOLECULE SPECTROSCOPY (1NA009)

C. B. Farmer
Jet Propulsion Laboratory, USA

The Atmospheric Trace Molecule Spectroscopy (ATMOS) investigation is designed to obtain fundamental information related to the chemistry and physics of the Earth's upper atmosphere using the techniques of infrared absorption spectroscopy. The investigation as proposed has two principal objectives. The first is the determination, on a global scale, of the compositional structure of the upper atmosphere and its spatial variability. The establishment of this variability represents the first step toward determining the characteristic residence times for the upper atmospheric constituents, the magnitudes of their sources and sinks, and, ultimately, an understanding of their effects on the stability of the stratosphere. The second objective is to provide the high-resolution, calibrated spectral information which is essential for the detailed design of advanced instrumentation for subsequent global monitoring of specific species found to be critical to atmospheric stability. This information will be disseminated in the form of a three-dimensional atlas of spectra obtained over a broad range of latitudes, longitudes, and altitudes in the stratosphere and mesosphere.

The spectra which will be acquired in the course of the ATMOS investigation will contain (in addition to the previously mentioned compositional data) a great deal of information related to the physics of the upper atmosphere. The experiment has been designed to return information for studying, among other things, vertical temperature structure, local thermodynamic equilibrium, regimes of dissociation, and radiative transfer processes. Investigators with special interests in each of these areas have been included in the ATMOS science team to insure that the instrument and experiment, as finally designed, will be capable of making the necessary measurements.

The experimental approach for acquiring the necessary data from Spacelab 1 will be to view the Sun with the ATMOS instrument during the periods just prior to entry into and shortly after emerging from solar occultation. Specifically, the viewing periods will be timed to occur when the ATMOS instrument's view of the Sun is being occulted by the upper atmosphere. During these periods, the instrument will make a set of interferometric measurements of the solar radiation incident upon it as a function of optical path difference within the instrument. Subsequent transformation of each of these measurements will produce spectra of the solar continuum between 2 and 16 micrometers, with the

characteristic absorption features of all the stratospheric species present superimposed upon it. Each set of measurements, generated at different stratospheric altitudes, will provide the information necessary to establish vertical composition profiles for the species of interest. The orbital geometry and occultation rate for Spacelab 1 will further provide for the acquisition of data sets at two latitudes and several longitudes.

The choice of the remote sensing method for acquiring the data is dictated by the need to obtain simultaneous concentration information for a large number of stratospheric species in times sufficiently short to provide useful spatial resolution. The one common characteristic possessed by almost all of the species of interest is that their rotational and vibrational transition frequencies lie in the infrared region, and thus simultaneous measurements can be made using infrared spectroscopic techniques. The transition frequencies are widely separated for different constituents, however, necessitating broad wavelength coverage in each observation. Moreover, in the Sun-looking mode from Spacelab, each observation must be made in times on the order of 1 to 2 seconds if useful vertical resolution is to be obtained. Interferometry, with its high energy throughput and multiplexing advantages, is the only infrared technique capable of satisfying these last two constraints. The ATMOS instrument will thus be a continuous-scanning Fourier spectrometer operating in the 2 to 16 micrometer wavelength region and capable of generating one interferogram each second with a spectral resolution of 0.02 centimeter^{-1}.

The ATMOS optical head consists of a suntracker, a telescope, and an interferometer. This part of the instrument will be located in the Spacelab module in the scientific airlock, with the associated electronics residing in a standard Spacelab rack. The preliminary optical layout is shown in Figures I-3 and I-4. The suntracker contains two single-axis, motor-driven mirrors and a silicon diode assembly for sensing and controlling the position of the mirrors with respect to the Sun. A 16 millimeter camera records the position of the instrument field-of-view projected onto the solar disc during each observation. An f/2 telescope system is used to concentrate the radiation received into a beam suitable for the interferometer. Cat's-eye retroreflectors replace the plane mirrors used in a conventional Michelson interferometer. A retroreflecting mirror double passes the radiation through the arms of the interferometer before it is recombined and sent to the detector. The use of the cat's-eye retroreflectors and double passing make the instrument insensitive to both angular and lateral motion of the moving elements. The detector is a HgCdTe type cooled to liquid nitrogen temperature. Its output is digitized and, together with the optical path difference position and housekeeping data, is multiplexed into a single data stream. A system controller coordinates all

instrument functions and operations; in addition, it formats the telemetry outputs and provides a responsive interface to the instrument microprocessor. Data-taking sequences are initiated manually or by preentered command.

The global survey described herein takes advantage of (1) the orbital geometry of the Shuttle to provide wide variations in stratospheric conditions and (2) the broad bandpass and high data rate of the proposed instrument to provide simultaneous concentration profiles with good vertical resolution for a large number of stratospheric constituents. It will, therefore, provide data on the three-dimensional variation of these constituents under different stratospheric conditions, which will be extremely useful for current modeling activities and will also provide the fundamental information regarding the composition of the stratosphere against which the results of future individual measurements can be assessed.

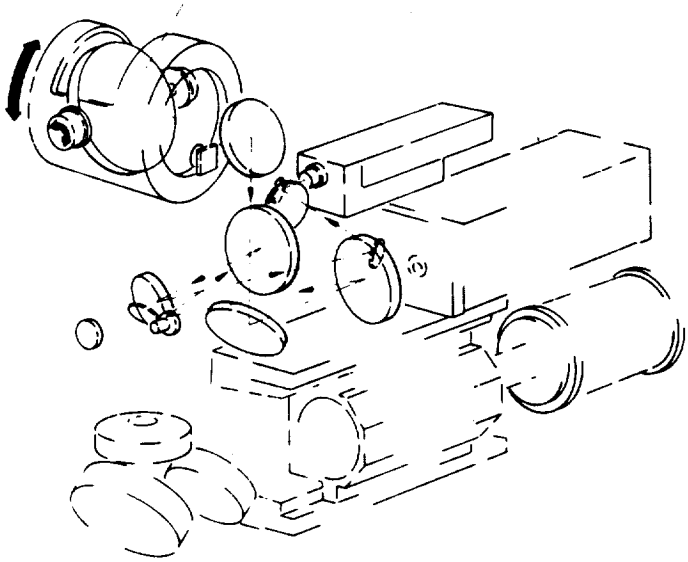


Figure I-3. ATMOS foreoptics and camera.

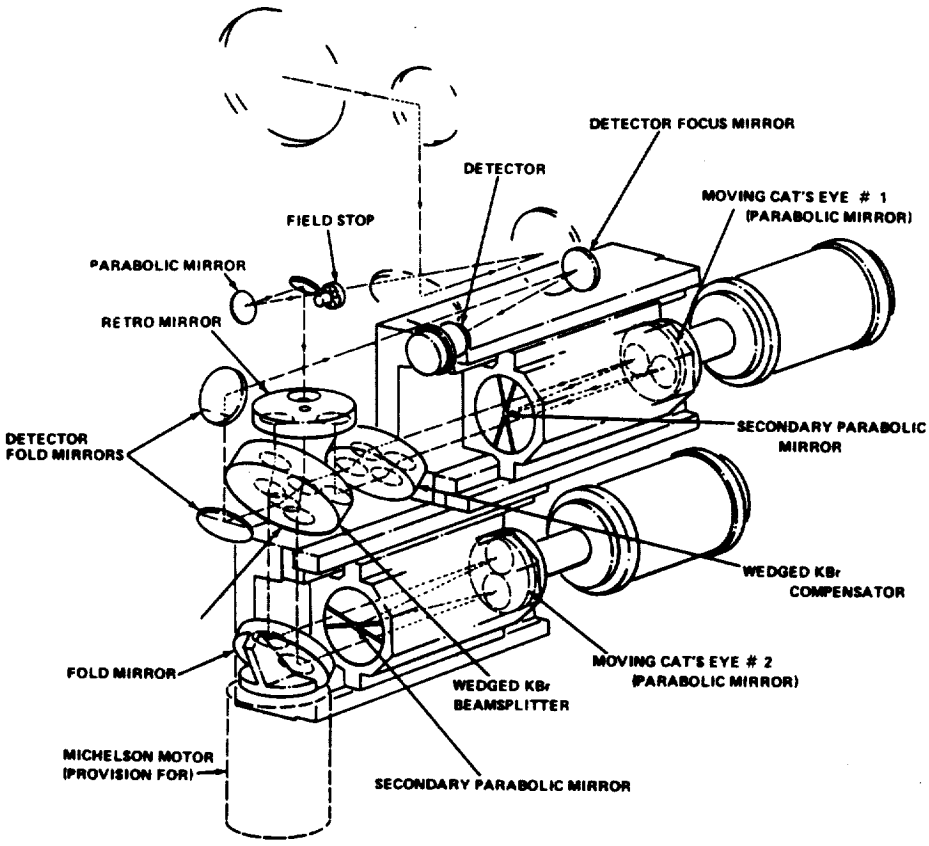


Figure I-4. ATMOS interferometer optical path.

GRILLE SPECTROMETER
(1ES013)

M. Ackerman
Belgian Institute for Space Aeronomy, Belgium

and

A. Girard
Office National d'Etudes et de Recherches Aerospatiales, France

The grille spectrometer has been proposed by two organizations: the Office National d'Etudes et de Recherches Aerospatiales in France and the Belgian Institute for Space Aeronomy in Belgium. Its purpose is to study, on a global scale, atmospheric parameters between 15 and 150 kilometers altitude. The investigation uses high-resolution (better than 0.1 centimeter^{-1}) infrared spectroscopic observations of the Earth's limb in the wavelength range characteristic of the vibrational-rotational lines of the relevant atmospheric constituents. Since major atmospheric constituents (O_2, N_2) are not active in the infrared, trace species (e.g., CO_2, H_2O, O_3, CH_4, N_2O, CO, NO, NO_2, HNO_3, HCl, HF, $CFCl_2$, $CFCl_3$, OH, O, etc.) will be observed. Most of the measurements will be performed in the absorption mode with a fast spectral scanning velocity (one spectral element in 0.1 second) using the Sun as the source at sunrise and sunset. This method of analysis of the minor constituents offers well-recognized advantages. The quantitative interpretation of the spectra can be performed with a high degree of accuracy; in particular, the knowledge of the temperature profile is not required. The vertical profile of number density is deduced readily with a set of observations at different solar zenith angles by the "onion peeling" processing method. The high resolution permits the unambiguous isolation of the spectral signatures even in the case of the components with the lowest number density.

In the emission mode, measurements of the infrared emissions of the trace constituents will be made by observing the Earth's atmospheric limb. Such measurements can be performed at almost any time during the night or day, the only limitation being the Spacelab attitude.

The grille spectrometer possesses the advantage of a luminosity approximately one hundred times better than the conventional slit spectrometer and, compared to the Fourier transform spectrometer, has the practical advantage of directly recording the spectral information in the very narrow spectral range where this information is relevant.

With a classical spectrometer, the entrance and exit slits make the luminosity and the resolving power strictly dependent on each other. In fact, high luminosity requires a large throughput for the spectrometer, and a high-resolving power requires a large range of transmission for the spatial frequencies in the focal plane of the spectrometer. The instrumental parameters determining these two properties can be made independent by placing, instead of slits, a plate (grille) with a large area and a set of alternatively reflecting and transparent zones, limited by equilateral hyperbolas. The grille, acting as a broadband width spatial filter, works by transmission at the entrance and by reflection at the exit. The luminosity depends on the area of the grille, and the resolving power depends on the width of the zones.

The resolved spectral interval is selectively modulated by a vibrating collimator which produces an oscillation with a small amplitude of the dispersed light coming from the spectrometer.

The spectrometer (Fig. I-5) will operate in the wavelength range from 2.5 to 13 micrometers. The light coming from the Sun through the Earth's atmospheric limb or from the atmospheric limb itself will be reflected toward a telescope by an orientable rectangular plane mirror. The telescope which will transmit the light to the spectrometer has a 0.3 meter diameter and a 6 meter focal length. Two detectors will be used simultaneously to cover the entire spectral range. All functions of the instrumentation will be programmable through a microprocessor which will be a part of the instrument electronics and will allow interaction between the payload specialist on board and the ground-based investigators. The instrument will be closed when not in operation. A built-in calibration light source will allow test at any time before and during flight.

Considerable valuable data have been obtained with similar instruments from balloon and aircraft platforms (Concorde and NASA Convair 990). Spacelab operation will provide global coverage, access to higher altitudes (mesosphere and thermosphere), and the acquisition of a large amount of data in a short time compared with the slow operation on other platforms.

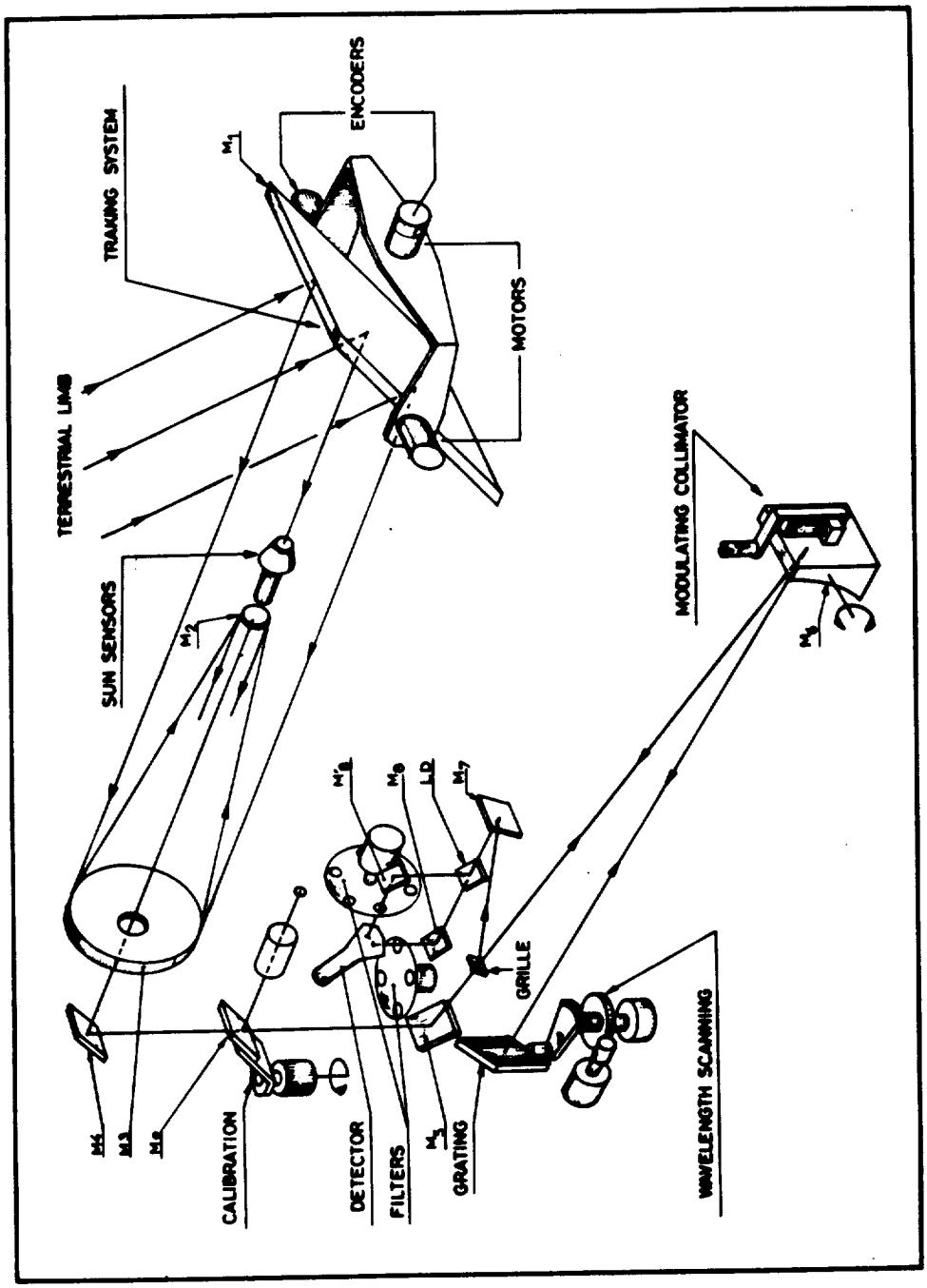


Figure I-5. Grille spectrometer optical principles.

TEMPERATURE, WIND IN MESOSPHERE AND THERMOSPHERE (1ES015)

G. Thuillier
Service d'Aeronomie du CNRS, France

Remote observations of electromagnetic radiation emanating from the Earth's atmosphere have proven to be important in atmospheric research, particularly in very recent years. Observations can be made over a wide spectral range and a variety of sources, including the thermal emissions, airglow, and scattered sunlight.

The scientific objective of this experiment is the direct measurement of the temperature and wind profiles in the mesosphere and thermosphere. Direct measurements are made by determining line widths and Doppler shifts. For this experiment, the lines to be utilized are those of the airglow spectrum of atomic oxygen and the (8-3) band of the OH radical. A field compensated Michelson interferometer will be used to record the spectral information.

Temperature measurements of the atmosphere can be obtained in different ways. Indirect measurements make use of the total density or density of a particular constituent or ion temperature measured by incoherent scatter radar. They are direct when the Doppler line width emitted by a thermalized atom is measured. Although many atmospheric models exist at the present time, the temperature versus altitude profile remains uncertain. Local daytime temperature profiles have been obtained by incoherent scatter radar, but a global coverage as well as measurements of latitudinal variations remain to be done.

Winds generally are poorly known due to the difficulty of their measurements. Classical techniques consist of chemical releases, incoherent scatter radar and lidar excitation. Due to the limited number of ground stations, latitudinal and longitudinal variations of the wind are not well known. At low latitude, the measurement of longitude effects (or magnetic declination effects) as observed on nightglow emissions will be very valuable for thermospheric dynamics.

For the Spacelab 1 mission, a field compensated Michelson interferometer (Fig. I-6) is used to demonstrate its ability to measure wind and temperature. It is a classical interferometer modified by placing a block of glass in one of the two paths. The result is that this instrument is much more luminous than a classical Michelson interferometer (i.e., accepts a larger field of light for a given spectral resolution).

To utilize the interferometer at its maximum spectral resolution, the spectral input is limited by interference filters, thus individually analyzing an emission line whose profile is theoretically known. In this case, atmospheric temperature and wind are determined from the line width and the Doppler shift of the line center, respectively. Measurements of the Doppler shift require a wavelength reference which is given by an He-Ne laser.

A telescope (Cassegrain) of 0.2 meter diameter and 1.0 meter focal length is used to collect the photons emitted from the limb. The horizontal field-of-view of the telescope is 2 degrees; the vertical field-of-view is 0.1 degree for mesospheric measurements and 0.4 degree for thermospheric measurements.

The Michelson interferometer can use a 2 degree × 2 degree field-of-view. To increase the time resolution, the field-of-view is analyzed simultaneously in five parts corresponding to five different altitudes. Five photomultiplier detectors are used, one for each part or altitude.

Altitude dependence of the temperature and wind is determined by recording the spectral line for each step as the field-of-view is scanned in a vertical plane. A vertical scan is made from the local horizontal plane to -16 degrees below this plane. A complete vertical scan (250 to 60 kilometers) is made in 34 seconds, which gives a latitudinal resolution of approximately 3 degrees. The vertical resolution is approximately 2 kilometers at 90 kilometers altitude.

The 630.0 and 557.7 nanometer OI lines and the 731.9 nanometer OII line of the airglow spectrum will be observed for thermospheric measurements. For mesospheric measurements, the 557.7 nanometer line and the 730.0 nanometer lines in the (8-3) band of the OH^+ radical will be utilized. To use these lines, the instrument is designed to be achromatic in the wavelength range of measurement. Spectral scanning is achieved by a small angle prism changing the optical path by approximately one wavelength. The line to be studied is isolated by a narrow-band interference filter. Background light for each spatial step is recorded by reflecting 5 percent of the incident light through a separate broadband interference filter to a detector.

The measurement sequences are under the control of a programmer which can be either remotely commanded or operated onboard by the payload specialist. However, measurement sequences, once started, are fully automatic. Data manipulation and control of the measurement sequences will be handled by a single microprocessor.

Very high resolution measurements of radiation emitted by the atmosphere can, in principle, be used to infer constituent density, atmospheric temperature, and motion (winds). Measurements of these atmospheric parameters, particularly with the broad coverage afforded by observations from Earth satellites, will serve, in the decade of the 1980's, to greatly increase man's understanding of the atmosphere. These early measurements, beyond their own scientific value, will pioneer the development of techniques that will ultimately enable a continuous surveillance of the state of this region of the atmosphere from orbiting instruments.

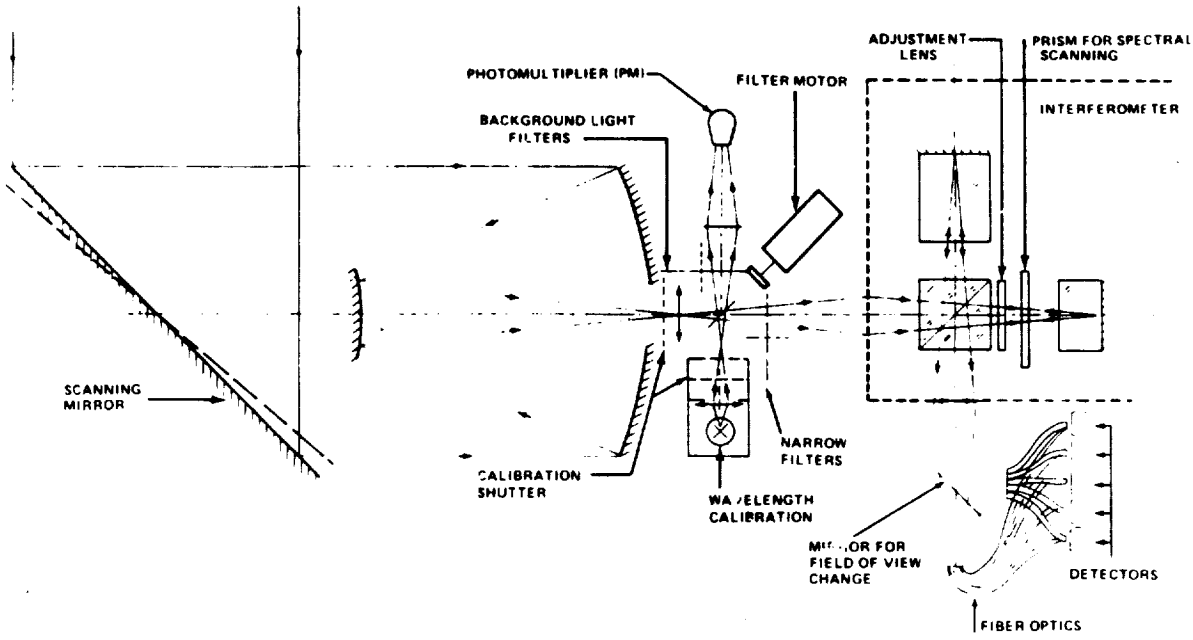


Figure I-6. Temperature and wind measurement instrumentation.

WAVES IN THE OH EMISSIVE LAYER
(1ES014)

M. Herse
Service d'Aeronomie du CNRS, France

The light of the night sky in photographs taken in the near IR frequently exhibits a patchy and striated structure. The striations or bright parallel bands occur in large cloud-like structures. Each large region is more than a 1000 kilometers in size, with roughly 40 kilometers between bright crests. The velocity of the movement of the bands is low, less than 20 meters per second. Parallax determinations place the altitude of the clouds at 85 kilometers. The only known species that emits light in the near IR and is localized at this altitude is OH.

The origin of the structure is not known, but it may be related to gravity waves or turbulences. To determine a correlation, one needs a larger coverage than is obtained from a single site. Observations from space permit such a coverage.

The scientific aim of this experiment is to photograph and measure the structures, i.e., sizes, velocities, contrast, evolution, etc. A better knowledge of the dynamics of the upper atmosphere at this altitude and possibly the causes of the structures will be obtained from these studies.

The instrument (Fig. I-7) is built with commercial parts. An objective forms the image of the sky on the photocathode of a microchannel image intensifier. A second objective (the camera lens) is used as a relay lens to record on photographic film the image of the output screen of the intensifier. An image intensifier is necessary because the emission is too faint to permit an exposure time compatible with spacecraft velocity. The spectral part of the airglow is delimited on the short wavelength side by a Wratten 88A filter (80 percent cutoff at 758.0 nanometers) and on the IR side by the sensitivity of the photocathode (50 percent cutoff at 830.0 nanometers). The camera is a 16 millimeter movie camera operated in a single frame mode. It will be turned on and off by commands initiated in the Spacelab module or on the ground. Approximately 2000 photographs are planned during the mission, using the Orbiter for pointing. The film will be processed post-mission and the structures projected on a geographical map to obtain the parameter values.

These OH natural emissions of the atmosphere rather than artificial tracers (e.g., barium) will allow wider geographical coverage for measurements of upper atmospheric parameters such as winds.

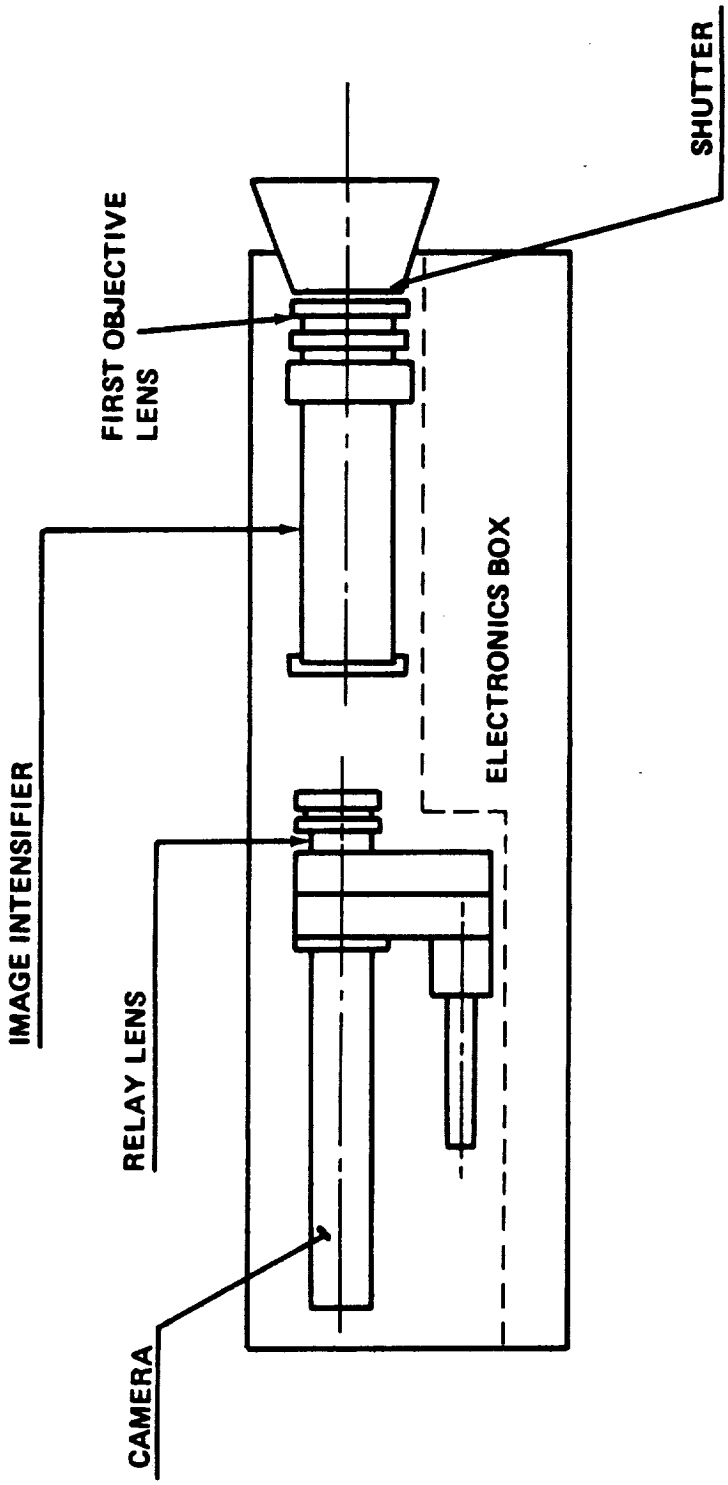


Figure I-7. Schematic of instrument for OH emissive layer experiment.

INVESTIGATION ON ATMOSPHERIC H AND D THROUGH THE MEASUREMENT OF THEIR LYMAN-α EMISSIONS (1ES017)

J. L. Bertaux
Service d'Aéronomie du CNRS, France

The scientific objective of this experiment is to study various sources of Lyman-α emission in the atmosphere, in the interplanetary medium, and possibly in the galactic medium. The instrument is a spectrophotometer associated with two absorption cells, one filled with hydrogen, the other with deuterium (Fig. I-8).

The main source of Lyman-α as seen from Spacelab is the result of resonance scattering of solar photons by atmospheric atomic hydrogen. This emission has been studied thoroughly with previous space experiments and is considered as "noise" in the present investigation; it is eliminated with the help of the hydrogen absorption cell run at a high absorption level. The other sources of Lyman-α are then studied (Fig. I-9).

Lyman-α emission of atomic deuterium (D) is identified with the help of the deuterium absorption cell. Its intensity and line-width are measured, yeilding the verical distribution of D from 90 to approximately 250 kilometers and its temperature. From this vertical distribution, the eddy diffusion coefficient K around 100 kilometers is derived and mapped on the whole sunlit Earth.

Lyman-α emission resulting from charge exchange is possibly present at various places: auroral zones, equatorial zones, and possibly at the foot of the polar cusps, where the solar wind interacts directly with the neutral atmosphere. The foot of the polar cusps could be located precisely through observations of these regions with a scanning mirror.

Some emission is also expected from the plasma guns placed on board Spacelab.

Interplanetary hydrogen (which comes from the nearby interstellar medium) is a source of Lyman-α. It prevents astronomical observation of diffuse galactic Lyman-α emissions. With the help of the absorption cell, the level of diffuse galactic emission will be determined. The use of the absorption cell on Spacelab is also a test for determining if the presence of geocoronal and interplanetary emission will prevent future astronomical observations of Lyman-α emissions.

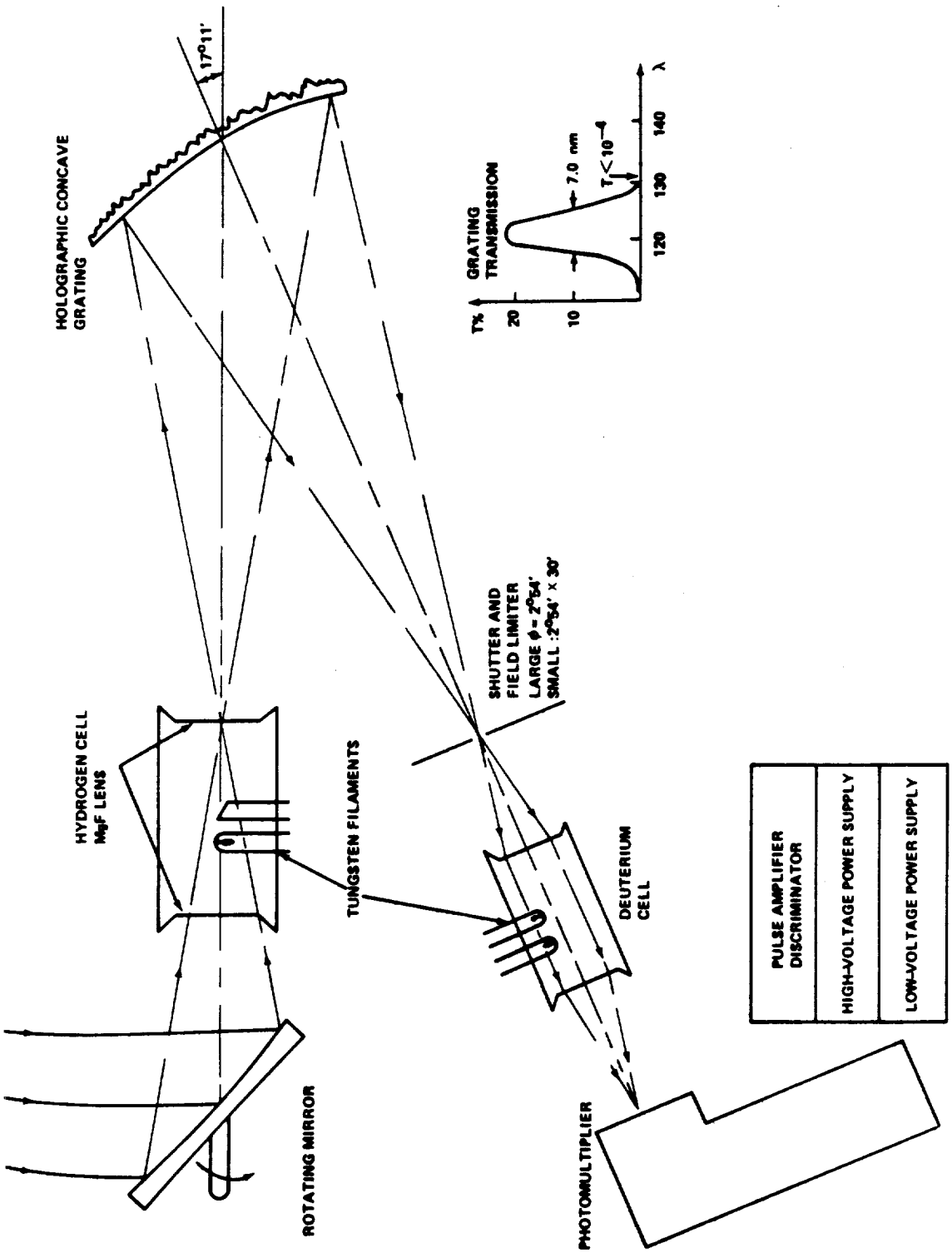


Figure I-8. Schematic of instrument for measurement of hydrogen and deuterium Lyman-α emission.

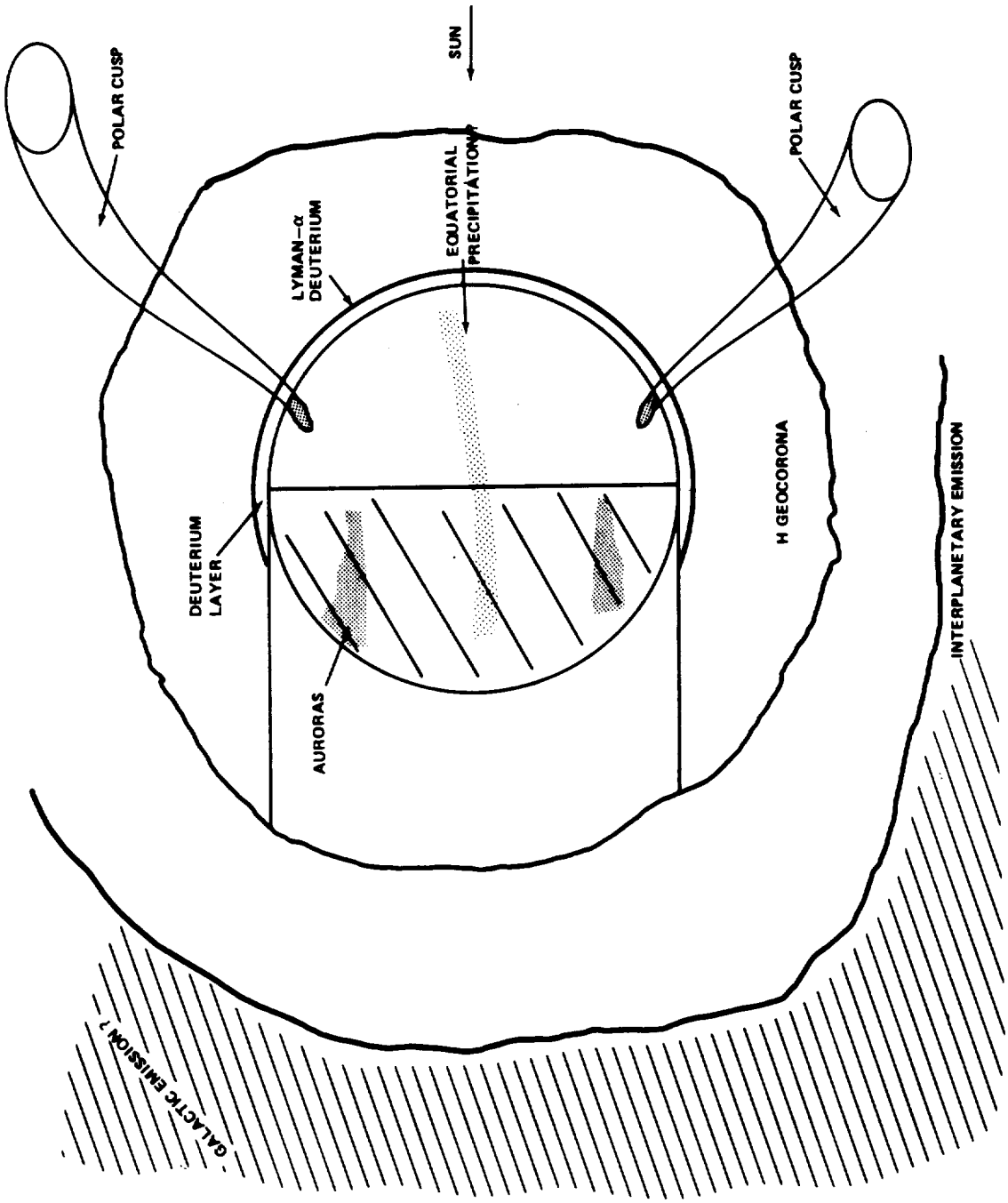


Figure I-9. Sources of Lyman-α emissions.

METRIC CAMERA EXPERIMENT
(1EA033)

M. Reynolds
ESA Facility

Considering the worldwide need for topographic mapping at medium to small scales for the planning of use of global natural resources and the need for deriving thematic maps on the basis of topographic maps, it is generally apparent to the mapping community that existing mapping techniques yield too slow a progress compared to the needs in (1) compiling topographic and thematic maps, especially in unpopulated or less-developed regions of the world and (2) updating and revising topographic and thematic maps in populated and developed regions of the world.

A possible remedy is the acquisition of high-resolution imagery from satellite altitudes using aerial survey camera systems. The purpose of the metric camera experiment is therefore to test the mapping capabilities of high-resolution space photography taken at the resolution limit of image motion on large film format (23 × 23 centimeters). The RMK 30/23 mapping camera chosen for the first Spacelab flight is expected to provide imagery with a photographic ground resolution of better than 20 meters, and it is therefore considered suitable for detecting details for mapping at small scales and for certain aspects at medium scale.

The metric camera system consists of the following components: camera body with optics and exposure meter, film magazines containing aerial film of 24 centimeters width, a remote control unit, and filters. An outline sketch of the camera installed in Spacelab is shown in Figure I-10, and Table I-1 gives the characteristics of the camera and experiment parameters. For operation, the camera has to be mounted behind an optical window and is therefore in the Spacelab module.

Three film magazines are foreseen. On the average, approximately 550 photographs can be obtained on one magazine, so that three magazines will yield a total of 1650 exposures. Each magazine may contain a different film type. The exposures will be taken cyclewise either with a 60 or 80 percent longitudinal overlap. At the present state of planning, there will be 32 cycles containing between 9 and 121 photographs. The cycle times will vary between 6 and 25 minutes.

For experiment control, the metric camera has its own microprocessor. The start times for each cycle are transferred by means of "scheduling commands" on a day-by-day basis.

After installation of the camera at the optical window, the payload crew is hardly involved in experiment operations except for changing film magazines and filters. Concerning monitoring activities, the crew is warned of an experiment error by a blinking indicator. In critical situations the experiment is switched off automatically. Consequently, the focal point for monitoring and control of the metric camera is in the payload operations control center.

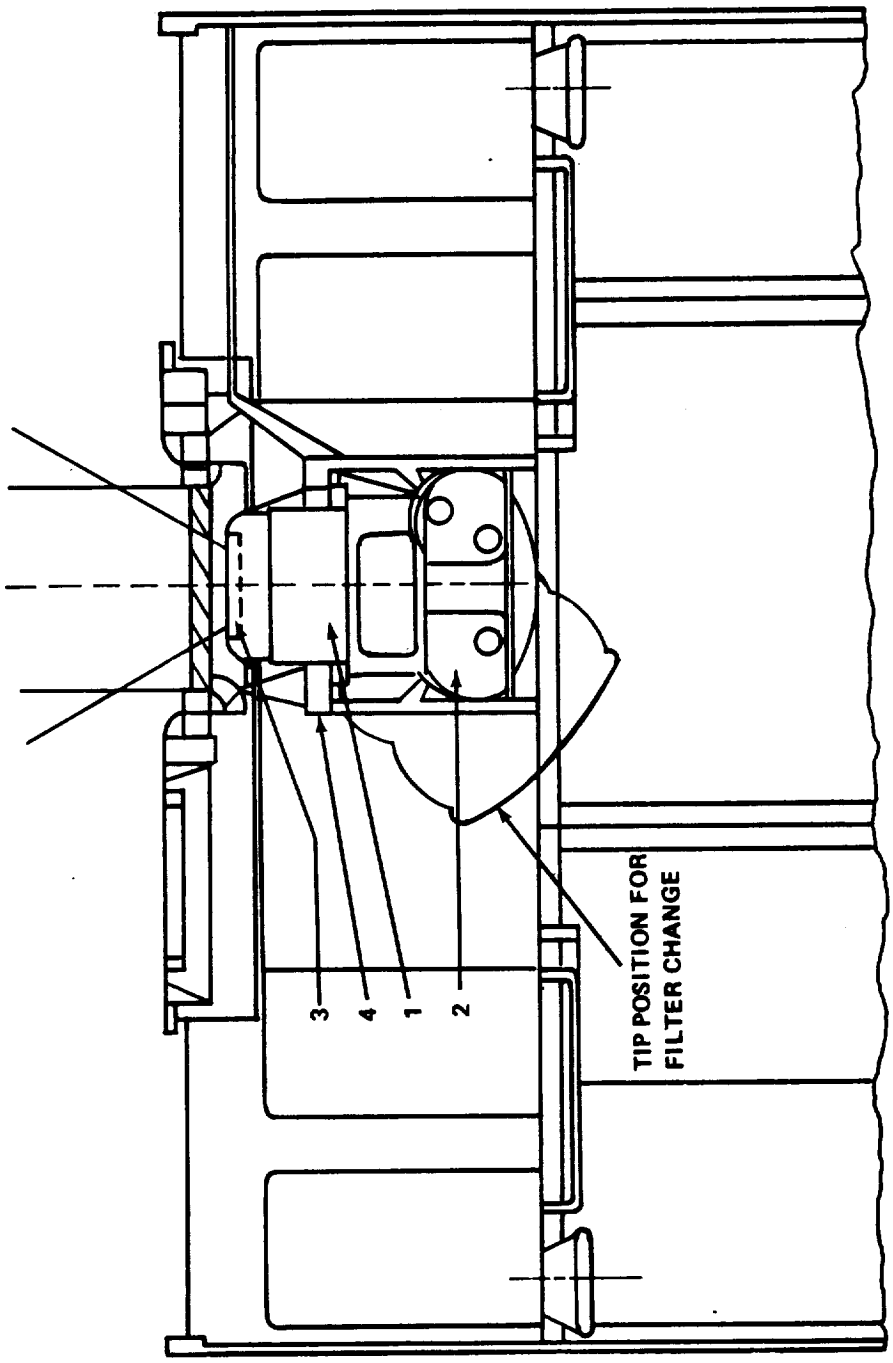
To get 80 percent longitudinal overlap of subsequent photographs at a Spacelab velocity of 7.7 kilometers per second there will be a time interval of Δt approximately 5 seconds between two successive exposures. This amounts to a total operation time of 2.3 hours for the camera (for 60 percent overlap, the total operation time is 4.6 hours). In this way strips 1800 to 2300 kilometers can be covered on the ground in each sequence.

In standard aerial photography, suitable illumination conditions exist only if the Sun elevation is higher than 30 degrees. However, the Sun elevation angle should be smaller than (90 degrees-α) in order to avoid interference due to solar reflection; α is 20.5 degrees to the edges of the photograph and 28 degrees on the direction of the diagonals. The second condition is fulfilled for the chosen orbit with inclination 57 degrees. However, the first condition (Sun elevation greater than 30 degrees) restricts the areas over which mapping photographs can be taken to a latitude 40 degrees or greater at the beginning of the mission and 30 degrees or greater at the end of the mission. For geological interpretation there may be some cases (e.g., over desert areas) in which photography with low elevation angle (between 30 and 15 degrees) is desired to enhance terrain relief by shadows.

This use of the camera in Spacelab will test the application of space photography over well-controlled regions, including perhaps areas of special characteristics both in Europe and other regions, particularly the developing countries.

TABLE I-1. CHARACTERISTICS OF THE EXPERIMENT

Camera	
Type:	Zeiss RMK A30/23
Lens:	Topar f = 305
Distortion:	5 μm maximum
Resolution:	40 lp/mm over whole image size (with Aviphot Pan 30 PE with a speed of 21° DIN and Perufin developer)
Field-of-View:	Diagonal 56°, Across 41.2°
Shutter:	Aerotop-rotating-disk-shutter (between lens shutter), Exposure: 1/100, 1/250, 1/500, 1/1000
Apertures:	1:5.6, 1:8, 1:11
Shortest Cycling Time:	2 sec (interval between two exposures)
Image Size:	23 × 23 cm
Film Width:	24 cm
Film Length:	120 to 150 m depending on film thickness
Experiment Parameters	
Scale of Images:	1:820 000
Image Size:	23 × 23 cm
Ground Coverage of One Image:	188.5 × 188.5 km
Spacelab Velocity:	~7.7 km/sec
Image Motion:	At 1/500 sec exposure time: 18 μm (= 16 m on the ground) At 1/1000 sec exposure time: 9 μm (= 8 m on the ground)
Base-to-Height Ratio at 60 percent:	1:3 (every second photo at 80 percent overlap)



3 FILTER
4 SUSPENSION MOUNT
2 FILM MAGAZINE
1 CAMERA BODY

Figure I-10. Metric camera in Spacelab.

MICROWAVE REMOTE SENSING EXPERIMENT (1EA034)

G. Dieterle
ESA Facility

The microwave instrument to be flown on the first Spacelab mission in 1980 will be the first European microwave remote sensing experiment to be placed in orbit. The design of the instrument is such that different sensor operating modes will be possible, enabling a range of experiments to be performed both during the first mission and during reflights of the instrument on subsequent Spacelab flights.

The Microwave Remote Sensing Experiment (MRSE) instrumentation is a radar facility. In the active modes the instrument transmits microwave energy in X-band (9.65 gigahertz) to Earth targets. A sensitive low noise receiver detects the backscattered radar signals. The same system is used in the passive mode to detect the microwave brightness temperature of the targets. The operation of the experiment is largely automatic, but it can be controlled by the payload specialist or from the ground.

The microwave instrument will operate in three modes: (1) a main mode as a two-frequency scatterometer (2 FS), (2) a high-resolution mode as a synthetic aperture radar (SAR), and (3) a passive mode as a passive microwave radiometer.

In the 2 FS mode, the instrument will measure the ocean surface wave spectra by using the complex backscattering of the ocean surface at two adjacent microwave frequencies. Calculations will deliver a cross-correlation term proportional to a component of the sea-wave spectrum depending on look angle, depression angle, and difference frequency; the radiometer signal is used for data correction. In this way, the long ocean wave spectrum components for waves between 10 and 500 meters will be detected. Rotation of the antenna will give wave direction. Data gathering will be done in ocean areas parallel to the Spacelab ground track. Calibration of the system is obtained by the comparison of space measurements with sea truth data from test areas.

In the SAR mode, areas of the Earth's surface will be imaged with the instrument operating in a synthetic aperture radar mode. The backscattered data are coherently recorded, and off-line processing will provide imagery with a ground resolution of 25 by 25 meters. Motion compensation is carried out

during the ground processing using data from the Spacelab attitude sensors. The SAR shall be used over land surfaces and over the ocean (sea ice, oil slicks).

The radiometer mode is an add-on mode to support the 2 FS sensor object study and will be used in time multiplex with other modes. This mode measures ocean surface temperatures.

The parts of the MRSE equipment which are located on the Spacelab pallet are the antenna with support tower and the high power amplifier (Fig. I-11). The antenna is designed as a parabolic offset system with horn feed. The main reflector dimensions are 2 meters in azimuth and 1 meter in elevation. The antenna gain is approximately 40 decibels with a sidelobe level of less than -24 decibels. The support tower houses the antenna feed, the low noise amplifier, the radio frequency switches, and the duplexer. The two-axis antenna pedestal allows depression angles from 25 to 55 degrees and azimuth angles from -35 to 40 degrees relative to the pallet coordinate system. The maximum angular velocity will be 5 degrees per second, and the pointing accuracy is ±0.1 degree.

The MRSE rack subsystem is installed in the Spacelab module. It contains the frequency generation system, the experiment dedicated processor with the interface to the Spacelab command and data management system, and the interface system to the high-rate multiplexer system (HRM).

During the mission all scientific data will be digitized onboard, formatted, and combined with auxiliary data. In all modes the data streams are delivered to the HRM of Spacelab for transmission to ground, where all data are stored.

The development of all-weather (microwave) remote sensing techniques will be an important element of the future European Remote Sensing Space Program. As a platform to conduct remote sensing experiments from space and to perfect instrument performance prior to integration into automatic satellite payloads, Spacelab is expected to play an important role in the development of a European microwave remote sensing capability.

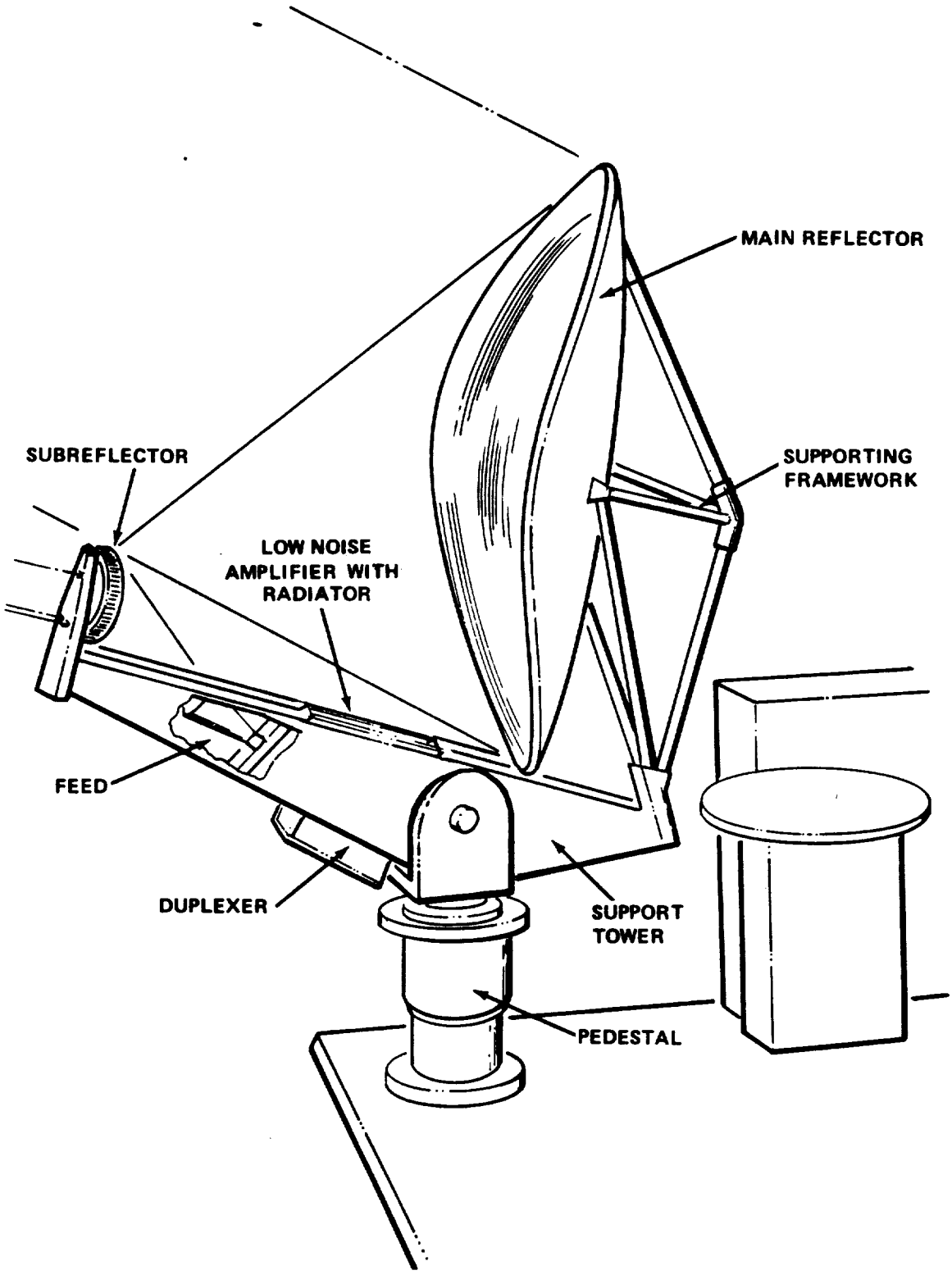
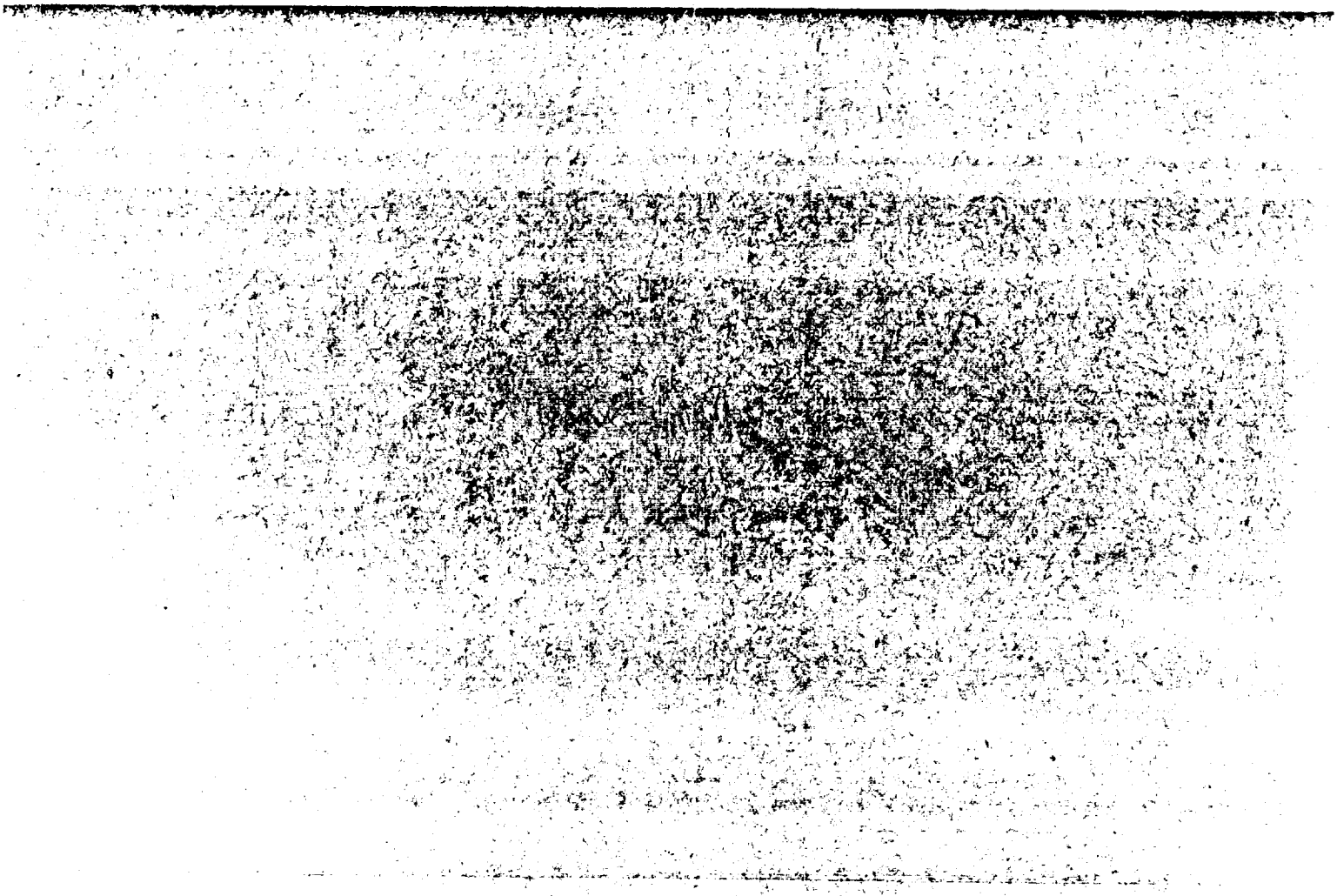
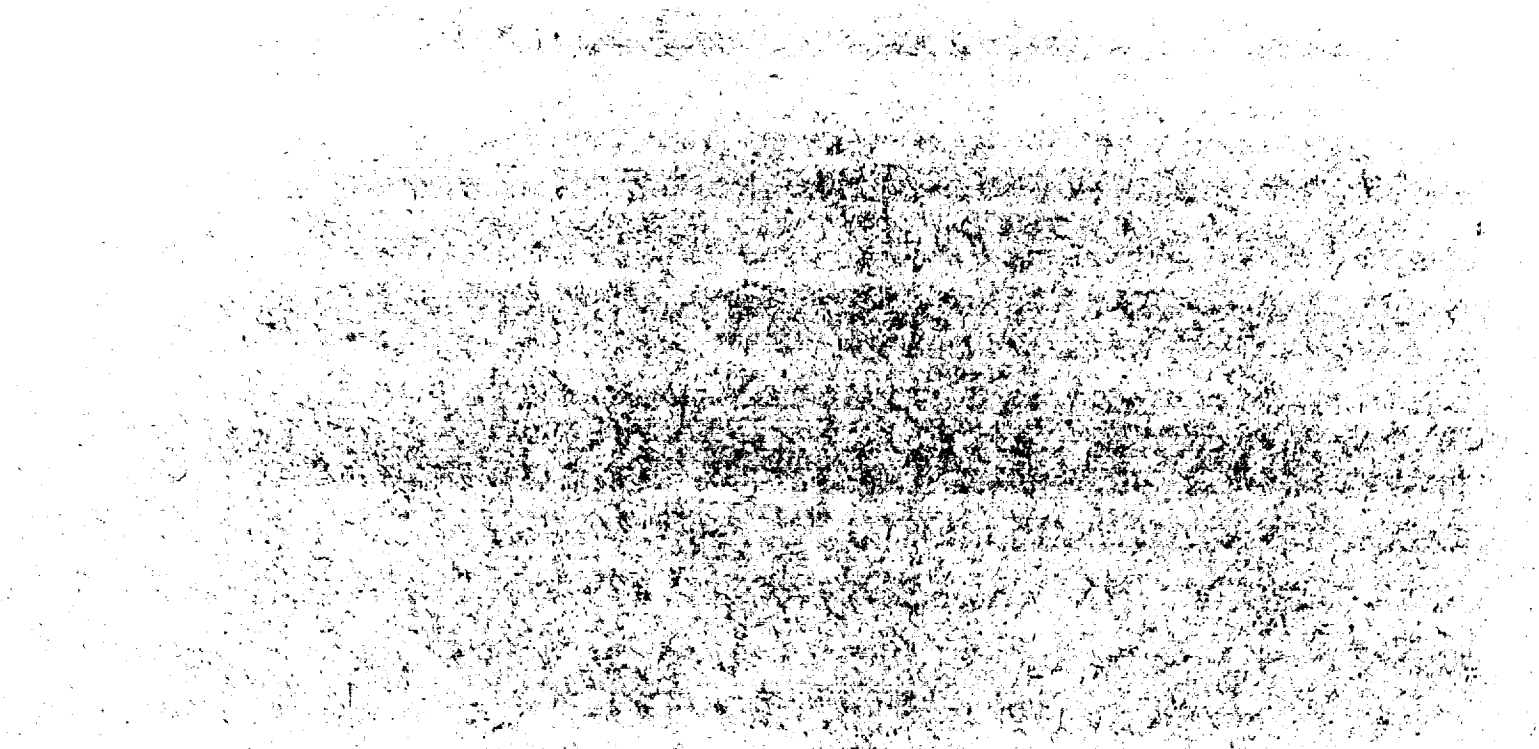


Figure I-11. Conceptional view of the antenna system.

SECTION II

SPACE PLASMA PHYSICS





SPACE EXPERIMENTS WITH PARTICLE ACCELERATORS (1NS002)

Tatsuzo Obayashi
University of Tokyo, Japan

The exploratory experimental programs of the past two decades have resulted in the accumulation of a vast amount of descriptive information concerning the near-Earth space environment. Nevertheless, the complexity of the geophysical and space-plasma phenomena encountered has in most cases limited man's ability to understand the fundamental controlling physical processes at work in the Earth's ionosphere and magnetosphere. It has been recognized for some time that controlled experiments, such as those performed in Earth-bound laboratories, will also be required for definitive results in the physics of space plasmas.

The purpose of Space Experiments with Particle Accelerators (SEPAC) is to carry out active and interactive experiments on and in the Earth's ionosphere and magnetosphere. It is also intended to make an initial performance test for an overall program of Spacelab/SEPAC experiments. The instruments (Fig. II-1) to be used are an electron beam accelerator, magnetoplasma dynamic (MPD) arcjet, and associated diagnostic equipment. The accelerators are installed on the pallet, with monitoring and diagnostic observations being made by the gas plume release, beam-monitor TV, and particle-wave measuring instruments also mounted on the pallet. Command and display systems are installed in the module.

Three major classes of investigations are to be performed by SEPAC. They are vehicle charge neutralization, beam plasma physics, and beam-atmosphere interactions. The first two are mainly onboard plasma physics experiments to measure the effect of phenomena in the vicinity of Spacelab. The last one is concerned with atmospheric modification and is supported by other Spacelab 1 investigations as well as by ground-based, remote sensing observations (Figs. II-2 and II-3).

The purpose of the vehicle charge neutralization investigation is to evaluate quantitatively the feasibility of launching electron beams from Spacelab. If the ability of the ambient plasma to return electrons to the Spacelab does not equal the current emitted by the accelerator, then Spacelab will acquire an electrostatic potential. If this potential exceeds the beam energy, electrons will not be able to leave Spacelab and the accelerator will be shut off automatically.

A systematic examination of various plasma coupling processes will be performed with the beam plasma physics investigations. The injection of an electron beam into a plasma often results in interactions which modify the structure of the beam and its velocity distribution while generating a wide variety of plasma wave phenomena. The instabilities responsible for these effects are of technological interest because they may place limits on the accessible range of parameters for electron beams used in magnetosphere probing experiments. They are of scientific interest because they are manifestations of basic physical processes that occur in beam plasma interactions.

The purpose of the beam-atmosphere interaction investigation is to study mechanisms for the formation of auroras and the excitation of airglow. The physical and chemical processes involved in the formation of natural auroras are complex. The dynamic nature of the aurora and associated rapid changes in the input particle distributions have severely limited the ability to understand the aurora through passive experiments alone. An auroral input-output experiment wherein a stable beam of electrons with a narrow spread in energy and pitch angle is fired into the atmosphere is planned by SEPAC and should advance the understanding of auroral phenomena significantly. Artificial auroras produced by firing the electron beam accelerator upward into the magnetosphere will be used to search for electric fields parallel to the magnetic field in the auroral zone. In addition, atmospheric airglow excited by firing the MPD arcjet into the environmental plasma can be used to investigate the plasma beam spreading and motions across geomagnetic field lines.

The SEPAC instrumentation is divided into three subsystems: the accelerators; the monitor and diagnostic equipment; and the control, display, and data management subsystem.

The electron beam accelerator, MPD arcjet, and neutral gas ejector are contained in the accelerator subsystem. The electron beam accelerator is capable of operating at voltages from 1 to 7.5 kilovolts at a maximum of 1.5 amps and with a variable pulse width of from 10 milliseconds to 1 second. The MPD arcjet uses argon gas and has an energy input of 2 kilojoules per pulse. The third accelerator component is a neutral gas plume generator which uses nitrogen as the gas.

Monitor and diagnostic equipment to be used are a beam monitor television, a photometer, an energetic particle analyzer, plasma probes, wave and field detectors, an accelerator-functions monitor, a beam current monitor, and vehicle charging and return current monitors.

The SEPAC is to be operated by firing the accelerator or accelerators appropriate to the investigation being performed at a predetermined position in orbit and in a given direction with respect to the Shuttle and the geomagnetic field lines. Data are taken with the diagnostic instruments.

Some initial controlled experiments have been conducted in the magnetosphere using ground-based transmitters and rocket-borne particle accelerators. While the initial results have been extremely significant and encouraging, it is evident that these experiments must be done from a number of selected locations and under varying geophysical conditions. The orbiting Spacelab should allow the accomplishment of the necessary controlled experiments using techniques that have been developed in the rocket-borne experimental programs. The instrumentation described here comprises a portion of a total particle and plasma accelerator system that has been designed to meet the long-term needs of the Spacelab experimental program.

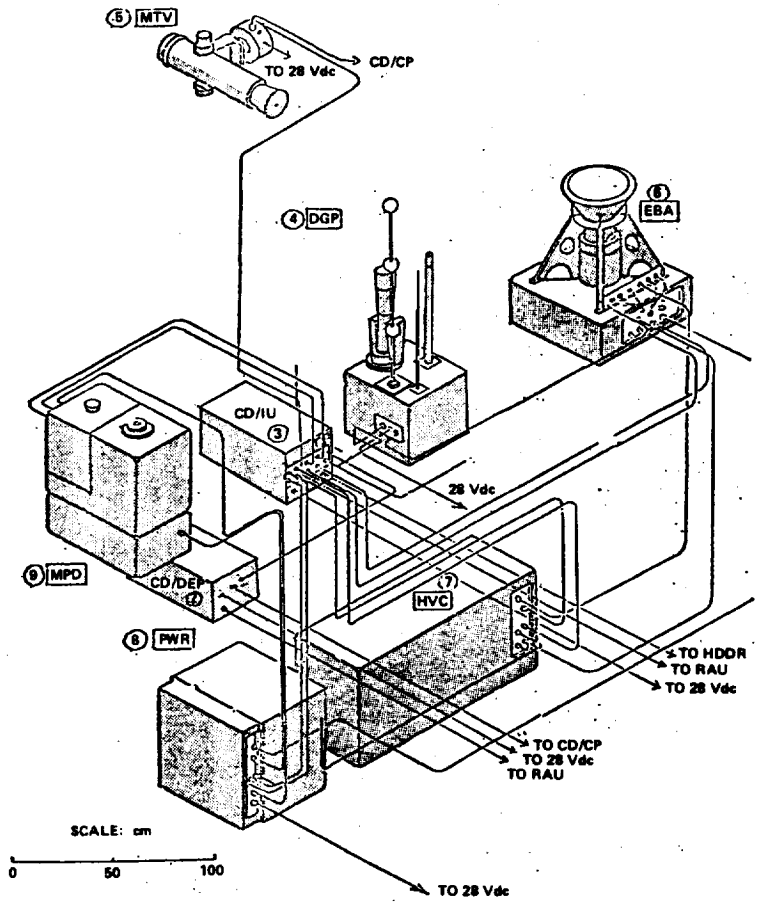


Figure II-1. Layout of SEPAC equipment.

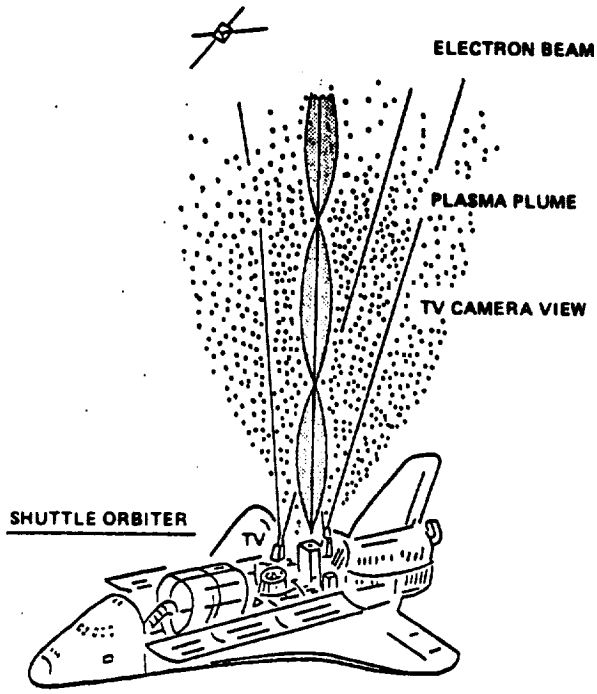


Figure II-2. SEPAC experiments in the vicinity of Spacelab: vehicle charge neutralization and beam plasma physics.

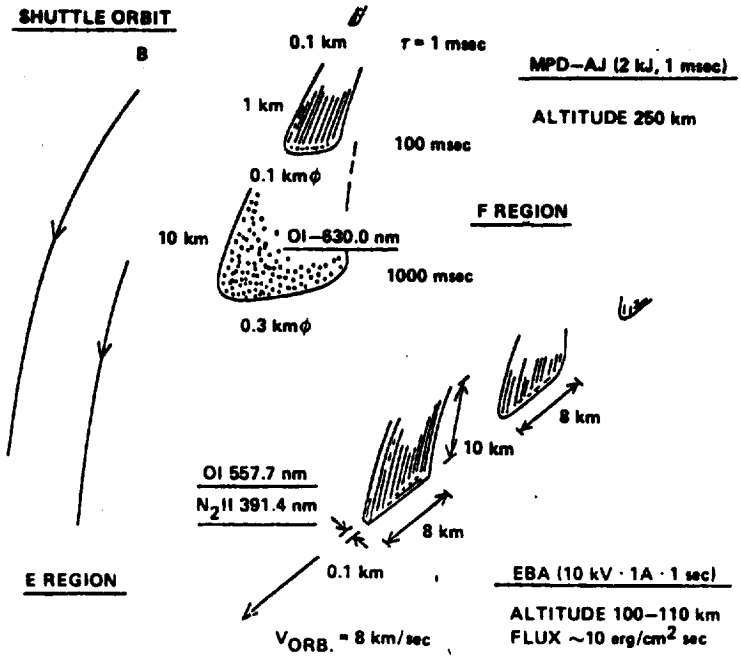


Figure II-3. SEPAC experiments on beam atmosphere interactions: artificial aurora/airglow excitations by EBA and MPD-AJ.

PHENOMENA INDUCED BY CHARGED PARTICLE BEAMS
(1ES020)

C. Beghin
CRPE/CNET/CNRS, France

This experiment is a forerunner for large and powerful particle injection experiments intended for future Spacelab flights. Among other applications in geoplasma physics, the injection of energetic particles along the Earth's magnetic field lines has been proposed as a remote sensing method to measure electric fields parallel to the magnetic field with good time resolution over the entire magnetic field. The measurement of the travel time back and forth to the point where the parallel velocity (for positive or negative particles) is reversed, combined with the known initial energies and pitch angles, leads to the knowledge of the parallel electric field position on a particular magnetic field line. There are many other possible interesting scientific applications of beam injection, such as artificial auroras and atmospheric studies. None of these ambitious objectives can be achieved fully at the present time without preliminary studies of special phenomena such as neutralization processes, return-current effects, dynamics of the beams, triggered instabilities, and waves.

Once these special phenomena have been investigated, the fundamental question about proper experimental conditions, such as energy, intensity and divergence of the beams, pitch-angle injection, ion species, proper probes and detectors and their location, and rendezvous conditions, will be resolved. The aim of this experiment is to provide a better understanding of these special physical processes and to provide some answers to questions concerning beam injection techniques.

Neutralization processes comprise the phenomena which naturally arise when high-intensity electron or ion beams are injected into the ionosphere. It is evident that one must know with a good accuracy the effective energy and pitch angle of the injected particles to study the interaction of the beam with the medium and to use the beam for geophysical measurements. This requires that the potential of the vehicle be known and that the question of neutralization by return current be well understood. Thus, the task of studying the physical processes involved in the neutralization of the vehicle is of prime importance, both for its own interest and to obtain sufficient information to make proper use of the beam.

Wave emissions have often been observed in association with active particle injection experiments. Not only are the processes responsible for the

production of the waves interesting, but they also represent a clue to the understanding of particle dynamics. Laboratory experiments have shown the existence of locally driven current instabilities (macroscopic drift instability) triggered by electrons and ion beams. The location of the plasma probe (and antennas) on Spacelab near the guns will allow a study of these instabilities.

Besides the beam-plasma interactions common to both electron and ion beams which govern their evolution during travel through the ionosphere and magnetosphere, the ion beams interact heavily with the ambient atmosphere along a significant part of their paths mainly via charge exchange reactions. This effect can be used to detect the reflected ion beam and measure the parallel electric field. One must note that little is experimentally known about charge exchange reactions of natural ions impinging on the atmosphere and that laboratory results are not abundant and often do not correspond to real ionospheric conditions. Thus, it is of interest to investigate the interaction of injected ions with the neutral atmosphere.

Optical measurements of the radiation emitted by neutral particles immediately after a charge exchange collision will be used. These measurements not only enable a determination of the charge exchange collision rate but will also indicate the lateral dimensions of the beam and, therefore, the conditions of its evolution during its path through the ionosphere.

The instrumentation (Fig. II-4) of this investigation consists of an electron gun, an ion gun, a plasma potential fluctuation probe, a suprathermal electron spectrometer, a return-current monitor, and an electron filter analyzer, all comprising the active package. A passive package contains a high-frequency antenna and plasma density fluctuation probe (both using the same probe), a low-frequency antenna and electron temperature probe (combined in the same probe), and an ac magnetic antenna. While the active package is mounted on the pallet, the passive package, when operating, will be mounted in the airlock.

The electron gun produces pulses of current up to 0.1 amp with electron energies up to 10 kiloelectron volts. The ion gun provides 10 milliamps of hydrogen ions up to 10 kilovolts. The antennas located in the airlock and separated from the gun will detect ac magnetic fields from 200 hertz and electrics fields up to 100 megahertz. The local plasma density and weak fluctuations associated with current-driven instabilities and wake will be measured by radio-frequency plasma probes. The particle detectors will monitor effects associated with the return current, and high time resolution could be used to correlate the particle flux with wave fields. These instruments will also monitor the environment of Spacelab. A microprocessor will be used to control the experiment and to correlate the gun pulses with the wave measurement sequences.

Active experiments using injection of electrons have been performed by the experiment investigators on rocket flights. A wealth of data has been obtained. Some results have not yet received an unambiguous explanation. Beam injection experiments from Spacelab with its advantages of long time in orbit and the variety of ambient plasma conditions offer a promising opportunity to add significantly to our knowledge of the Earth's magnetosphere.

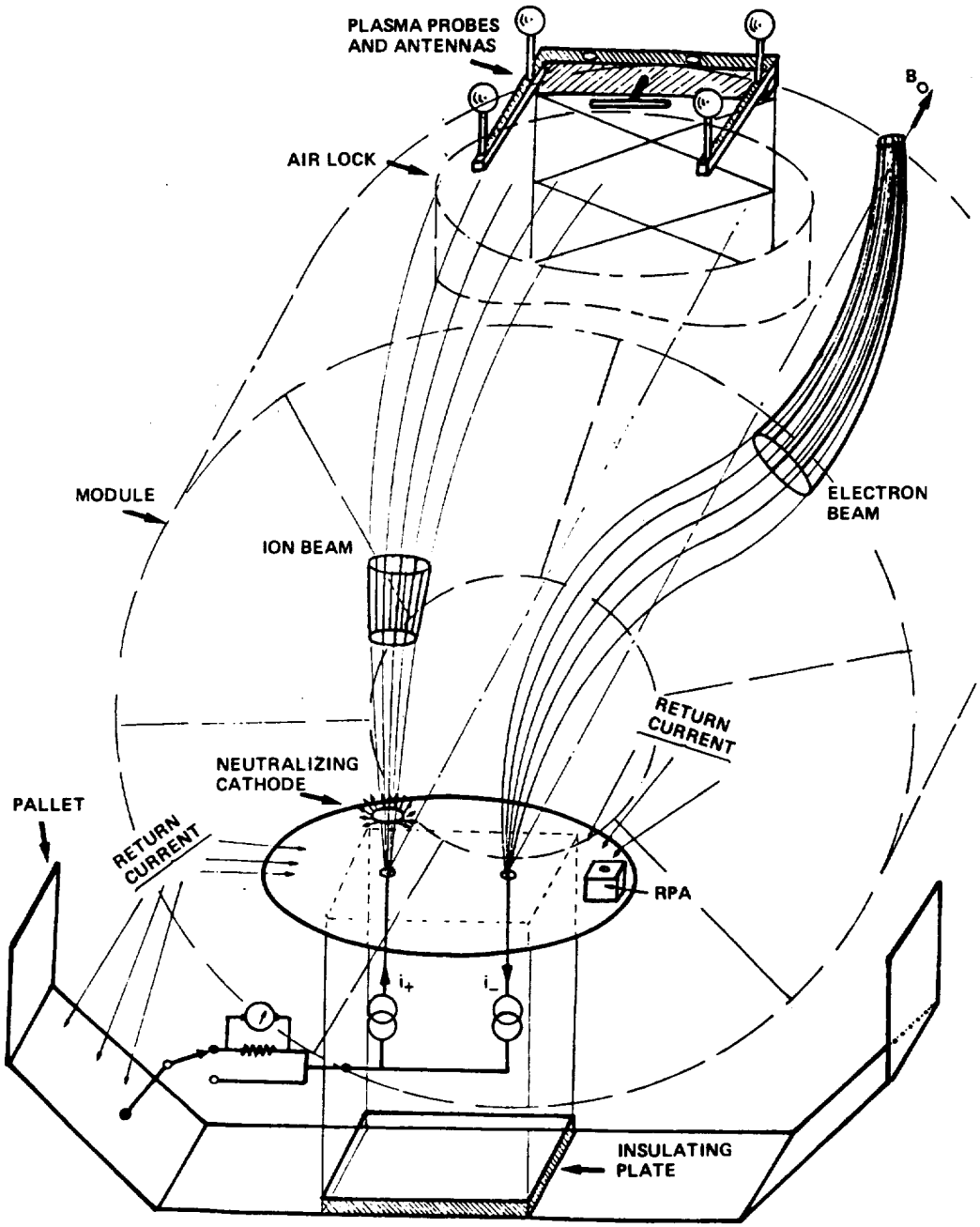


Figure II-4. Charged particle beam experiment schematic.

ATMOSPHERIC EMISSION PHOTOMETRIC IMAGING (1NS003)

S. B. Mende
Lockheed Palo Alto Research Laboratories, USA

The atmospheric emission photometric imaging experiment has five broad objectives: (1) the investigation of ionospheric transport processes by observing Mg^+ ions, (2) support of magnetospheric electron bounce experiments, (3) measurement of electron cross sections for selected atmospheric species, (4) the detection of small particle contamination, and (5) pilot studies of natural auroras.

Ionospheric transport processes involve global patterns of electric fields and neutral winds. Knowledge of ion motion is important to understand the cause-effect relationships on upper atmospheric dynamics. Recent observations show that there is an observable quantity of Mg^+ ions in the F region. The direct imaging of the resonance radiation of the Mg^+ ions would enable us to study these effects using the natural Mg^+ as the ionospheric "tracer" in the manner that Ba is used as an artificially injected tracer. Natural phenomena of interest which could be investigated by this technique are the mechanism of equatorial spread F formation, intertropical red arc ionization transport mechanisms, wind shear (sporadic E), electric field, and neutral wind drift motion.

For these observations, the Mg^+ resonance line will be imaged at 279.5 and 280.2 nanometers. Special visible blocking filters will be used to reduce any possible leakage through the filters at the visible wavelengths. Because of the ozone absorption, the Earth background should be dark at these wavelengths. However, narrowband filtering is still essential to minimize it. The simplest observation geometry is produced by viewing toward the ultraviolet terminator while the Orbiter is in darkness.

Particle and plasma accelerators on Spacelab 1 will fire particle beams into the magnetosphere to study interactions leading to artificial auroral excitation and wave generation and to determine particle trajectories for field tracing and measurement of magnetospheric electric fields. Central to the success of such a program is the ability to detect the low-light-level spots that will identify spatial and temporal beam interactions with the ionosphere. Support of these controlled active magnetospheric experiments is a prime objective of the proposed low-light-level television (LLLTV) system.

In conjunction with the electron beam experiment (SEPAC), an electron beam is shot downward or upward from the Spacelab. The electrons precipitate, either directly or after having been mirrored at the opposite hemisphere, causing artificial auroral emissions which will be detected by the LLLTV system looking down toward the Earth.

The objective of the "induced equatorial aurora" experiment is a measurement of several electron impact cross sections of atmospheric constituents. The experiment involves the ejection of an electron pulse on a magnetic equatorial crossing by the Orbiter and viewing the emission returning from the beam path with passive instruments from the Spacelab. The measurement results will include the effective excitation cross section for producing $O^+(^2P)$ and other atomic metastables from their atmospheric ground states. Pulsed afterglows will also permit a measure of the collisional deactivation rate for some of the highly quenched metastable states. For $O^+(^2P)$, simultaneous sensing of emissions having different emission probabilities (i.e., 731.9 and 247.0 nanometers) will provide a direct measure of total collisional deactivation at the altitude of observation.

One of the major concerns in the use of the Space Transportation System (STS) for astronomical observation is the possible presence of small particles in the vicinity of the spacecraft. The LLLTV will monitor the environment of the STS by directly observing the scattered light due to small particles.

Because of the offset of the geographic and geomagnetic poles, the 57 degree inclination orbit will provide auroral zone coverage. The nightside auroral zone extends down to an invariant latitude of 65 degrees, which is well within the Spacelab orbit of 57 degrees geographic latitude at two specific locations. Depending on the launch schedule, one or both of these locations will be in the nightside of the orbit. However, because of the relatively low frequency of the auroral overpasses, natural aurora investigations will be pilot observation programs in preparation for later STS missions with higher inclination orbits. Nevertheless, valuable information can be obtained on Spacelab 1. Investigations of natural auroral phenomena which will be performed are: (1) monitoring the extent and structure of the plasma sheet, (2) comparison of ultraviolet auroral features with visible forms, (3) coordinated particle and optical auroral observations, and (4) small-scale auroral morphological studies.

The equipment required for making the low light flux observations (Fig. II-5) at selected wavelengths consists of a dual-channel video system mounted on a stabilized two-axis gimbal system (mounted on the pallet) with associated

optics and data handling electronics. Similar optical systems consisting of sunshields, collecting optics, and filter wheels for both narrowband and broadband filters will be used with the two detection systems. One detector will consist of the LLLTV SEC vidicon with a microchannel plate-type intensifier for high-sensitivity, high-resolution operation. The field-of-view for this detector will be selectable to 6 or 20 degrees. The other detection channel will utilize a low-resolution (10×10 element) microchannel plate photon counting array with discrete anodes operating in a photon counting mode with a digital data handling and recording system. Its field-of-view will be fixed at 6 degrees.

The housekeeping information will be added to the TV data which will be processed by a video field memory for onboard inspection by means of a TV monitor. The data from the 100-element photon counting array will be multiplexed for transmission and displayed inside the Spacelab 1 module. The experiment controller controls all experiment hardware, enabling the payload specialist to aid in the control in an operator-interactive manner.

The LLLTV instrument is not limited to the investigations proposed herein. It is an instrument that is modular and evolutionary in nature. It will accommodate future programs in atmospheric, magnetospheric, and some astrophysical related sciences with minor system changes (filters, etc.) and offers evolutionary flexibility and growth to a rapidly developing image array technology.

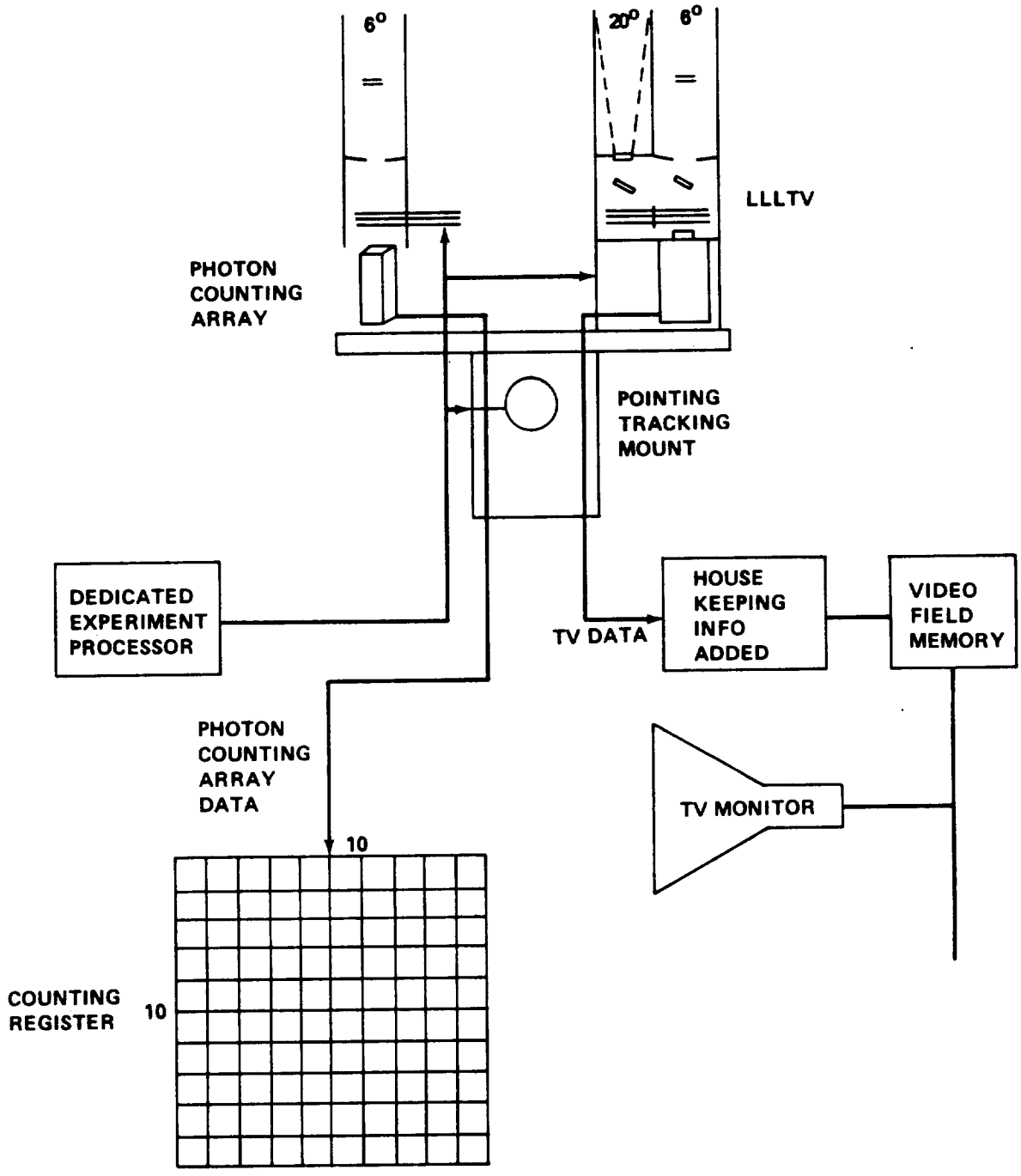


Figure II-5. Atmospheric emission photometric imager.

LOW-ENERGY ELECTRON FLUX AND ITS REACTION TO ACTIVE EXPERIMENTATION ON SPACELAB (1ES019)

K. Wilhelm
Max-Planck-Institut für Aeronomie, Germany

Sounding rockets and automated spacecraft have proven that the cause of the discrete aurora is the precipitation of low-energy particles, primarily electrons, into the atmosphere. Contrary to first expectations, the particles do not travel directly from the Sun into the atmosphere but are subject to complicated processes taking place in the magnetized plasma surrounding the Earth. Early hypotheses assumed that the magnetic field lines were equipotentials and that particles thus should not be influenced by electrostatic fields directed along the magnetic field. In recent years, however, many observations and theoretical arguments have indicated that this concept probably is not correct under all circumstances.

This experiment is intended as a forerunner of a method that will utilize artificially accelerated electrons as tracer particles for electric fields parallel to the magnetic field (E || B). This will be done by detecting fast echoes produced by electrons that have been injected by electron accelerators onboard Spacelab upwards along the field line and are subsequently reflected within a parallel electric field region. Only those beams with insufficient parallel energy to surmount the potential barrier will be reflected downwards, producing an echo. Measurements of the energy and the pitch angle dependence of the transit time of the echoes will provide information on the location of the potential barrier and the field strength.

The full achievement of the scientific objectives of the E || B experiment cannot be obtained on the first Spacelab flight because of the restrictions to be observed during the mission. Nevertheless, valuable preparatory investigations can be performed. These studies will concentrate on effects that are of importance either as means of detecting the echo beam or as causes of beam perturbations (e.g., spacecraft charging effects and electron background). The experiment will use electron accelerators as a tool to probe magnetospheric processes rather than to modify them.

The instrument will be capable of observing the natural electron flux in the energy range from 0.1 to 12.0 kiloelectron volts. These electrons are not only the main contributors to the excitation processes that lead to auroral light

emissions but are also carriers of electric currents and of kinetic energy that is deposited in the atmosphere. The experiment can also be utilized for observations relating to effects of the electron accelerator operation. High injected currents will lead to substantial spacecraft charging effects which can be investigated by observing the influence on natural electron fluxes. Differential spacecraft charging with and without accelerator operation can be investigated by observing the effects of the local electrostatic fields on the natural electron flux.

The detection of artificially injected electrons reflected at the potential barriers is possible only with instruments that can observe extremely anisotropic fluxes with high time resolution. Therefore, it is necessary to use a special detector capable of observing electron fluxes in a large field-of-view with directional resolution. This detector, when looking with its axis parallel to the magnetic field, is designed to detect particles in a 360 degree azimuthal range and will, in addition, provide a sweep of the viewing cone in an 80 degree pitch angle range. Thus, the instrument covers a field-of-view of almost 2π solid angle. It utilizes the direct detection method for low-energy electrons by means of continuous channel electron multipliers. It has to be pallet-mounted with little obstructing material within its viewing angle of half a sphere. Pitch angle and energy selection will be done by electrostatic deflection devices. A sketch of the cylindrically symmetrical instrument is shown in Figure II-6. The instrument and experiment parameters (e.g., energy and pitch angle sweeps) are commanded and controlled by a microprocessor. Data from the experiment and housekeeping data are transmitted to ground or recorded on the Spacelab data recorder.

For observing natural electron fluxes, the instrument has to be switched on at high-latitude portions of the Shuttle orbits. Internal energy and angle scans are the main features during this kind of operation. Typical cycle times at suitable geomagnetic location will be 10 minutes, during which detailed measurement of electron energy and pitch angle distribution functions will be performed. The need to work in conjunction with other instruments (e.g., electron accelerators, auroral television and magnetometer systems) is another aspect of the operation of this experiment requiring crew and computer assistance. This cooperation is essential for achieving the scientific objectives because the complexity of geophysical events can be studied only by an integrated approach.

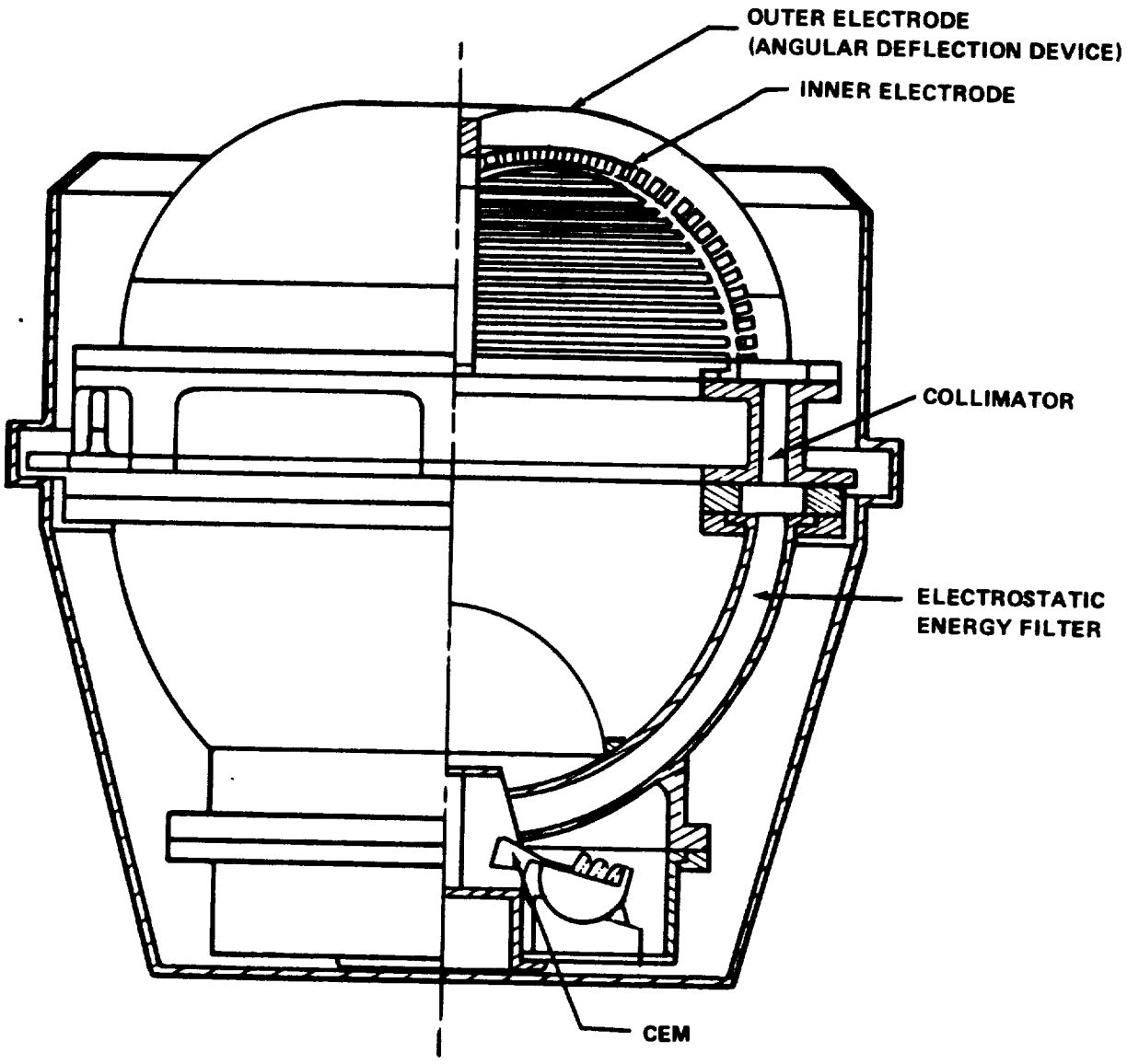


Figure II-6. Low-energy electron spectrometer with approximately 2π field-of-view. The schematic shows (from top to bottom) the angular deflection device as a toroidal electrostatic system, the collimator, the hemispherical electrostatic energy filter, and the continuous channel electron multipliers.

DC-MAGNETIC FIELD VECTOR MEASUREMENT (1ES019B)

R. Schmidt
Space Research Institute of the Austrian Academy of Sciences, Austria

The Earth's magnetic field can be depicted as a dipole field. Therefore, the flight direction of precipitating electrically charged particles will be dominated by the magnetic field vector. The motion of the particles, (e.g., electrons or protons) has three components: (1) a gyration around the field line, (2) an oscillation between mirror points, and (3) a drift around the Earth.

A problem which has not been clarified is the correlation between electric and magnetic fields in the magnetosphere. To contribute to the understanding of this problem, some experiments onboard Spacelab will make measurements on low-energy particles. This will be done in collaboration with other active and passive experiments on Spacelab. Under certain circumstances the electrons ejected by electron guns (accelerators) will be reflected by a potential barrier, and some of them will be subsequently detected by an electron spectrometer. If one measures the distance to the reflection point, then the electric field strength can be calculated if other parameters are known. An important parameter for calculation of the distance to the reflection point is the strength and direction of the local magnetic field. The basic requirement is to inject the electrons into the magnetic field with a well-known pitch angle and energy. This magnetic field will be composed of the Earth's field and an unknown spacecraft field. Therefore, the objective of the magnetometer experiment is to determine the local magnetic field by measuring the total of these two contributors. The measured field vector components are available to all onboard experiments via the Spacelab command and data management system.

The experiment consists of two parts, an electronic box and the magnetic field sensor. The sensor will include three independent measuring flux-gate magnetometers, each measuring one component. The physical background is the nonlinearity of the B-H curve of a ferrite material. Two coils wound around a ferrite rod are necessary. One of them, a tank coil, pumps the ferrite rod at approximately 20 kilohertz. As a consequence of the nonlinearity, many harmonics will be produced. The second coil (i.e., the detection coil) resonates to the first harmonic. If an unknown dc or low-frequency magnetic field exists, the amplitude of the first harmonic is a measure for the unknown magnetic field. The voltages detected by the sensors will be digitized and transferred to the command and data management system. The calculated B-field data are available for all other experiments.

It is planned to have the experiment functioning during the entire mission to achieve a very long duration of measuring so that the field strength can be mapped over large geographic and temporal areas.

ISOTOPIC STACK — MEASUREMENT OF HEAVY COSMIC RAY ISOTOPES (1ES024)

R. Beaujean
Institut für Reine und Angewandte Kernphysik der
Universität Kiel, Germany

The isotopic stack is designed to measure heavy cosmic ray nuclei with nuclear charge, Z, equal to or greater than 3. The stack consists of passive visual track detectors which remain sensitive throughout the entire mission. The scientific data are stored in latent tracks which are produced by heavy ions and which can be revealed in the investigator's laboratory after recovery. During the mission, only housekeeping data have to be collected.

The exposure onboard Spacelab 1 allows the study of two cosmic ray components:

1) The chemical composition and energy spectrum will be measured for particles which have energies in the range 20 to 100 million electron volts per atomic mass unit. These particles originate most likely from the solar wind. Such low-energy particles can be detected only outside the atmosphere and behind a minimum amount of shielding matter. In addition, a time resolving system enables one to determine after recovery the arrival time of the particles. Arrival times can be correlated with the orbital position of the Orbiter and, thus, to a position in the geomagnetic field. The Earth's magnetic field rejects all particles with rigidities pc/Ze (p = momentum; c = velocity of light; Ze = charge) less than a threshold value (geomagnetic cutoff) which varies along the orbit and can be calculated. Using the energy measurement obtained from the range of the track in the plastic detectors, the maximum possible charge of the particle for a given rigidity can be deduced. Thus, the existence of partially stripped particles can be verified — a point of great interest for theories explaining how particles propagate within the solar system.

2) The isotopic composition of heavy galactic cosmic rays with energies in the range 100 to 1000 million electron volts per atomic mass unit will be measured. These particles give information on the source, acceleration, and propagation of the cosmic rays. The exposure on the pallet of Spacelab 1 takes place under minimal shielding. Therefore, almost no disturbing background of fragmentation products is involved. Also, most of the particles can be correlated to the orbit position of the Orbiter by the previously mentioned time resolving system. Thus, "geomagnetically forbidden" cosmic ray particles can be observed by taking advantage of the decreasing geomagnetic cutoff with increasing latitude.

The experiment hardware is located on the pallet where it is mounted on a cold plate (Fig. II-7). The experiment weight is 20 kilograms; the physical dimensions are 50 centimeters diameter and 7 centimeters height. The field-of-view of the stack is 2π steradian solid angle.

The main stack for the measurement of the high-energy galactic cosmic rays consists of approximately 8 grams per square centimeter of types of plastic visual track detector sheets that have well-established response (cellulose nitrate and Lexan polycarbonate). It is housed in an aluminum container which provides structural support and thermal contact to the cold plate.

Approximately 20 detector sheets will be exposed on top of the main stack outside the container under minimal shielding to measure low-energy particles. Some layers of this top stack will be rotated to achieve a time resolution by measuring the angular displacement of the track segments with respect to the segments in the fixed part. This allows the correlation of arrival time of the particles with the orbital position of the Orbiter (i.e., a correlation between the particle and the geomagnetic cutoff).

On top, the total stack is sealed by a thin-coated polyester foil which provides a residual pressure for the detector foils and avoids environmental contamination due to outgassing. The position of the moving part is monitored by means of an angular encoder; the temperature on the top and bottom of the stack is measured by temperature sensors. The output data for position and temperature are periodically sampled after each step command. Each step command is generated by the command and data management system and initiates a small rotation step. Motor, encoder, gears, and electronic parts are housed in a small box which is fixed to the main aluminum container.

Heavy ions stopping in or passing through the plastic sheets of the stack produce latent tracks which can be revealed by chemical etching in the laboratory. Further analysis can be done under optical and electron microscopes by measuring the shape and length of the etched cones (Fig. II-8). These parameters strongly depend on the energy loss along the trajectory of the incoming particle. The nuclear charge and mass determination is based on the cone length versus residual range method, which is equivalent to a multiple dE/dx-E method.

Plastic track detectors have registration thresholds which make the detector system insensitive to electrons and protons; therefore, they do not produce any background. Plastic material with different registration thresholds is used to obtain an optimum mass resolution for the different nuclear charge regions. The applied technique is capable of detecting isotopes separated by approximately 0.5 atomic mass units.

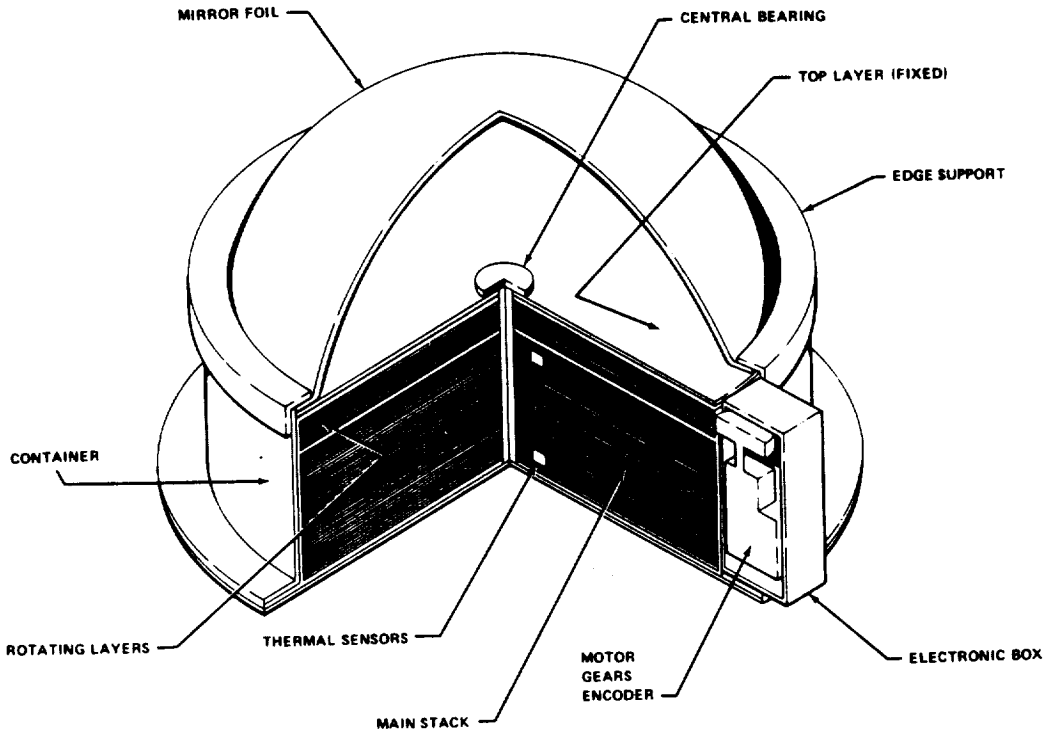


Figure II-7. Sketch of isotopic stack (not to scale).

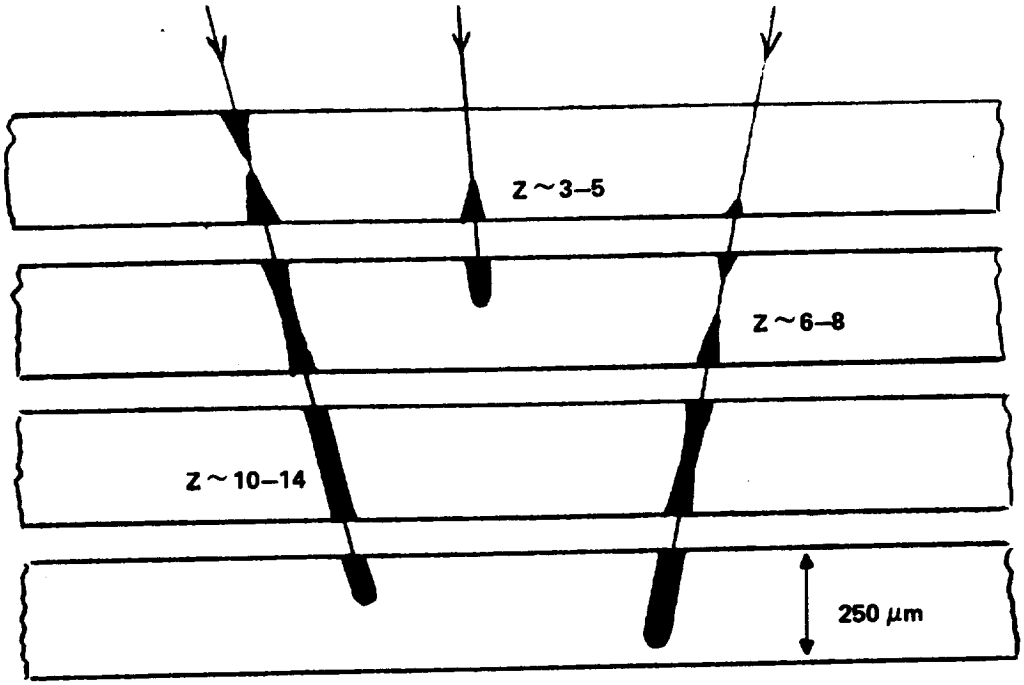


Figure II-8. Image of different stopping heavy nuclei in plastic track detectors after etching (not to scale).

STUDIES OF THE IONIZATION STATES OF SOLAR AND GALACTIC COSMIC RAY HEAVY NUCLEI (1NS004)

S. Biswas
Tata Institute of Fundamental Research, India

Cosmic ray nuclei of galactic origin have been studied during the past 20 years and energetic solar nuclei during the past 15 years in an attempt to understand the characteristics of their sources and the nature of their acceleration processes. Until recently the chemical composition and energy spectra of these nuclei were determined only for energies equal to or greater than 50 million electron volts per atomic mass unit. Recent studies at lower energies indicate that the charge and energy distribution of low-energy cosmic rays are different from that of high-energy cosmic rays. Observations of the flux of medium nuclei (C, N, O) at 10 million electron volts per atomic mass unit appear to indicate that the nuclei may be partially ionized in contrast to high-energy nuclei which are completely ionized; i.e., all electrons are stripped from the nucleus. The origin of this new component of cosmic rays in unknown.

Enhancement of abundances of heavy nuclei (e.g., Mg, Si, and Fe) at low energies relative to solar photospheric abundances and anomalously high abundances of iron relative to oxygen nuclei at low energies were recently discovered in solar energetic particles studied at low energy. These phenomena are not understood at present. It is believed that they are probably related to the partly ionized states and acceleration processes.

The proposed experiment is designed to study the recently discovered anomalous component of low-energy galactic cosmic ray ions of C, N, O, Ne, and Ca to Fe of energy 5 to 100 million electron volts per atomic mass unit in regard to their ionization states, composition and intensity, and to study the ionization states of heavy elements from oxygen to iron in energetic solar particles emitted during flare events. The same detector system will serve for both studies, with the second objective being given priority if there are any solar particle events during the mission.

The detector system (Fig. II-9) consists of stacks of thin sheets of special plastics such as cellulose nitrate (CN) and lexan polycarbonate which are efficient low-noise detectors for heavy nuclei. The stacks are in the shape of a cylindrical module with a diameter of 40 centimeters and a height of approximately 5 centimeters. There are two distinct stacks, a major lower stack (5 centimeters thick) which is slowly rotated at the rate of 4 degrees per hour with respect to a thin, fixed upper stack (0.5 centimeter thick) with a separation of 0.05 centimeter.

An energetic particle entering through the top stack and stopping in the bottom stack leaves a damage trail along its path that can be revealed optically by a suitable chemical treatment in the laboratory. The identity and energy of the particle can then be determined from measurements on the geometry of the tracks and the range traversed in the stack. Also, by identifying the segments of the same track in the top and bottom stacks, the arrival time of the particle can be determined from the displacement between the segments. The arrival time can be measured to the nearest 20 seconds in the present design, and this coupled with the arrival direction gives the lower bound on the magnetic rigidity (momentum/effective charge) of the particle as determined by the Earth's magnetic field configuration. Thus, the combined information permits the determination of the particle's charge state.

The structure housing consists of an approximately cylindrical enclosure of approximately 44 centimeters diameter and 25 centimeters height, the top of the enclosure being covered by a thin spherical shell of aluminum. Inside the housing a high-resolution stepper motor rotates the lower detector stack with respect to the fixed upper one in steps of approximately 40 arc seconds once in 10 seconds, so that full 360 degree rotation is completed in 90 hours. The rotation history of the detector stack is recorded and monitored with a 15 bit optical absolute shaft angle encoder. The instrument enclosure is maintained at one-tenth atmospheric pressure. The operation of the instrument is controlled by the onboard experiment computer through a Spacelab provided remote acquisition unit. Thermal control of the instrument is provided by the pallet cold plate on which the instrument is mounted and by a reflective coating on the outer surface.

The information obtained is of two kinds. One, which is telemetered to the ground together with time and Spacelab attitude vectors, is the output of the angular motion of the shaft angle encoder. The other is the data obtained from the measurements on particle tracks in the detectors with optical microscopes. Analysis of these data is carried out for identifying nuclear charge and energy using an interactive program package employing graphic displays. Combining this information allows the determination of ionization states of solar and galactic cosmic ray heavy nuclei of 5 to 100 million electron volts per atomic mass unit energy.

The direct measurements of the charge state of low-energy heavy ions are crucial to the understanding of new particle phenomena observed by the present investigator on Skylab and by several investigators on other satellites. Information on the ionization states of solar heavy nuclei which may be provided by this experiment (depending on the occurrence of solar flares) is of immediate interest in the understanding of the acceleration and confinement of energetic nuclei in the Sun.

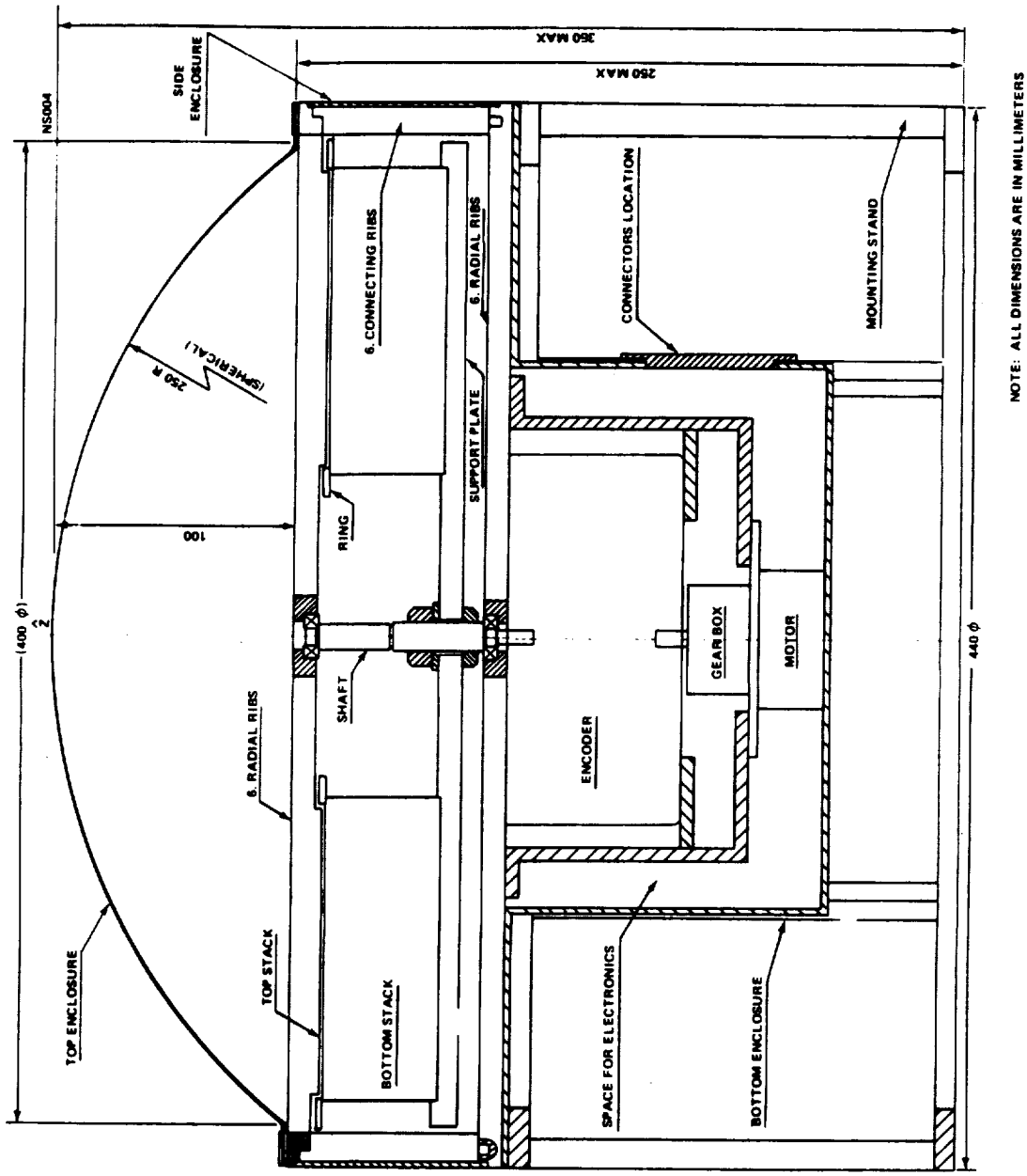
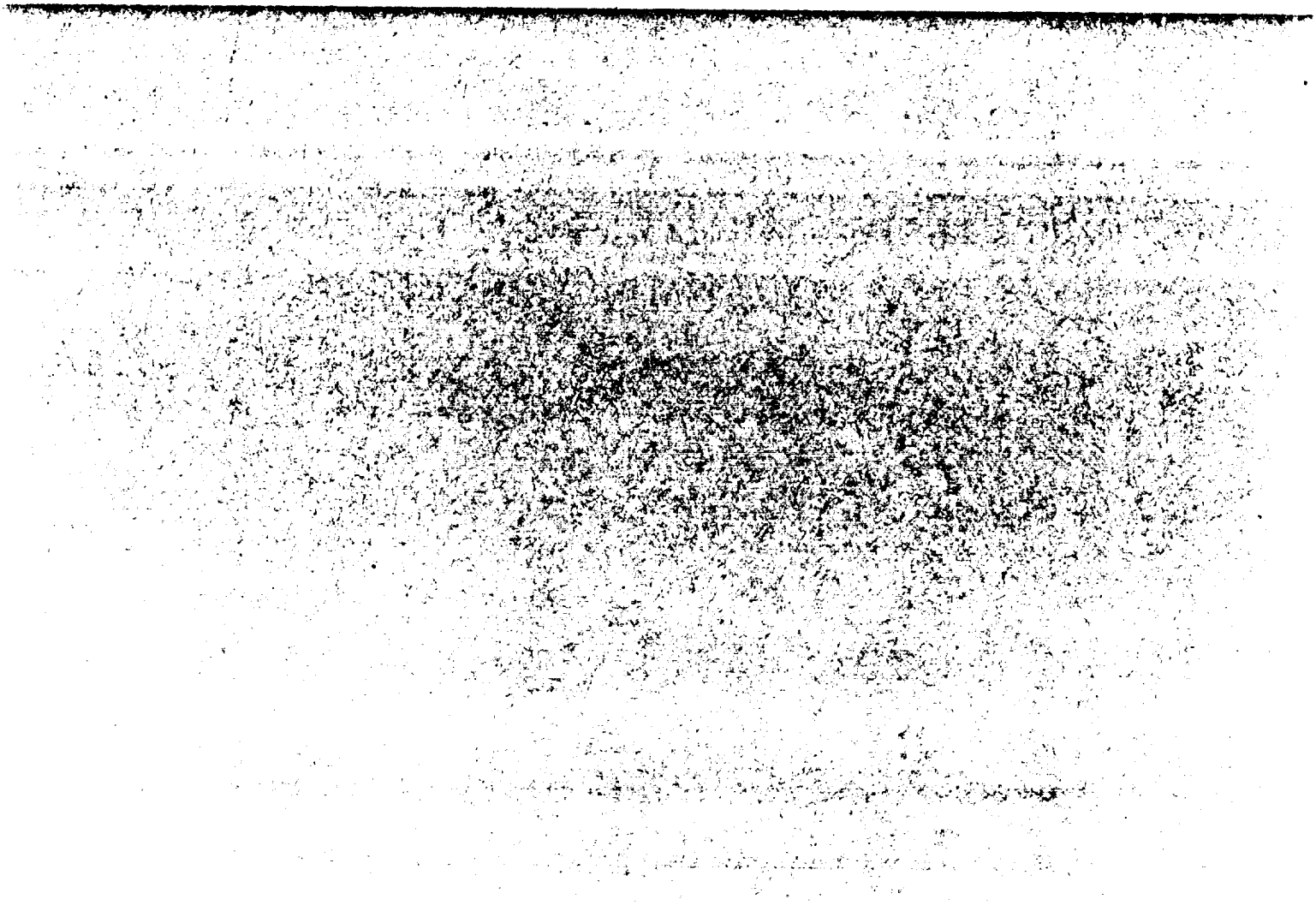


Figure II-9. Sketch of the detector assembly (sectional view).

SECTION III

MATERIAL SCIENCES AND TECHNOLOGY





MATERIALS SCIENCE
(1ES300)

U. Huth, ESA Headquarters, France

Y. Malmejac, CEA, France

L. Napolitano, University of Naples, Italy

and

H. Weiss, University of Erlangen, Germany

The materials science facility for the first Spacelab payload includes 36 different experiments. Whereas most of these experiments will be performed with the help of multiuser facilities (e.g., furnaces), there are seven experiments which require special equipment (autonomous experiments). All the hardware, with the exception of two elements (covering three experiments), will be integrated in a Spacelab double rack called the "Materials Science Double Rack" (MSDR).

The payload experimental facilities are intended to meet two main objectives: (1) to perform, during the first Spacelab mission, a number of significant pilot experiments in the fields of crystal growth, fluid physics and metallurgy, and, at the same time, to flight-verify the materials science hardware items developed (e.g., various furnaces, process chambers, etc.), and (2) to make a significant contribution to the establishment of a materials science equipment pool, which will be an important feature of the future program.

The first materials science payload will include the following categories of hardware: (1) multiuser facilities, (2) common-support equipment, and (3) a number of autonomous experiments.

Facilities

The Isothermal Heating Facility (Fig. III-1) is a multiuser facility for different types of experiments, including solidification studies, diffusion fundamentals, casting of metals and composites, and preparation of new and/or improved glasses and ceramics.

The material to be investigated must normally be placed in cartridges. To allow simultaneous heating and cooling of two different samples, a cooling and a heating chamber are provided. The samples in the cartridges which are attached to the sample holder will remain stationary during the entire performance, whereas the heating and cooling parts of the furnace can be moved.

The heating facility can be equipped with an acoustic mixing device or an acoustic positioning device. The atmosphere in the furnace can be helium or vacuum and in the cooling chamber helium or air. Technical data for the Isothermal Heating Facility are given in Table III-1.

TABLE III-1. TECHNICAL DATA FOR THE ISOTHERMAL HEATING FACILITY

Operating Temperature:	200 to 1600°C
Measurement Accuracy:	±5°C (at 250°C)
	±10°C (at 1500°C)
Accuracy of Adjustment:	±5°C
Isothermal Zone Dimensions:	100 mm in length, 40 mm in diameter
Temperature Gradient in Isothermal Zone:	0.5°C/cm
Operating Pressure (Minimum):	10^{-2} N/m^2
Operating Pressure (Maximum):	1.2×10^5 N/m^2
Operating Atmosphere:	Vacuum or helium
Heating rate for a standard nickel sample in the 20 to 1250°C range:	60°C/min
Maximum Sample Dimensions:	40 mm diameter × 100 mm

The Gradient Heating Facility I for Low Temperatures is defined to be a multipurpose facility for different types of experiments (e.g., crystal growth, unidirectional solidification of eutectics, etc.).

The furnace (Fig. III-2) allows for parallel injection of three cartridges which can be heated with three heating elements which are independently controllable, so that a variety of temperature profiles (also isothermal) can be achieved. Thermal insulation is provided by axial heat shields, a low conductivity radiation shield, multifoil insulation, and an outer protective shield.

Vacuum and noble gas supply provisions are part of the facility. Quenching can be obtained by purging the furnace with helium. Table III-2 gives technical data for this facility.

TABLE III-2. TECHNICAL DATA FOR THE GRADIENT HEATING FACILITY I FOR LOW TEMPERATURES

Volume: for 3 cartridges of 275 mm length, 25 mm diameter
Maximum Temperature: 1200°C on the cartridge
Gradient: up to 100°C/cm
Maximum Heating Rate: 1.5 h to reach 1200°C
Cooling Rate: from 1200°C to 50°C achievable in 4 h (fastest rate) or up to 20 h (slowest rate)

The Mirror Heating Facility is an experimental facility which is particularly suitable for investigating crystal growth using the melt zone or traveling solvent methods.

This facility consists of an optically heated zone furnace and ancillary devices (e.g., a pulling and turning device). The key elements of the zone furnace are two ellipsoidal mirrors with coincident optical axes and a common focus (Fig. III-3). Halogen lamps acting as heat sources are located in the other two foci. The actual space for samples (the melt zone) is located at the common focus. Samples can be inserted here by means of two holders perpendicular to the optical axis. Two viewing ports are provided for optical monitoring and pyrometric temperature measurement or control. Table III-3 lists the technical data for the Mirror Heating Facility.

The Fluid Physics Module, which is being developed for the first Spacelab payload, serves a variety of scientific objectives in the field of fluid phenomena, fluid physics in its widest sense.

The Fluid Physics Module (Fig. III-4) consists mainly of a structure fitted with two discs which can be rotated separately, at the same or different speeds, and in either direction. A "floating zone" will be set up either on one of the discs or between the two.

TABLE III-3. TECHNICAL DATA FOR THE MIRROR HEATING FACILITY

Maximum Sample Diameter: 20 mm
Zone Length: 10 to 20 mm
Maximum Growth Length: 110 mm
Maximum Feed Length: 150 mm
Minimum Turn Velocity: 0.1/min
Maximum Turn Velocity: 10/min
Minimum Feed Velocity: 10^{-3} mm/min
Maximum Feed Velocity: 10 mm/min
Maximum Variation for Turn and Feed for One Run: 1:20
Operating Temperature Range: 200 to 2100°C depending on sample diameter and material
Temperature Setting Accuracy: ±5°C
Temperature Constancy: ±0.5°C
Atmosphere: Vacuum or Helium
Operating pressure (minimum): 10^{-2} N/m^2
Operating pressure (maximum): 1.2×10^5 N/m^2
Heat-Up/Cool-Down Rates: Selectable, very fast rates possible

One of the discs can be moved axially (liquid injection side). The amount of liquid injected and the dimensional features of the floating zone are controlled by the combined movement of this disc and the tank which is fitted on a second slide independent from the first.

The opposite disc can move laterally and vibrate axially at different vibration frequencies and amplitudes. Temperature gradients and differences in electric potential can be set up between the two discs. The liquid tapped from the tank operates in an air-tight test chamber.

Two of the "auxiliary systems" which are an integral part of the Fluid Physics Module are as follows:

1) Visualization System — Detects the shape and size of the floating zone as well as local speed of the operative fluid. For detecting the fluid motion range, a duplicate filming system has been adopted (i.e., one at right angles to the lighted meridian plan for recording the shape and speed in the meridian

plane and one along the axis of rotation for recording speed in a plane at right angles to the axis).

2) Air-Circulation and Liquid-Recovery System — Cleans out the test chamber if the floating zone is broken and also controls temperature and moisture inside the chamber.

The form and diameter of the end plates may be modified according to the experiment objectives. Even special containers can be mounted, rotated, etc., with the help of the end plates. Different fluids with or without tracers can be used. Data describing this facility are given in Table III-4.

TABLE III-4. TECHNICAL DATA FOR THE FLUID PHYSICS MODULE

Test Volume (Zone):	130 mm maximum height, 100 mm maximum diameter
End Plate Diameters:	40 and 60 mm at injection side; 40, 60, and 100 mm at opposite end
Rotation Speed of End Plates:	5 to 100 rpm ±1% or ±0.1 rpm (separate operation possible)
Rotation Axis:	Parallel within 0.01 degree
Liquid Injection Speed:	0.5 to 6 cm^3/sec
Tank Capacity:	1.3 liters
Oscillations:	0.1 to 2 Hz, 0.05 to 0.5 mm amplitude
Lateral Offset:	Preset steps of 0.1 mm to a total of 2 mm
Heat-up Capabilities:	Up to 60°C (both end plates)
Electrical Potential:	±100 Vdc at one end plate
Photographic Recording:	Dual system with 16 mm cine-camera plus 16 mm cine-camera or 35 mm still camera
Resolution:	0.03 mm for cine-camera; 0.012 mm for still camera
Visualization of Inner Flow:	Solid tracers envisaged

The "common-support equipment" comprises a central control console, vacuum control, noble and inert gas supply, liquid coolant, special power supplies, acceleration and pressure measurement, workbench, and sample storage.

The autonomous materials science experiments are individual, black-box type experiments which, in general, require only the provision of power, data, and heat rejection. They do not need other facilities or commom-support equipment and will normally be developed by the experimenters themselves.

Experiments

Space material sciences (also called space processing) cover a variety of fields which have as a common bond the fact that the physical mechanisms involved are adversely affected on Earth by the presence of gravity. The sciences include crystal growth, metallurgy, fluid physics, glass and ceramics technology, and electrophoretic separation. (Table III-5 lists all the material science experiments on the first Spacelab mission.) Absence of gravity is the main advantage that space systems offer for these disciplines. In addition, use can be made of the unlimited pumping capability offered by the space environment.

Crystal growth in space is characterized by the microgravity environment which means, in the ideal case, the absence of gravity-induced convection. It is expected that semiconductor crystals can be grown with a degree of perfection and chemical homogeneity not otherwise obtainable. Model substances such as InSb for fundamental studies and technically important crystals such as silicon have been chosen to clarify the nature and effect of convection currents. Use is also made of the possibility that the near gravity-free environment allows crucible-free zone melting of materials without decomposition and negligible vapor pressure. These experiments will, in general, study the influence on crystal growth of factors such as the presence of a container, nucleation conditions, convection, and diffusion. The purpose is to improve the desired properties of the crystals. Improvements are obtained, for example, by improving the homogeneity and lowering the defects in a crystal, by an improvement in the homogeneity of dopant distribution, or by just growing large single crystals (e.g., crystals of proteins like 2β hemoglobin and β-galactosidase).

The large number of metallurgy experiments selected for the first Spacelab mission fall into several categories. One category concerns the solidification of immiscible alloys (i.e., systems containing a liquid-phase miscibility gap). The possibility exists that materials that are immiscible on Earth can be processed in space to make products with unusual structures and properties. Typical immiscible alloy systems chosen for the first mission are AlIn, AlPb, and ZnPb.

TABLE III-5. MATERIAL SCIENCE EXPERIMENTS OF THE FIRST SPACELAB MISSION

Experiment Number	Title	Experimenter
Experiments Using the Isothermal Heating Furnace		
1ES301	Solidification of Immiscible Alloys	Prof. H. Ahlborn, Universität Hamburg, Germany
1ES302	Solidification of Technical Alloys	Dr. D. Neuschütz, F. Krupp GmbH, Germany
1ES303	Skin Technology	Dr. Sprenger, Maschinenfabrik Augsburg-Nürnberg AG, Germany
1ES304 1ES305	Vacuum Brazing	Dr. Wycisk, Bundesanstalt für Materialprüfung, Germany Prof. R. Stickler, University of Vienna, Austria
1ES306	Emulsions and Dispersion Alloys	Dr. Poeschel, Battelle-Institut e. V., Germany
1ES307	Reaction Kinetics in Glass	Prof. H. G. Frischat, Technische Univeristät, Germany

TABLE III-5. (Continued)

Experiment Number	Title	Experimenter
1ES308	Composites (He-Glass)	Dr. H. M. Rosenberg, University of Oxford, United Kingdom
1ES309	Metallic Emulsions AlPb	P. D. Caton, Fulmer Research Institute Ltd., United Kingdom
1ES310	Fibre and Particle Composites	P. G. Cappelli, Centro Ricerche FIAT, Italy
1ES311	Bubble Reinforced Materials	P. Gondi, Istituto di Fisica dell' Università, Italy
1ES312	Nucleation Behaviour of Ag-Ge	Dr. Y. Malmejac, CEA — DMECN, France
1ES313	Solidification of near Monotectic ZnPb Alloys	Prof. H. Fischmeister, Montan University, Austria
1ES314	Dendrite Growth and Microsegregation	Dr. H. Fredriksson, The Royal Institute of Technology, Sweden
1ES315	Composites with Short Fibres and Particles	Prof. Deruyttere, Université Catholique de Louvain, Belgium

TABLE III-5. (Continued)

Experiment Number	Title	Experimenter
Experiments Using the Low Temperature Gradient Furnace		
1ES316 1ES317	Unidirectional Solidification of Al-Zn, Al-Al_2Cu, Ag-Ge Eutectics	Dr. C. Potard/ Y. Malmejac, CEA — DMECN, France
1ES318	Growth of Lead Telluride	Mme. H. Rodot, CNRS Laboratoire d' aérothermique, France
1ES319	Unidirection Solidification of Eutectics (InSb-NiSb)	Prof. H. Weiss, Universität Erlangen, Germany
1ES320	Thermodiffusion in Tin Alloys	Dr. Y. Malmejac CEA — DMECN, France
Experiments Using the Mirror Furnace		
1ES321	Zone Crystallization of Silicon	Prof. R. Nitsche, Kristallographisches Institut der Universität, Germany
1ES322	Traveling Solvent Growth of CdTe	Dr. H. Jäger, Battelle Institut e.V., Germany
1ES323	Travelling Heater Method of III — V Compounds (InSb)	Dr. K. W. Benz/Prof. Weiss, Universität Stuttgart, Germany

TABLE III-5. (Continued)

Experiment Number	Title	Experimenter
1ES324	Crystallization of Silicon Spheres	Dr. Kölker, Consortium für Elektrochemische Industrie GmbH, Germany
1ES325	Unidirectional Solidification of Cast Iron	Ir. T. Luyendijk, Laboratorium voor Metaalkunde, The Netherlands
Experiments Using the Fluid Physics Module		
1ES326	Oscillation Damping of a Liquid in Natural Levitation	Mne. H. Rodot, CNRS Laboratoire d'aérothermique, France
1ES327	Kinetics of Spreading of Liquids on Solids	Dr. J. M. Haynes, University of Bristol, United Kingdom
1ES328	Free Convection in Low Gravity	Prof. L. G. Napolitano, Università degli Studi, Italy
1ES329	Capillary Surfaces in Low Gravity	Dr. J. F. Padday, Kodak Limited, United Kingdom
1ES330	Coupled Motion of Liquid-Solid Systems in Near Zero Gravity	Dr. J. P. B. Vreeburg, National Aerospace Laboratory NLR, The Netherlands
1ES331	Floating Zone Stability in Zero Gravity	Prof. I. Da Riva, Ciudad Universitaria, Spain

TABLE III-5. (Concluded)

Experiment Number	Title	Experimenter
Single Experiments Using Special Equipment		
1ES332 1ES333	Organic Crystal Growth	Dr. K. F. Nielsen, Technical University of Denmark, Denmark
	Growth of Manganese Carbonate	Prof. A. Authier, Université Pierre et Marie Curie, France
1ES334	Crystal Growth of Proteins	Dr. W. Littke, Chemisches Laboratorium der Universität, Germany
1ES335	Self- and Interdiffusion in Liquid Metals	Dr. Kraatz, Technische Universität, Germany
1ES338	Growth of HgJ_2 Single Crystals	Dr. C. Belouet et al., Laboratories d' Electronique et de Physique Appliquée, France
1ES339	Interfacial Instability and Capillary Hysteresis	Dr. J. M. Haynes, University of Bristol, United Kingdom
1ES340	Adhesion of Metals UHV Camber	Prof. G. Poletti, C.I.S.E., Italy

Another category of interest for space processing is isotropic composite materials, which are produced by homogeneous dispersion of short fibers and/or particles in a molten matrix metal. It is expected that in space homogeneous distributions and large numbers of hard particles in the molten matrix of, for example, high-conductivity material for electrical contacts can be achieved. Examples of composite material experiments selected for the first Spacelab flight are Al_2O_3 powder and fibers (SiC) in Al and in a Cu-matrix material.

In the field of growth of eutectic alloys, advantages may be expected from the space environment because eutectic materials under conditions on the ground include a great number of defects which have been attributed to convection movements in the liquid phase. In general, the solidification process in space should be more regular, leading to a better structure which determines the properties of the solidified alloy. Initial experiments will be made with Al-Al_2Cu and AgGe eutectic alloys.

It is also intended to study the possibility of a controlled unidirectional solidification of an AlZn vapor emulsion having a fine regular dispersion of voids. Under normal gravity conditions (i.e., 1-g) there is a very low stability of the gas-liquid emulsion caused by the gravity field.

Another experiment concerns the unidirectional solidification of Te-doped InSb-NiSb eutectics in which the NiSb needles grow perpendicular to the phase boundary liquid solid. Since both length and direction of the NiSb needles and the distribution of the dopant are influenced by gravity, it is expected that the space-grown material will show superior properties.

An experiment of practical interest is the gas turbine blade investigation which has the objective of improving the mechanical properties at high temperatures. The blades based on directionally solidified eutectics of chromium alloys are coated with a thin refractory layer by plasma spraying, chemical vapor deposition, and cementation. In space the turbine plate will be remelted and solidified without changing the blade geometry.

Two diffusion experiments also have been selected for the first mission of Spacelab. In microgravity in the absence of convection the thermodiffusion will become very important due to larger temperature gradients and will result in composition changes (called Soret effect). In space it will therefore be much easier to measure the thermodiffusion parameters and their temperature dependence. The study will be performed on Sn+Sb, Sn+In, and Sn+Ag systems.

One of the diffusion experiments concerns the self- and interdiffusion in liquid metals. This self-diffusion experiment will help to determine which of the current theories of diffusion in liquids (quasi-crystalline fluctuation and critical volume) is correct. On Earth, one is unable to decide which of the current theories is the most probable because the accuracy of measurements is limited by the unavoidable convection.

The objective of another experiment is to investigate how the characteristics of mating surfaces affect adhesion and friction as well as to discriminate between the relevant mechanical and chemical mechanisms. The aim of this experiment is to obtain information about the field of force of atoms at an interface.

The only glass experiment on the first Spacelab mission concerns the investigation of reaction kinetics in glass melts. On Earth a separation of mass transport due to diffusion and due to convection is not possible. Microgravity conditions will be used to enlarge the range of temperatures within which undisturbed diffusion experiments can be realized. Since silicate systems (Na_2 0.3 SiO_2/Rb_2 0.3 SiO_2) are important for both glass and ceramic technology, binary alkali-silica systems have been chosen for the experiments.

The Fluid Physics Module will be used to study several phenomena connected with the hydrodynamics of floating liquid zones. Floating zone techniques are widely used to avoid container contamination in crystal growth in terrestrial laboratories. The maximum stable length of a vertically suspended liquid zone is determined by the balance between the surface tension forces and the hydrostatic pressure on Earth. In the microgravity environment of space the constraints imposed on the length of a zone and the buoyancy-induced convection are strongly reduced, which renders the zone more accessible than on Earth.

One investigation will study the adhesion between phases (liquid/solid) in the absence of electric and magnetic forces. Since the forces (van der Waals forces) involved in adhesion and cohesion fall off very rapidly with distance, gravitational forces mask all attempts to study these forces in larger macroscopic systems in experiments conducted on Earth. In the Fluid Physics Module experiment it is intended to study the properties of a liquid bridge zone between the two solid discs (end plates) of the module. From the shape of the liquid bridge the interaction forces will be derived and the critical point at which the bridge becomes unstable will be determined.

A related experiment will study the kinetics of spreading of liquids on solids. The objective is to study the flow of a liquid in response to forces generated at the nonequilibrium line of intersection of a liquid/vapor interface with a plane solid surface. In microgravity it is feasible to study large systems in which the curvature effects are small and fluid flow is predominantly driven by movements of the contact line.

Another Fluid Physics Module experiment will study coupled motions of liquid-solid systems in microgravity. Coupled motions represent an unsolved classical problem in analytical mechanics. The experiment uses a number of differently shaped containers partially or completely filled with liquid. The containers will be fixed to one end plate and the Fluid Physics Module system will be used to excite the liquid motion by spinup from rest and by forced vibration sweeps. The internal liquid motions and the free-surface behavior will be examined.

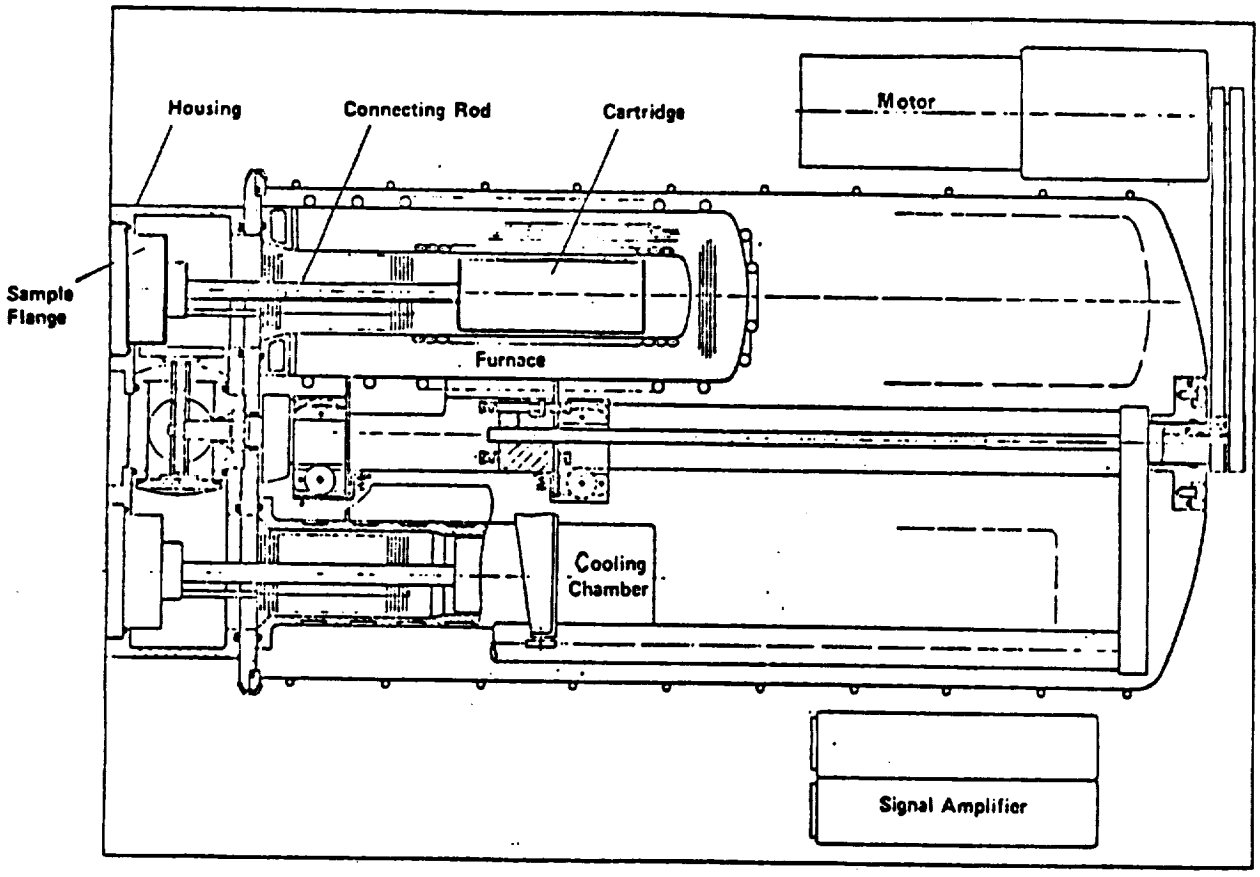


Figure III-1. Schematic of Isothermal Heating Facility.

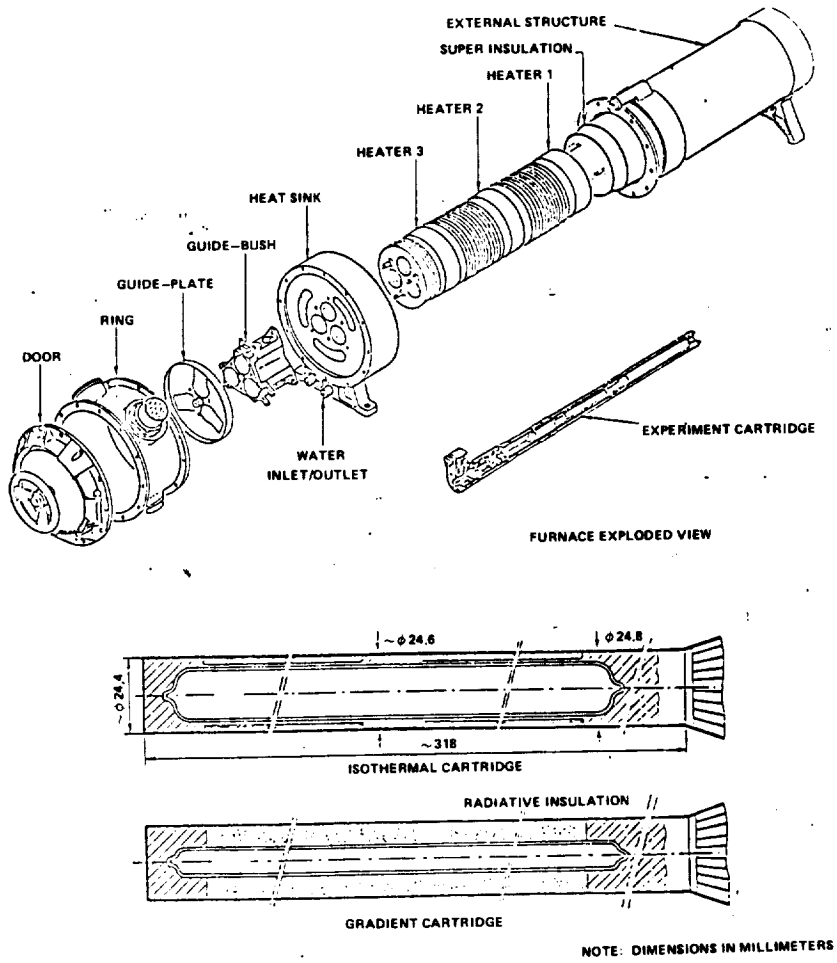


Figure III-2. Schematic of Gradient Heating Facility.

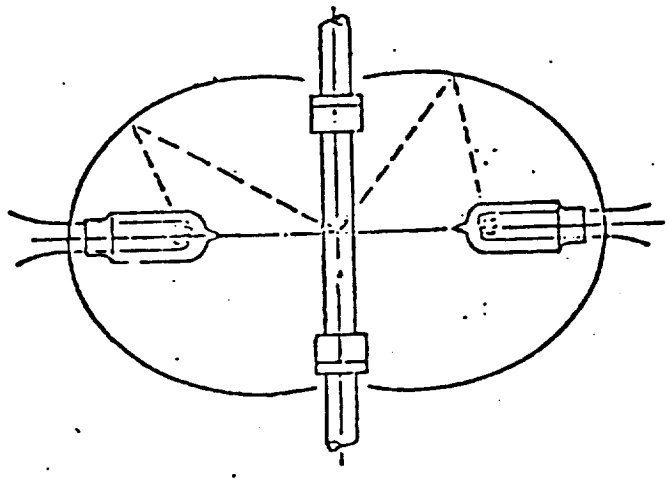


Figure III-3. Schematic of Mirror Heating Facility.

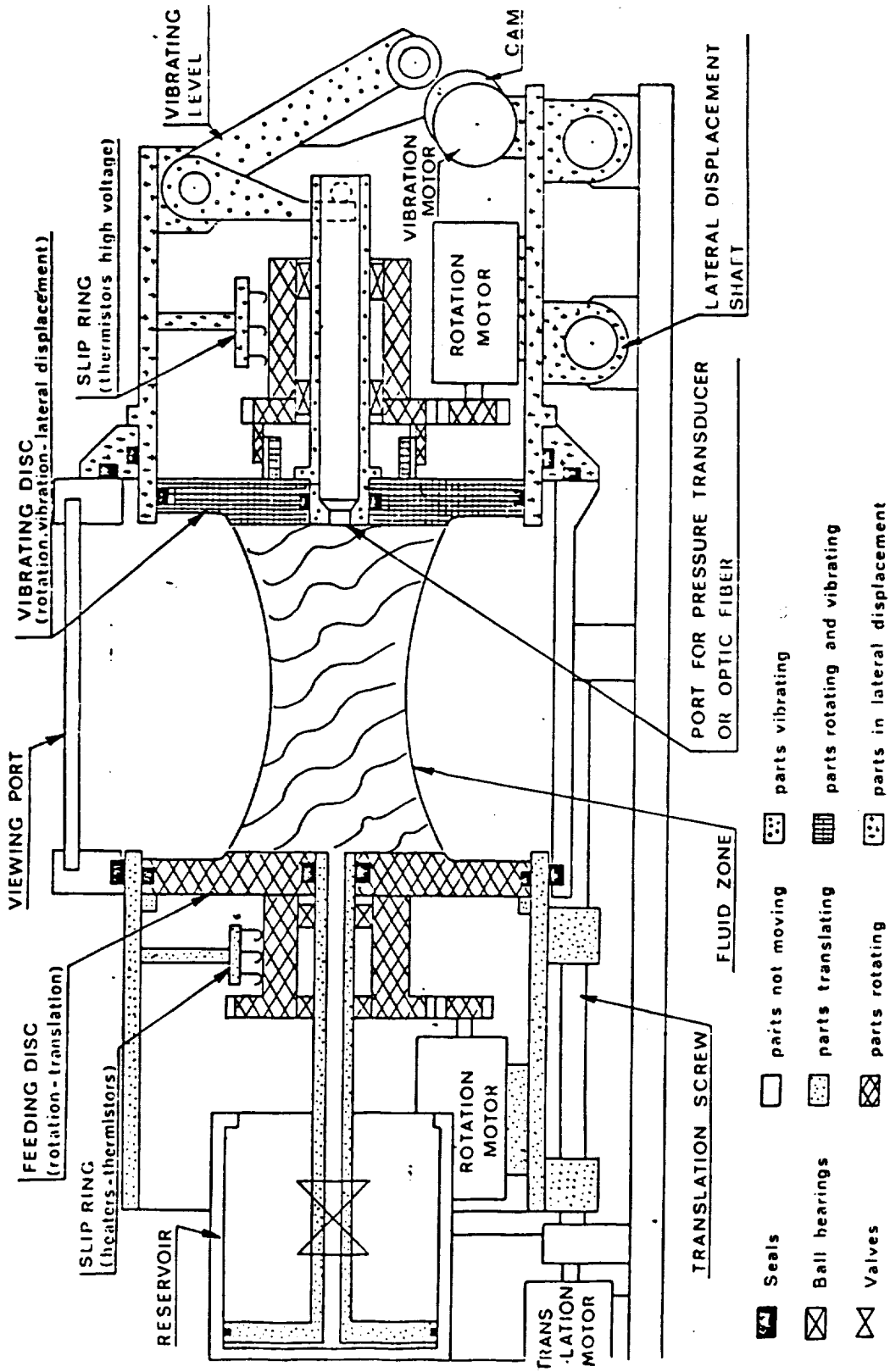


Figure III-4. Fluid Physics Module.

WETTING, SPREADING, AND OPERATING CHARACTERISTICS OF BEARING LUBRICANTS IN A ZERO-GRAVITY ENVIRONMENT (1NT011)

C. H. T. Pan
Shaker Research, USA

and

Ann F. Whitaker and Raymond L. Gause
NASA/Marshall Space Flight Center, USA

Spreading and wetting of a lubricating oil over surfaces occur in all lubrication systems. Examples are listed in Figure III-5. In many circumstances, long-term distribution and movement of the lubricant determine the useful life of the bearing. The phenomenon has many facets (Fig. III-6). Some isolated factors can be measured routinely (e.g., shadow photography of contact angle illustrated at the bottom of Fig. III-6). The total phenomenon cannot be accurately observed in the Earth environment because the relevant forces are overwhelmed by the gravitational force. The prolonged zero-gravity condition in a Spacelab flight provides a unique opportunity to obtain such technological data.

The zero-gravity environment also provides an opportunity for further research on the dynamic stability mechanism of a journal bearing which is believed to be associated with the two-phase fluid boundary. A journal bearing is a common mechanical device which works by developing a load-supporting film under the loaded direction. The thickness (h) of this film is a complex function of the rotating speed (n) and the fluid viscosity (μ) and is an inverse function of the bearing load (w):

$$h = f\left(\frac{n\mu}{w}\right) \quad .$$

In zero-gravity the load w approaches zero, and the bearing theoretically becomes unstable. The proposed experiment will determine the mechanisms of instability and the reaction of fluid films to zero gravity and will also test several concepts for preventing the onset of instability.

Two types of experiments will be conducted [viz., wetting and spreading on stationary surface(s), and two-phase boundary in a journal bearing configuration]. In each case, the fluid-surface combination will be the primary control parameter.

The experiment on stationary surfaces will be performed on a pre-assembled specimen. Upon commencement of the experiment, an automated dispenser will place a standard amount of the lubricant at the center of the surface specimen. Sequential or cinema photography of the front view will record the progression of the spreading boundary. Inclined mirrors will present simultaneous views showing the geometrical and size variations of the central drop.

Four journal bearing concepts will be investigated. These will include a plain journal bearing, a three-lobed bearing, a magnetic-ferrofluid bearing, and a plane bearing with eccentricity locked in. Photographs will be used to observe the movement and response of the fluid films under zero-gravity operating conditions, and vibration or displacement transducers will be used to record the movement of the bearings.

Both the wetting and spreading and the journal bearing portion of the experiment will be located in a drawer in Rack 7 of the Spacelab module (Fig. III-7).

This drawer will contain, in addition to four fluid wetting and spreading modules and four journal bearing modules, associated support equipment such as a camera, film, lenses, three-axis low-gravity accelerometer system, electronic controls, and a power supply.

The data to be obtained will have both scientific and engineering significance. The basic knowledge of fluid behavior in a low-gravity environment will be greatly advanced and provide a sound basis for the design of reliable and efficient fluid handling hardware for future spacecraft. The data generated from the journal bearing experiment should provide fundamental information on bearing and fluid dynamics to support theoretical work on hydrodynamics and engineering design of bearings for long life in a space environment.



DISTRIBUTION OF ROLLING ELEMENT COMPONENTS:

- RETAINER
- RACES
- BALLS AND ROLLERS

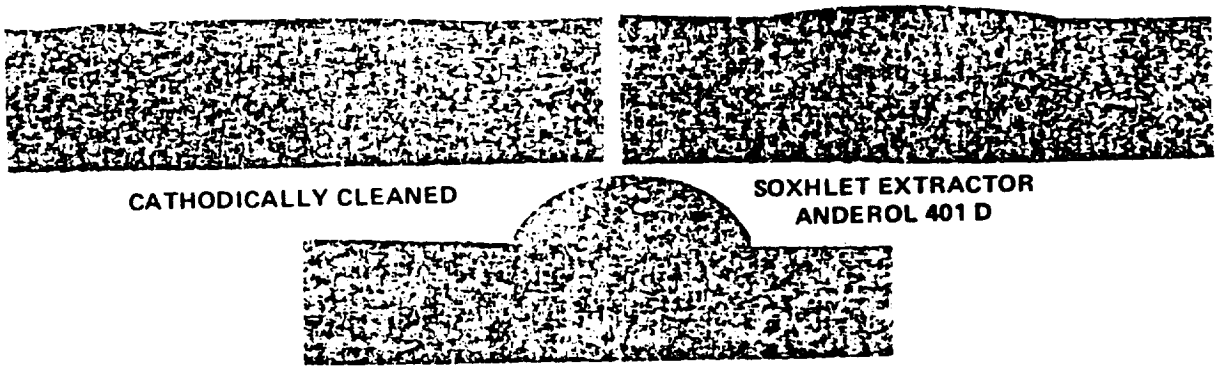
LONG–TERM MIGRATION/DEPLETION:

- SLIP RING
- INSTRUMENT BALL BEARING

FORMATION OF TWO–PHASE BOUNDARY:

- JOURNAL BEARING
- SQUEEZE–FILM DAMPER

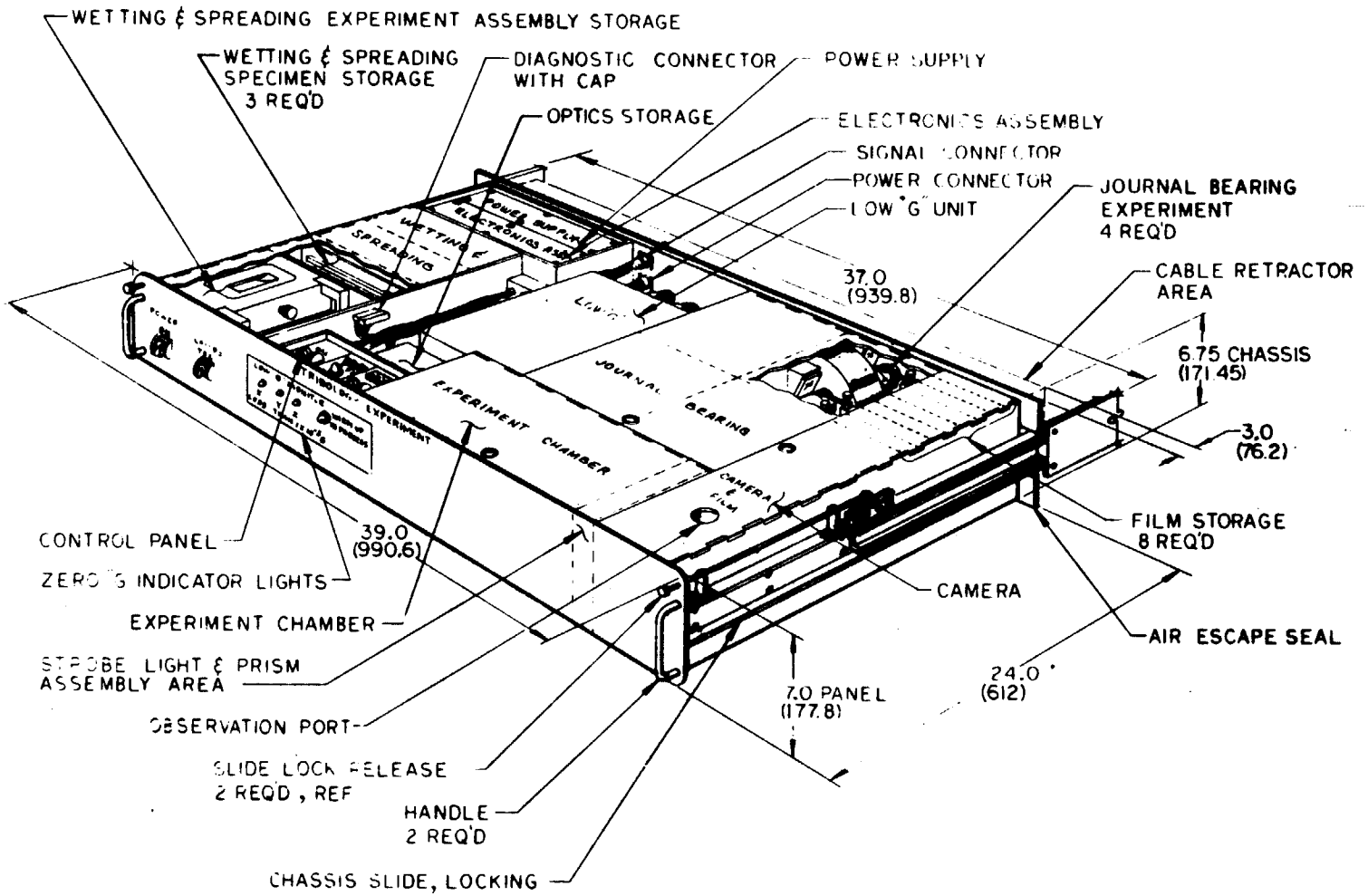
Figure III-5. Roles of wetting and spreading.



ANDEROL 401 D TRAPPED
WITHIN BARRIER FILM
CIRCLE

- BASE FLUID PROPERTIES:
  – SURFACE TENSION
  – VISCOSITY
- BLENDING
- SURFACE FREE ENERGY
- ADDITIVES
- SURFACE TOPOGRAPHY/TEXTURE
- EVAPORATION
- FLUID MOTION

Figure III-6. Influencing factors.



NOTE: DIMENSIONS IN INCHES (MILLIMETERS)

Figure III-7. Tribology experiment assembly.

GEOPHYSICAL FLUID FLOW EXPERIMENT
(1NT012)

John E. Hart
University of Colorado, USA

The primary purpose of the geophysical flow experiments is to simulate large-scale baroclinic (density stratified) flows which occur naturally in the atmospheres of rotating planets and stars and to gain insights and obtain answers to crucial questions concerning the large-scale nonlinear mechanics of the global geophysical flows. In particular, the investigator hopes to identify those external conditions related to fluid viscosity, rotation, gravity, etc., which allow qualitatively different modes of instability or waves in the model. In a geophysical context he is trying to understand why Jupiter and Saturn have axisymmetric cloud patterns as compared to the Sun which, as a rotating convecting body like Jupiter, seems to have a preferred orientation of large eddies from pole to pole.

Theoretical models of planetary circulations indicate that the planetary curvature plays a crucial role in the dynamics of rotating atmospheres because the two major constraints on flow, rotation (Coriolis forces) and gravity (buoyancy forces), vary with latitude relative to each other. Previous laboratory models of planetary atmospheres could not incorporate the curvature effect because, given the uniformity of terrestrial gravity, a rotating tank experiment was always required to have parallel rotation ($\vec{\Omega}$) and gravity ($\vec{g}$) vectors.

Simulation in the present experiment will be accomplished through the use of a dielectric fluid confined between concentric, rotating, electrically conductive spherical shells (Fig. III-8). The dielectric fluid will have a dielectric constant which is temperature dependent so that upon application of a voltage between the spheres an electric field will occur and a radially directed body force will act on the fluid in a manner exactly analogous to the gravitational body force which acts on oceans and stellar and planetary atmospheres. Because of the low-gravity environment of Spacelab, this experiment (unlike previous Earth-bound experiments) will contain the correct vector relationship between the rotation vector $\vec{\Omega}$ and gravitational body force vector (per unit mass) $\vec{g}$ of a planet; i.e., $\vec{\Omega} \times \vec{g}$ = maximum value at equator and $\vec{\Omega} \times \vec{g} = 0$ at poles.

The apparatus includes a convection cell, temperature controllers for maintaining thermal boundary conditions at the inner and outer boundaries of the cell, a servo-controlled rotation drive to set the rotation speed, and a high-voltage supply (Fig. III-9). A camera is positioned above the cell at an angle to view a quadrant of approximately 90 degrees longitude and from equator to pole in the northern hemisphere. Visualization of the flow pattern is attained either by (1) injecting dye lines into the working fluid by exciting photochromic molecules and photographing the displacement of the dye or by (2) photographing the distortion of a set of ruled lines on the outer spherical shell caused by refractive index changes in the fluid. In either case it will be possible to ascertain the state of the fluid — steady no-motion, steady axisymmetric, banded, unsteady, etc. In addition, the principal wavelengths and frequencies of the unstable modes will be measured.

Each experimental run is made with the rotation ($\vec{\Omega}$) and applied voltage fixed, while the applied temperature difference ΔT is raised slowly past a critical value which distinguishes simple axisymmetric unicellular motion from a more complicated state which may include banding or traveling waves. The nature of the instability for various thermal boundary conditions (constant temperature on inner and outer boundaries or meridionally varying temperature on inner boundary) will be determined. Of particular interest is the generation of mean zonally averaged flows by the eddies and any characteristic difference in the eddy structure between polar and equatorial regions.

The geophysical fluid flow cell experiment will permit the laboratory study in space of the large, planetary-scale dynamics of the Earth's oceans and atmosphere. The experiment should be able to verify existing theories of moderately nonlinear fluid systems on spherical surfaces and provide basic data on flows which are more strongly nonlinear than can currently be handled on a computer or by asymptotic methods. Of particular interest is the orientation of flow instabilities at various external conditions.

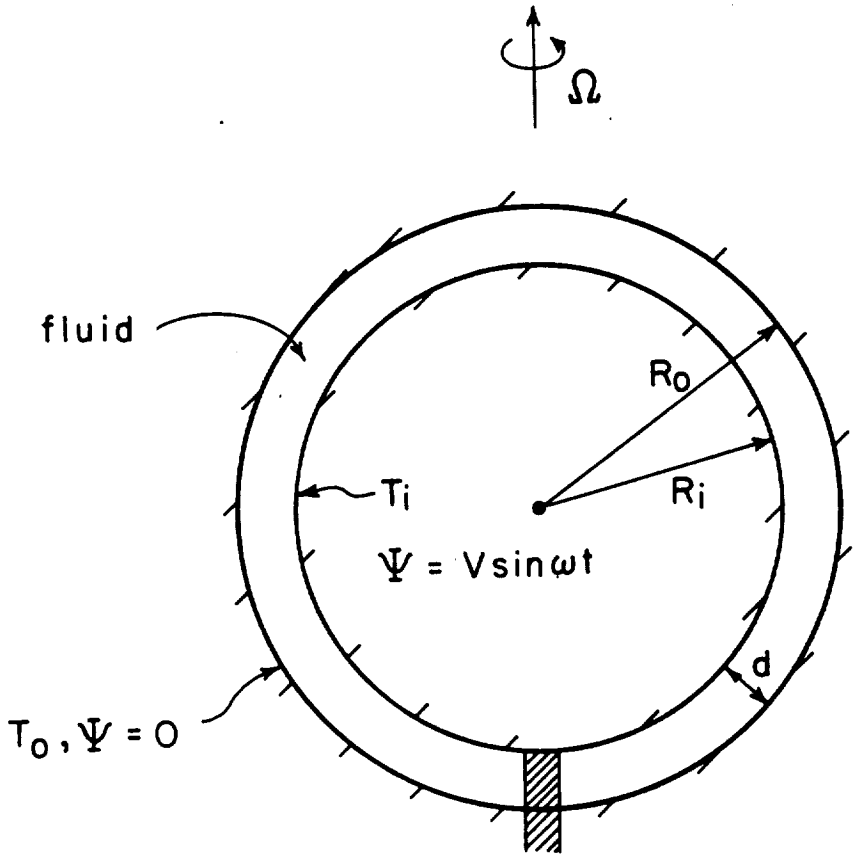


Figure III-8. Geometry of the rotating spherical shell experiment. The outer shell at radius R_o is maintained at temperature T_o, voltage $\Psi = 0$. The inner shell at radius R_i is at temperature T_i, voltage V sin ωt. The applied frequency is 60 hertz. The temperature difference $\Delta T = T_i - T_o$ (> 0 for unstable convection). The entire apparatus is rotated about its axis. The interior is fed via a supporting neck.

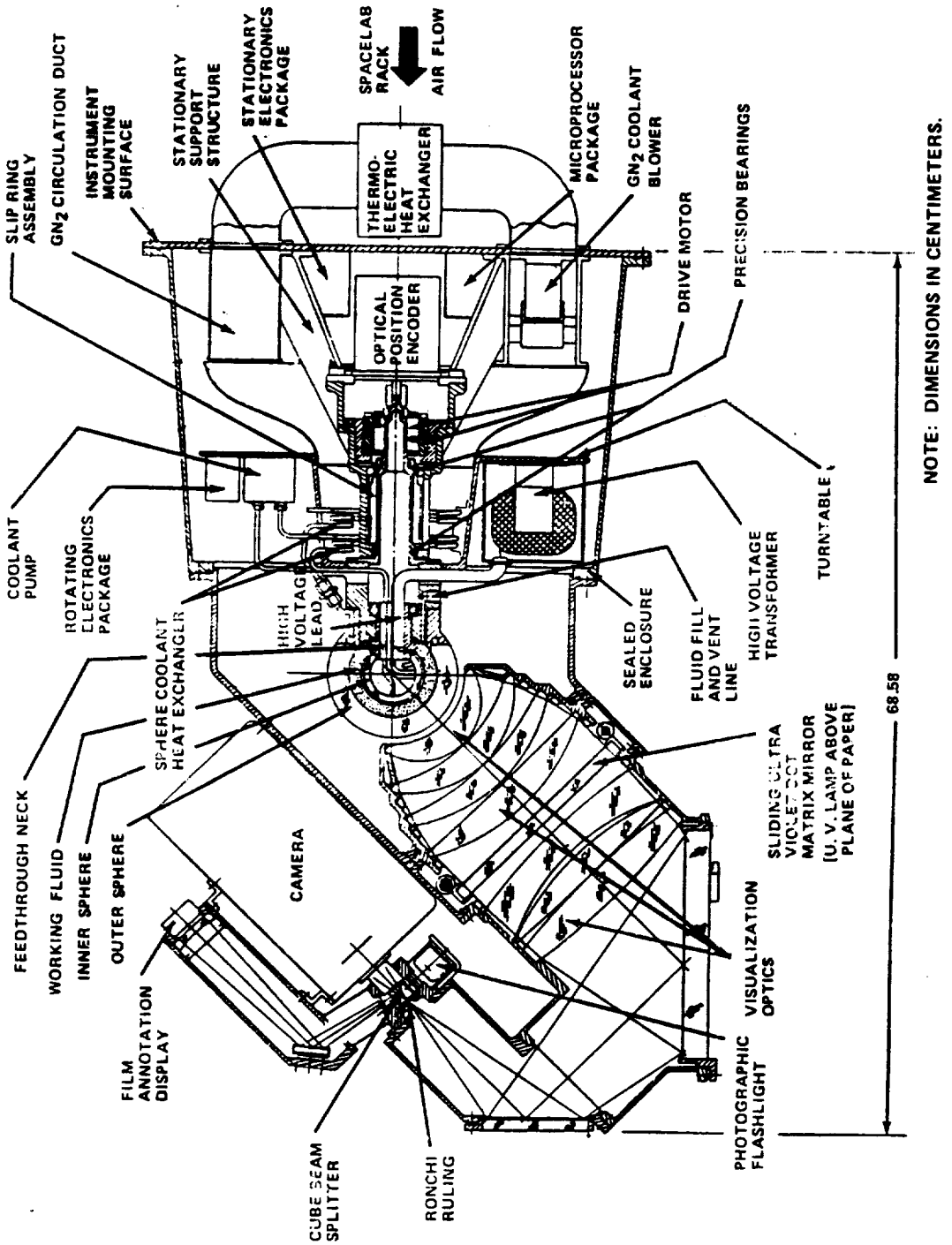
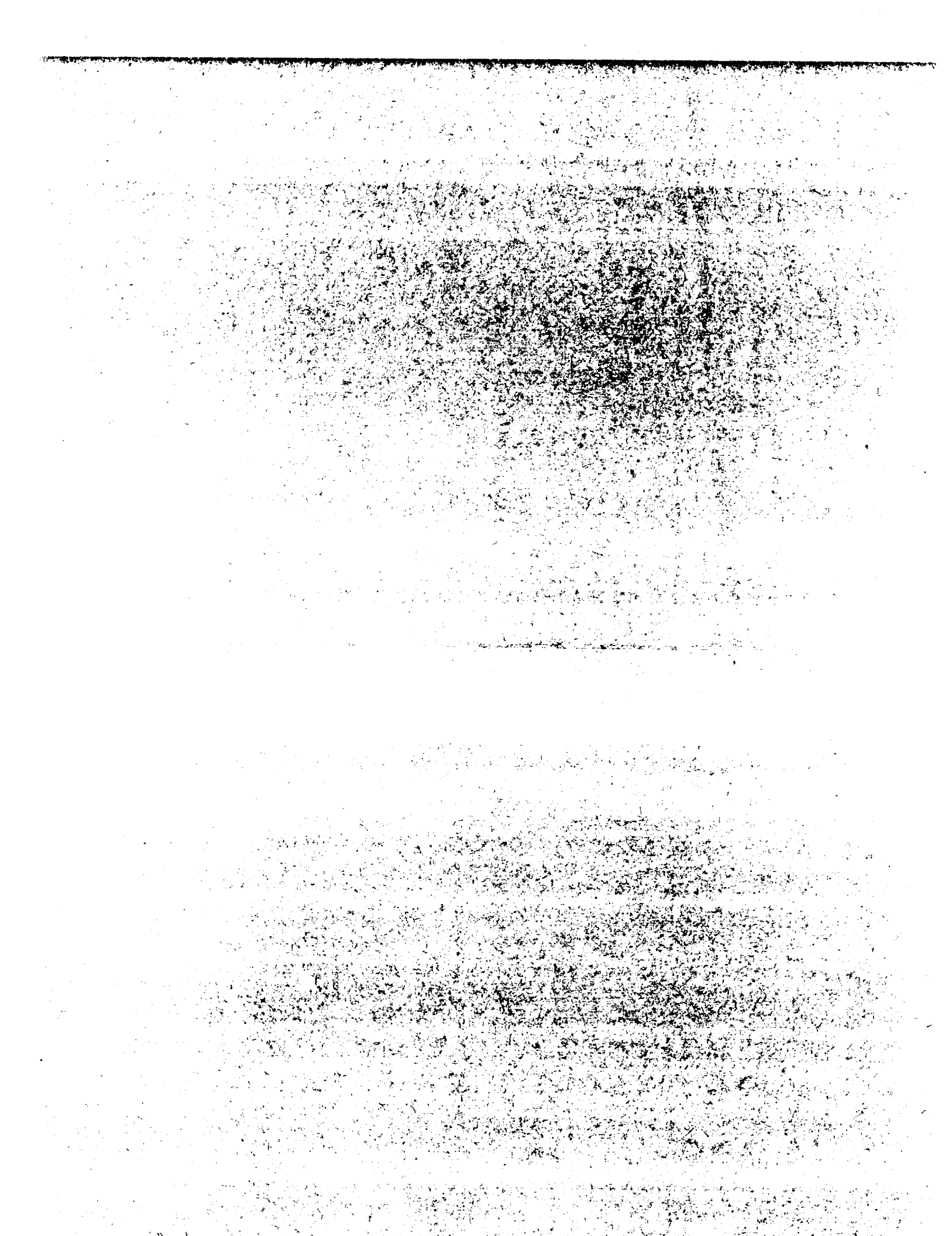


Figure III-9. Geophysical fluid flow cell design.

SECTION IV

ASTRONOMY AND SOLAR PHYSICS



FAR ULTRAVIOLET ASTRONOMY USING THE FAUST TELESCOPE (1NS005)

C. S. Bowyer
University of California (Berkeley), USA

The Far Ultraviolet Space Telescope (FAUST) is a compact, wide field-of-view, far ultraviolet instrument designed for observations of extended and point sources of astronomical interest. The instrument was developed by the Laboratoire d'Astronomie Spatiale and the French Space Agency (CNES); it has been used previously in sounding rocket work by both French and American investigators.

The prime experiment objective is to observe faint astronomical sources with sensitivities higher than previously available. The experiment will cover the 110 to 200 nanometer band, which is inaccessible to observers on Earth. Several scientific programs will be conducted; these will include a search for a class of sources known as ultraviolet stars which are predicted to exist at the stage of evolution prior to the final death of a star. A second program will consist of observations of galaxies and quasars. Such observations are important in understanding the activity at the cores of galaxies and in providing the data necessary for interpretation of observations of galaxies at very high redshifts. Joint programs with other Spacelab 1 experiments will also be conducted.

The secondary experiment objective is to verify the suitability of the Spacelab as a platform for far ultraviolet astronomy. In particular, data will be provided on the ultraviolet background levels due to astronomical, terrestrial, and spacecraft-generated sources; the levels of contaminants which affect ultraviolet instruments; and the capability of the Orbiter for stable pointing at celestial sources for useful periods of time.

The instrument (Fig. IV-1) is an f/1.12 Wynne camera with an effective collecting area of 150 square centimeters and a field-of-view of 7.5 degrees. The imaging capability is better than 2 arc minutes in the entire field-of-view. The detector system uses a microchannel plate image intensifier in conjunction with a 60-exposure, 35 millimeter film pack of Kodak 103a0. The overall instrument, which includes a sealed container with a mechanical door, is a cylinder 48.8 centimeters in diameter and 131.3 centimeters in length. When used in a

photometric mode with a bandpass of approximately 100 nanometers, the limiting magnitude for a 2 minute observation is V = 17 to 18. Diffuse sources as faint as 27th magnitude per square arc second can be detected. In the alternate spectroscopic mode, with a calcium fluoride objective prism which permits a wavelength resolution of between 3 and 20 nanometers, the limiting magnitude is V = 14 to 15. The photometric mode will be used on Spacelab 1.

The instrument will be hard-mounted on the pallet and will be operated by the payload specialist using a control and display box in the Spacelab. The pointing requirements will be met by the Orbiter pointing capability for observing times between 1 and 10 minutes. The payload specialist will be responsible for selection of targets at a given observing opportunity, readying the instrument and checking its health, selection of observing parameters, and initiation of the observing sequence. The primary data are photographic and, hence, require no data management beyond return to the experimenter for processing. Secondary data concerning observation parameters and housekeeping data will be available to the payload specialist and to the experimenter at the payload operations control center.

A typical astronomical observing program would consist of obtaining a series of photographs during spacecraft nighttime. The targets will include hot stars and nebulae in our own galaxy, the cores of nearby galaxies, and objects of cosmological interest such as quasars. Detailed investigations will potentially include (1) search for ultraviolet stars in areas of low obscuration in our galaxy, (2) search for hot stars in globular clusters, (3) peculiar stars (such as interacting binaries) in our galaxy, (4) the far ultraviolet background as a function of ecliptic and galactic coordinates, (5) nearby clusters of galaxies (such as the Virgo cluster) to study the spatial distribution of far ultraviolet emission in the galaxy cores, and (6) magnitudes of quasars and BL Lacertae objects. To perform the secondary objective, exposures at different orbital coordinates and Orbiter attitudes will be compared. Any degradation in instrument performance due to Spacelab and/or Orbiter generated contaminants or instrument deterioration will be monitored by reobserving sources of known intensity.

The experiment is a good example of the effective use on Spacelab of existing instrumentation at low cost. It will help establish the suitability of Spacelab for astronomical observations. Secondly, the experiment has a potentially high scientific return which will not have been achieved before the Spacelab, and it has a good reflight potential.

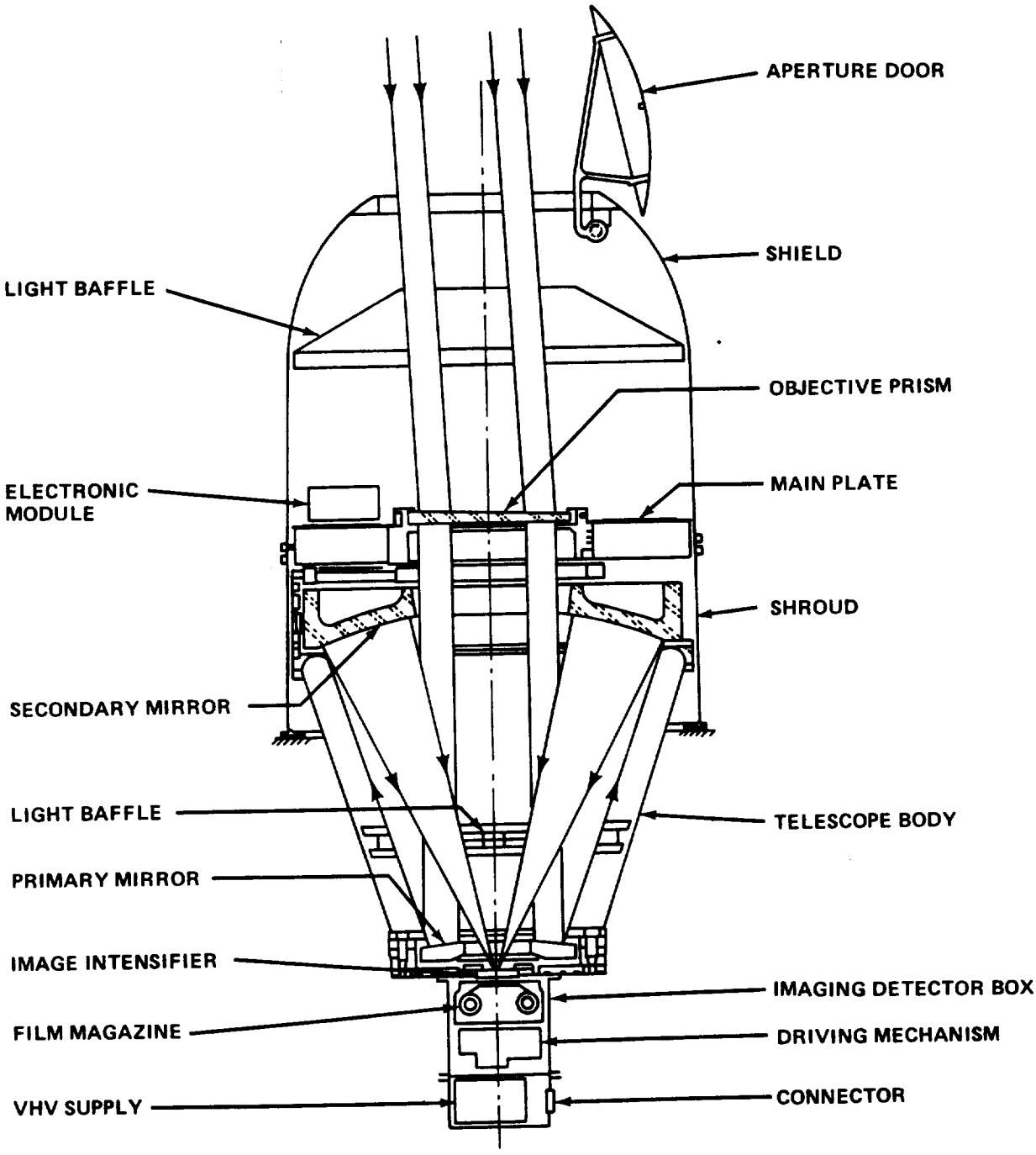


Figure IV-1. Far Ultraviolet Space Telescope (FAUST).

VERY WIDE FIELD CAMERA
(1ES022)

G. Courtes
Laboratoire d'Astronomie Spatiale, France

Past and present astronomical satellites have been designed for the study of stellar spectra of relatively bright stars. Only a few direct photographs have been obtained. Some wide fields in the Milky Way (120 × 80 degrees) have been photographed in the near ultraviolet (260 nanometers), easily detecting the Milky Way and the zodiacal light as well as 10th magnitude O spectral type stars. It is anticipated that the Very Wide Field Camera (VWFC) will have a limiting magnitude (sensitivity) of V_{lim} = 12 to 12.5 for a normally reddened early B spectral type star.

Astronomical observation using instruments with a very wide field-of-view is relatively new. It is faster and easier to interpret than systematic spectral scanning of many points over a large field, allows constant comparison with a large part of the sky background and photometric reference stars, and is compatible with the conditions of the Spacelab (i.e., large field available and relatively poor stabilization). Such observations will give a first evaluation of the most interesting large-scale phenomena. This kind of wide field survey has been to date entirely neglected as a precursor of more sensitive deep survey programs.

The proposed experiment will make a very general ultraviolet survey of a large part of the celestial sphere. The objectives are to study galactic and faint extragalactic extended sources and peculiar ultraviolet objects. A camera with a very wide field-of-view will be operated in the ultraviolet in two modes: photometric and spectrometric.

The photometric mode is direct photography through filters for observation of the following sources:

1) Large-scale distribution of ultraviolet radiation in the Milky Way. The stellar clouds must be studied as a whole for their geometrical extension and their energetic spectral distribution.

2) Diffusion of the galactic light above the galactic plane and in front of the large absorbing clouds. Observation of this source permits the detection of large extensions of the galactic material and studies of possible connections with

the local group of galaxies. A general study of the sky background will allow discrimination of the galactic and extragalactic light from sunlight scattered by interplanetary dust (zodiacal light and gegenschein).

3) The optical emission of the interstellar matter. Until recently these emissions have been observed in only a very few cases.

4) Stars, especially the peculiar ultraviolet objects found with the TD1 satellite, and star-like objects with diameters less than 3 arc minutes (galaxies, globular clusters).

It is in the photometric mode that the field-of-view is 54 degrees (this is the field size with no cat's eye, but the overall useful field allowed by the intensifier is nearly 65 degrees with a maximum light loss of 15 percent). Filters to be used are centered at 155, 190, and 250 nanometers.

In the spectrometric mode (nebular spectrograph), the light from the center of the photometric field is concentrated on a slit covering 10 degrees by 10 arc minutes on the sky. The wavelength range detected in this mode is 130 to 270 nanometers, with the most sensitive range being 155 to 192 nanometers. In the latter wavelength region the resolution is 0.5 to 0.8 nanometer.

In the camera (Fig. IV-2), a hyperbolic primary mirror is followed by a Schmidt camera placed at the long focal length of the hyperbolic mirror. With this primary mirror one can obtain an image of the sky at f/13 and a large object field. The Schmidt camera gives a final plane image with a large aperture ratio of f/2 and a small apparent field. The small convergence of the beam ahead of the Schmidt camera allows placement of various devices (interference filters, gratings, etc.) into the beam and does not impose a high positional accuracy for the optical elements. The geometrical properties of the hyperboloid artificially stopped at one of its geometric foci render the system relatively insensitive to field aberrations. The entrance pupil seen from the various object fields is always circular. Its area increases as off-axis angle increases, tending to increase sensitivity to stars as one goes farther off axis. However, the sensitivity to extended sources is constant over the field since there is no limitation to the solid angle subtended by the pupil as a function of field angle.

Data are recorded on photographic film. An image intensifier is used in both modes to shorten integration time. Once a sequence is initiated, it is completed automatically by computer control; provisions have been made for manual operations.

Pointing is accomplished with the Orbiter since the camera is rigidly mounted in the Spacelab scientific airlock. The sources are the ultraviolet radiation of interstellar matter of diffuse galactic light, stars, and star-like objects. Spectrograms of these sources will be the first nebular space spectrography in this ultraviolet wavelength range.

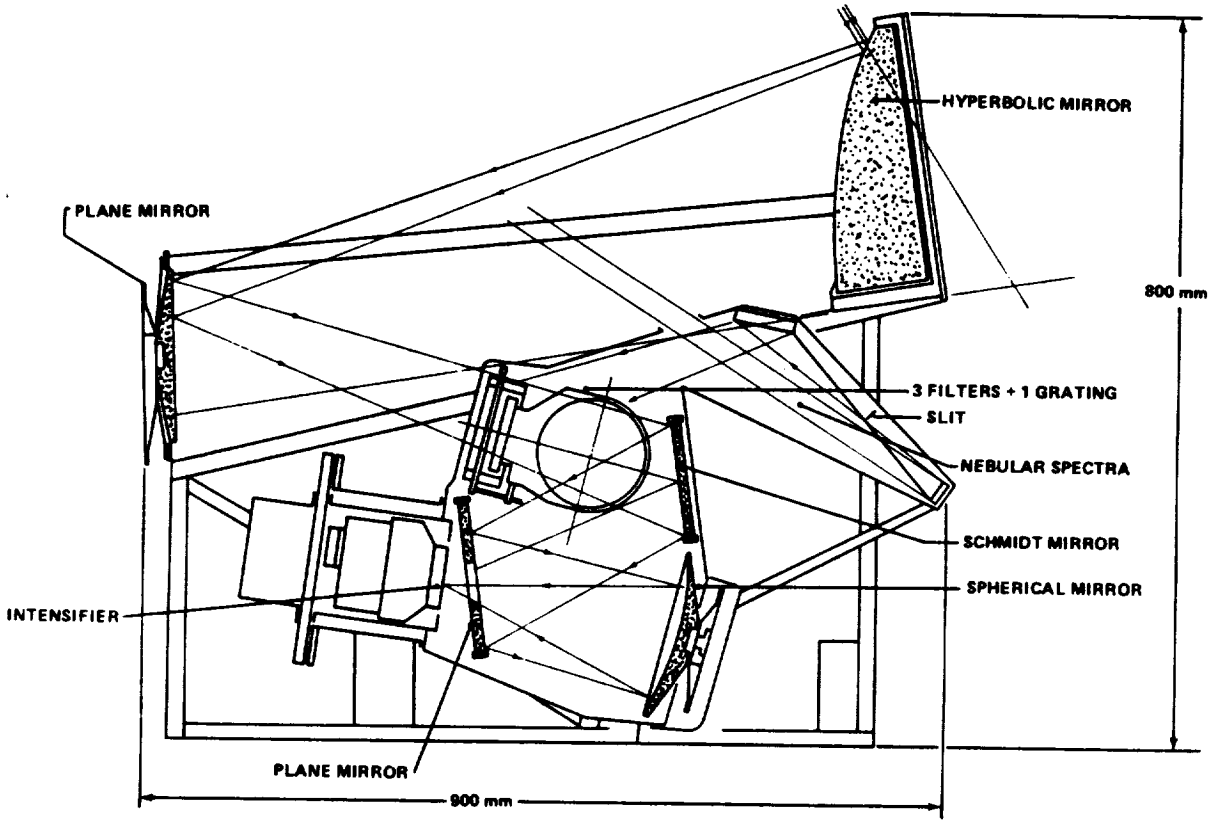


Figure IV-2. General design for the Very Wide Field Camera (VWFC).

SPECTROSCOPY IN X-RAY ASTRONOMY
(1ES023)

R. Andresen
ESA/ ESTEC, The Netherlands

The primary scientific objectives of this experiment are the study of detailed features in cosmic X-ray sources and their associated temporal variations over a wide energy range.

Unlike solar X-ray spectroscopy, which is a fairly well-developed field (several emission lines have been observed in the 0.14 to 20.0 nanometer band from the corona and solar flares), cosmic X-ray spectroscopy is at its beginning. Recent observations on rocket flights, and particularly with the satellites Ariel 5 and OSO-8, indicate excess emission and absorption at approximately 6 to 7 kiloelectron volts in the spectra of supernova remnants, binary X-ray sources, and clusters of galaxies. The emission feature is probably a complex of Kα lines of highly ionized iron.

The results obtained so far derive from proportional counters operating in the range 0.1 to 30 kiloelectron volts, with the low spectral resolution inherent to this type of detector. Bragg crystal spectrometers and solid-state detectors have been limited by low efficiency and narrow bandwidth. For the missions which will be carried out before Spacelab, only HEAO-B will carry spectrometers with sufficient resolution to tackle the problem in the spectral range below 1 kiloelectron volt, but these leave unexplored the higher energies such as that relating to the iron complex.

To fulfill the scientific objectives of this experiment, a gas scintillation proportional counter (GSPC) will be used as the detector system. In the gas scintillator, where the initial electrons are accelerated sufficiently by an electric field to excite the gas and yield photons, yet insufficiently to produce charge multiplication, the principal limitation is due to the statistics of the initial ionization process only. In theory, the limiting resolution is approximately 7 percent full width at half maximum (FWHM) at 6 kiloelectron volts. In practice, 10 percent FWHM or better has been obtained with large area counters in the investigator's laboratory. Both values compare well with those for conventional proportional counters (i.e., a theoretical 14.5 percent FWHM and the approximately 25 percent FWHM achieved in practice).

The concept of the GSPC is shown in Figure IV-3. It is pointed toward a target using the Orbiter system. X-rays from the target, after passing through conventional collimators defining the field-of-view, enter through the window (beryllium of 300 micrometer thickness) into the chamber filled with xenon gas. The upper energy limit of the device is determined by the stopping power of the drift region given by the product of gas depth and pressure. The electrons from the conversion drift to the first grid and are then accelerated to the second grid, producing a burst of scintillations in the ultraviolet for the well-defined time taken by the electrons to cross the scintillation region. X-rays which are absorbed in the scintillation region or charged particles entering the detector produce scintillation burst times of significantly different lengths. A conventional photomultiplier is used to observe the scintillations. Data from the photomultiplier tube are stored on magnetic tape after transmission to the ground and are analyzed after the mission. For each "event" detected, the pulse height of the photomultiplier signal is analyzed to yield the energy and the time of arrival recorded; the length of the scintillation burst is measured to monitor event validity.

For X-ray astronomy, the development of a large-area GSPC is crucial, since the associated X-ray source intensities are low. The development has been hampered by the variation in light yield with position across the counter entrance window. This results from the varying solid angle presented to the photomultiplier tube at various radial positions in the scintillation region of a linear electric field GSPC. The situation has been overcome by the focusing of the primary electron cloud in the photoabsorption region. This is achieved by the introduction of a spherically symmetric field formed by partially spherical grids and X-ray entrance window.

The recent observations of what appear to be emission lines in the X-ray region indicate the advent of cosmic X-ray spectroscopy as a new science; it is clear, however, that its potential for a decisive role, similar to that played in optical and radio astronomy, will not begin to be realized until X-ray lines are seen at higher resolution.

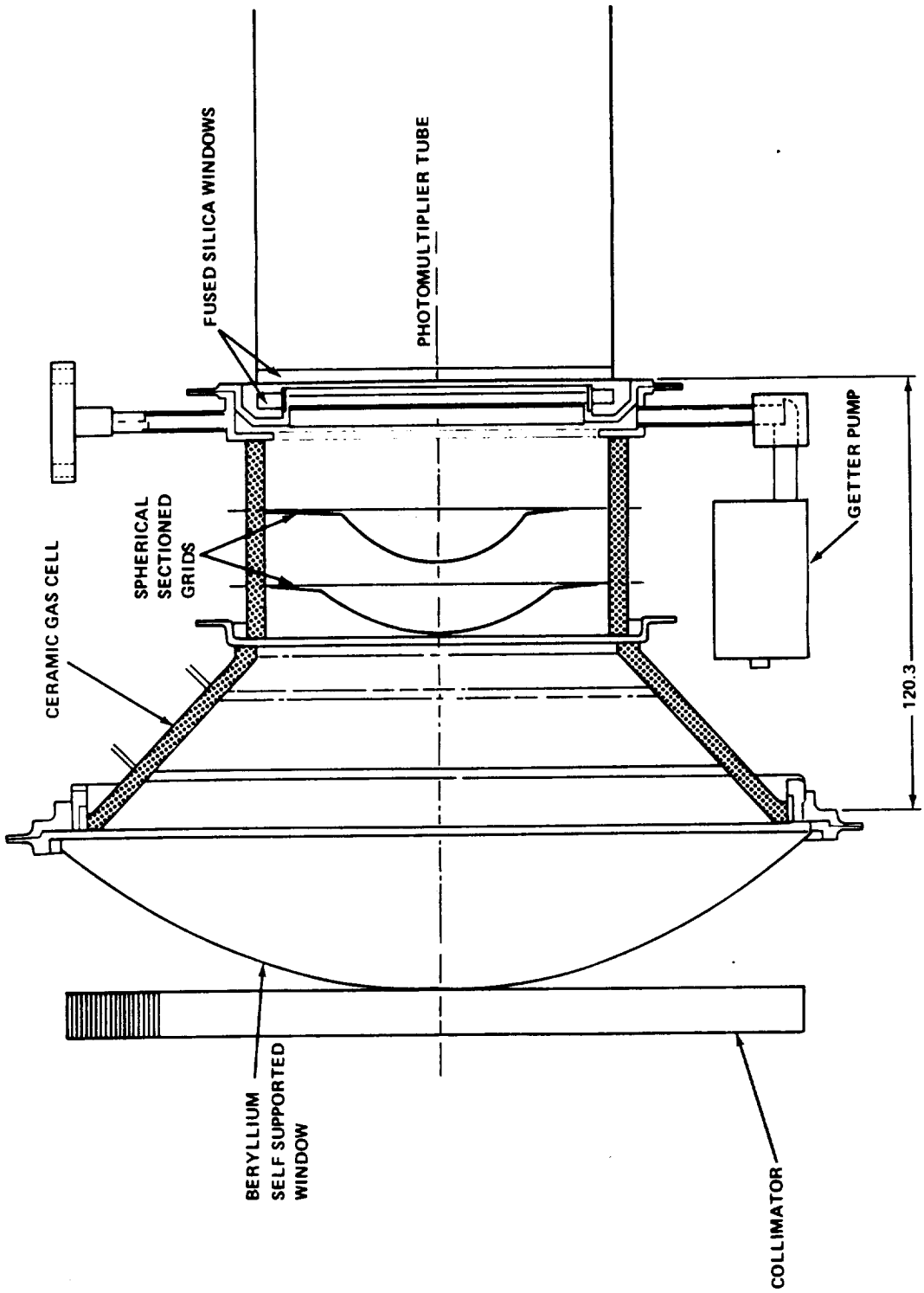


Figure IV-3. Gas scintillation proportional counter (GSPC).

ACTIVE CAVITY RADIOMETER IRRADIANCE MONITOR (1NA008)

R. C. Wilson
Jet Propulsion Laboratory, USA

The objective of the Active Cavity Radiometer Irradiance Monitor (ACRIM) experiment on the Spacelab 1 Mission is the measurement of the total solar irradiance with state-of-the-art accuracy and precision. This experiment is part of an on-going long-term program of extra-atmospheric observations to determine the magnitude and direction of possible variations in the total solar output of optical energy. The principal use of this information is in the study of the Earth's climatology and the physical behavior of the Sun.

The total solar irradiance from far ultraviolet through far infrared wavelengths will be measured by three Type IV active cavity radiometer (ACR) detectors. These detectors are electrically self-calibrated, cavity pyrheliometers, each capable of defining the absolute radiation scale with an uncertainty of ±0.1 percent in the International System of Units (SI) at the solar "constant" level.

The primary driving force for the circulation of the Earth's atmosphere and the formation of weather systems is the interaction of the Sun's optical radiation with the Earth-atmosphere system. Small variations in the Sun's total or spectral radiant output would have substantive effects on the weather and climate of the Earth. The exact magnitude of the effect predicted for a solar constant change is somewhat dependent on the climatological model. A decrease of 6°K in mean global temperature in response to a -1 percent solar constant change is predicted by one model. Another indicates that runaway glaciation producing 100 percent ice cover would occur if the solar constant decreased by more than 6 percent below its present level. The effects of much smaller changes on ocean level and climate would be dramatic. Clearly, such changes might occur over long periods of time, and to observe such trends, the highest possible absolute measurement accuracy and reproducibility are required. The ACRIM experiment will provide solar "constant" observations with an SI uncertainty of ±0.1 percent, which corresponds to the threshold of solar variability of significance to present climatological modeling.

Pyrheliometers have been constructed in various forms, but they all have certain features in common. They are calorimeters in which the heating effect of unknown irradiant flux on a detector is compared with that of an electrical current passed through a heating element placed in intimate thermal contact with the detector. An accurate knowledge of the effective absorptance of the detector for the irradiant flux, the area over which the detector is irradiated, and the cavity electrical heating power facilitates the accurate measurement of irradiant fluxes on an absolute basis in terms of SI.

The three detectors of the Spacelab 1 ACRIM are each equivalent to that shown in Figure IV-4. Two right, circular, conical cavity detectors are connected to the heatsink by two thermal impedances. All four parts are electrodeposited 99.99 percent pure silver. The interiors of the cavities are coated with a specular black paint. A low temperature coefficient heater winding is bonded to the back of each cavity in the region corresponding to solar irradiance of the cavity interior. Resistance temperature sensors are bonded to the cavity apertures. The primary cavity is irradiated through a precisely machined and accurately measured aperture. The detector's field-of-view is defined by an extension of the heatsink. The heatsink assembly is insulated from the outer case. Figure IV-5 shows the ACRIM flight configuration.

The dissipation of a fixed amount of power in each primary cavity will produce a constant temperature drop across the thermal impedance. This drop, transduced by the resistance temperature sensors, is used by an electronic servo-system which automatically maintains constant cavity power dissipation by controlling the dc voltage supplied to the cavity heater. The primary cavity detector of the ACR is accurately maintained at a slightly higher temperature than the heatsink at all times.

The ACR operates in a differential mode. A shutter alternately blocks solar radiation from, and admits it to, the primary cavity. In the shutter-closed or reference phase of the measurement, the ACR views its own heatsink. Electrical heating provides the necessary power to balance the cavity's conductive and radiative losses and maintains the constant cavity-heatsink temperature difference. When viewing the Sun in the shutter-open or observation phase, the power supplied by the electronics automatically decreases by an amount proportional to the solar irradiance of the cavity aperture. Absolute irradiance measurements are derived from the difference in the electrical power supplied to maintain the constant cavity-heatsink temperature difference in the two phases of measurement.

The ACRIM detectors will be independently shuttered. Their cycles of operation will be different. Channel A will be used routinely to monitor the total solar irradiance. It will be able to define the solar flux in SI units with an absolute uncertainty of 0.1 percent and a precision of 0.02 percent. Short-term fluctuations at the precision level will be observable at a 1 hertz maximum rate. The time constant for a reference or observation phase step function of solar "constant" magnitude will be less than 2 seconds. Shuttering cycles will be 60 seconds open and 60 seconds closed. The second detector (Channel B) will be intermittently compared with Channel A to establish A's long-term stability or to calibrate any apparent degradation. The third channel (C) will, after initial comparison with A and B, be used only to resolve ambiguities arising from the operation of the first two.

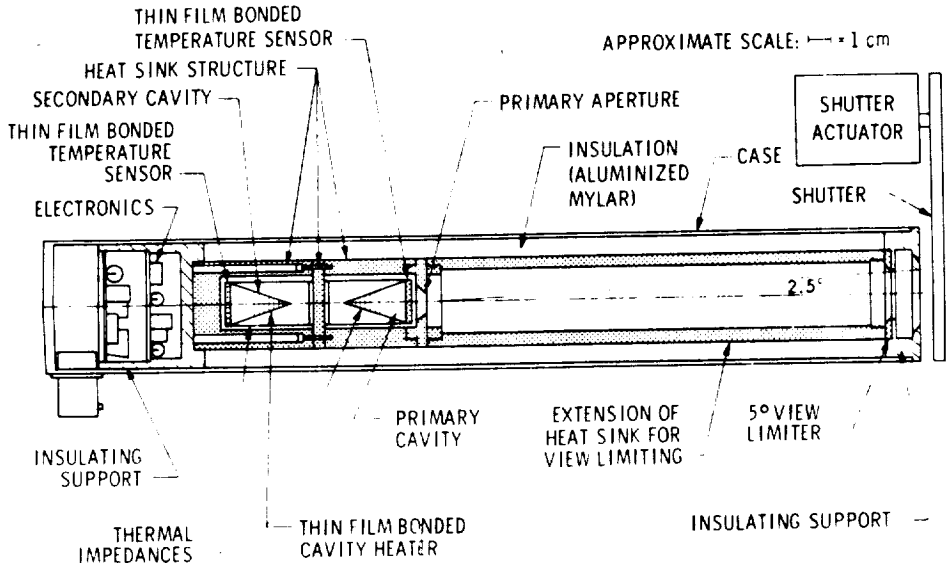


Figure IV-4. Schematic of Jet Propulsion Laboratory's ACR Type IV.

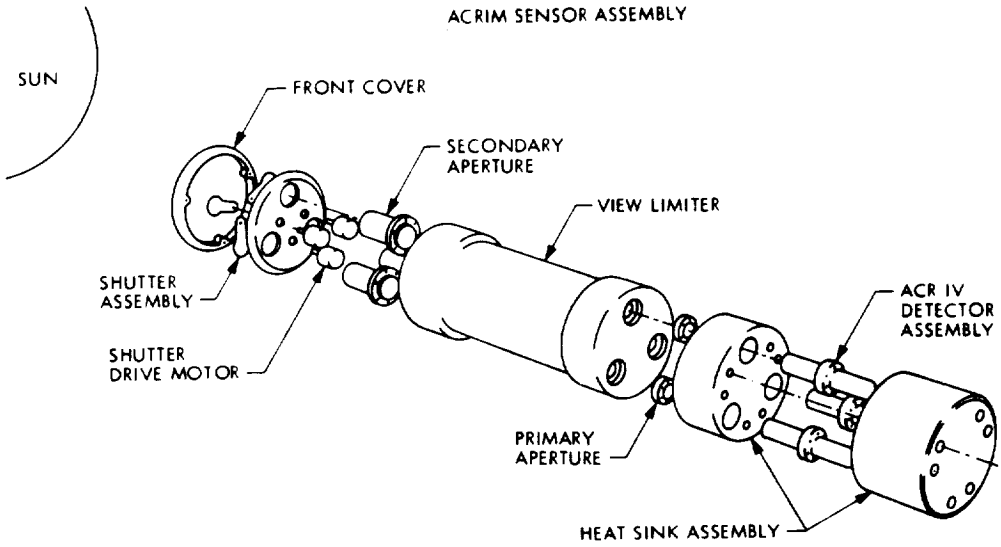


Figure IV-5. Jet Propulsion Laboratory's ACRIM for Spacelab 1.

MEASUREMENT OF THE SOLAR CONSTANT (1ES021)

D. Crommelynck
Institut Royal Meterologique de Belgique, Belgium

The objectives of this investigation are (1) to measure the absolute value of the solar constant with improved accuracy and (2) to detect and measure long-term variations that may exist in the absolute value of the solar constant.

The solar constant is the total irradiance of the Sun at a distance of one astronomical unit. This will be measured directly in space by an absolute self-calibrating radiometer with an absolute accuracy estimated to be of the order of ±0.1 percent and a sensitivity better than 0.05 percent.

The values for the solar constant obtained by measurements since 1960 lie between 1353 ± 20 watts per square meter and 1392 ± 14 watts per square meter; the most probable value is stated as 1371.0 ± 4.8 watts per square meter. This dispersion is caused by the inaccuracies and scale problems of the instruments which have been used and the need to correct measured values for atmospheric attenuation. The use of an absolute radiometer removed from the effects of the atmosphere with its calibration tested in situ is the only way in which a truly accurate measurement of the solar constant can be made.

The need for an accurate measurement of the solar constant has been recognized for some time, and improvement of the value has been strongly recommended by several scientific bodies. The absolute value of the solar constant is a critical term in the determination of the Earth's radiation budget as well as for the studies of Earth albedo. In addition, it is one of the main components in the energy balance equation and is responsible for the dynamic behavior and circulation of the atmosphere and, thus, also of climate. The importance of an accurate knowledge of the solar constant (its value and variations) for climatology and atmospheric physics in general cannot be overstressed.

The special feature of this radiometer (Fig. IV-6) is that it has two channels which enable any degradation of the black surfaces to be detected and compensated and the self-consistency of the radiometric system to be determined in space. The radiation measurement will be made by using a heat balance

system driven automatically by a feedback system. The precise knowledge of the electrical, optical, mechanical, and thermal characteristics makes this radiometer an absolute instrument which does not need to be calibrated by radiative sources.

Each of the two radiation sensors has an independently controlled shutter. The radiometer is operated by using various combinations of open and closed shutters and a reference electrical power source which has a stable and known output.

At the beginning and the end of each measurement sequence, the correct behavior of the radiometer system is ascertained by having the shutter of both channels closed, applying the reference power source to one heater, and using the servo-system to adjust the power applied to the other until heat flux balance is achieved. The roles of the channels are then reversed and the same procedure followed. The measurement of the electrical power applied to each channel for the two cases gives a value for the precision of the servo-system. Because the power of the reference electrical source is already known, this is a simultaneous check of the data processing system.

The actual radiation flux measurements are made by pointing the radiometer to the Sun' s center and opening the shutter of the channel to which the servo-system power is attached. The servo-system compensates for the extra heat input until heat flux balance is achieved again. The shutter is then closed, and the servo-system should adjust the power back to its previous value. The difference in the power applied with the shutter opened and closed is a function of the incident radiation flux. The absolute total irradiance can be calculated from the known characteristics of the instruments. This sequence of opening and closing the shutter will be repeated several times, always using the same channel for the measurement.

On the first and last measurement sequences of the mission the roles of the channels will be reversed for just one step, and the shutter of the channel that is normally closed will be opened. In this way the radiation measurements of the two channels can be compared to detect and compensate for any aging of the black paint of the absorption surface that is repeatedly exposed to the Sun.

The strategy for these long-term observations using the proposed radiometer should be guided by the following principles: (1) direct and absolute measurement of the solar constant on the first Spacelab and/or OFT flights, (2) repetition of the measurements using the same radiometer on subsequent flights,

and (3) comparison between subsequent flights of the radiometer with spare models and other absolute radiometers on the ground, ascertaining the link with the new International Radiometric Reference.

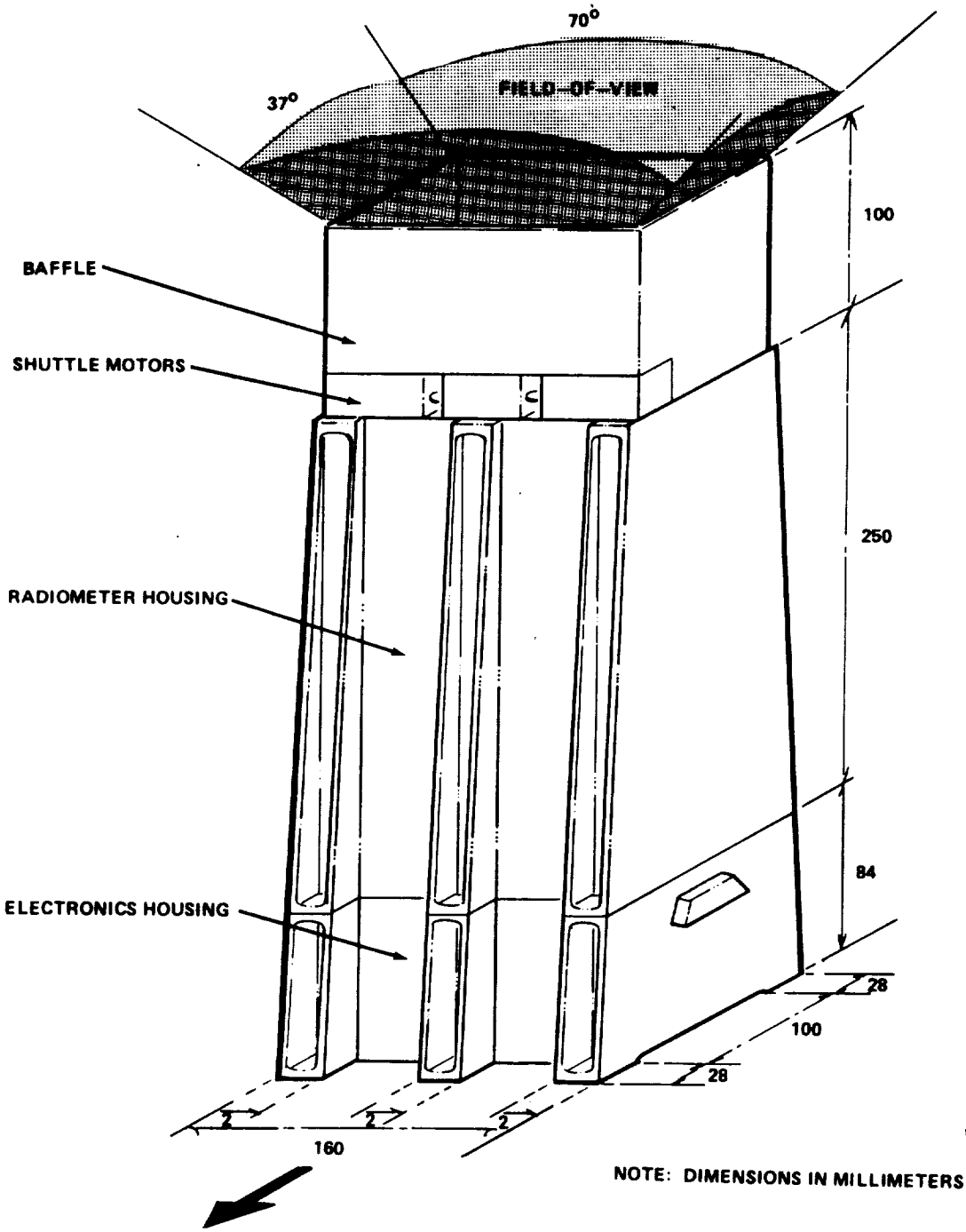


Figure IV-6. Radiometer.

SOLAR SPECTRUM FROM 170 TO 3200 NANOMETERS (1ES016)

G. Thuiller
Service d' Aeronomie du CNRS, France

The total incoming solar radiation, called the solar constant, is the primary external source of energy for the Earth' s atmosphere. Any change in its value directly affects the radiation budget and, consequently, the climate. A drift of approximately 0.5 percent per century would suffice to explain the little ice age of the 16th and 17th centuries. But solar constant variability remains uncertain. Because the standard deviation of all solar constant determinations since 1966 is 1 percent, no conclusion concerning the variability of the solar constant can be based on experimental data available up to now.

It is important to know which wavelength ranges of the solar spectrum are involved in the variability of the solar constant. In fact, consequences of changes in the solar irradiation flux are directly related to the wavelength range involved. Variability below 300 nanometers influences mainly the photodissociation of ozone and the photochemical equilibrium in the stratosphere, while variability above 700 nanometers is mainly related to water vapor and carbon dioxide absorption which takes part in the thermal budget of the terrestrial atmosphere.

Ultraviolet solar radiation between 250 and 300 nanometers contributes 0.97 percent of the solar constant. Variation in this spectral range is generally considered negligible, but recently variations of 50 percent at 250 nanometers and 20 percent at 300 nanometers over the 11-year cycle have been theorized. These variations would lead to changes in the solar constant of the order of 0.3 percent, but the variations have not yet been confirmed rigorously.

The purpose of the proposed experiment is to measure the spectral irradiance of the Sun between 170 and 3200 nanometers to determine with accuracy the solar constant, its possible variation with the solar cycle, and the wavelength range responsible for the observed variations. This objective requires measurements over very long time periods (10 years) involving flights of the same instrument on future Spacelab missions.

The range 170 to 3200 nanometers of the solar spectrum will be studied by means of three spectrometers, one covering the ultraviolet, one the visible, and another the near infrared range. The ultraviolet spectrometer will cover from 170 to 370 nanometers, the visible spectrometer will cover 350 to 900 nanometers, and the infrared spectrometer will cover the range from 800 to 3200 nanometers.

The instrument consists of four parts: dispersive elements, an in-flight calibration device, detectors, and counting system. The basic instrument (Fig IV-7) is a double monochromator using two holographic gratings as a dispersive element. The two gratings are mounted on the same mechanical axis to provide high accuracy for the bandpass. The input window is a grind which reduces the effect of an angular variation (±2.5 degrees) between the optical axis and the Sun. Colored filters are used to eliminate the second order. For the three spectrometers, the rotation angle of the two gratings in cascade is 30 degrees. The three sets of gratings rotate on the same axis. The detector for the ultraviolet and visible spectrometers is a photomultiplier tube. The infrared spectrometer will use a PbS cell as detector.

Calibration lamps are used to monitor any change of the sensitivity of the instrument. They are not used as a photometric standard but as a reference. Their light follows the same optical path as the Sun' s light. A hollow cathode lamp is used to check the wavelength position of the spectrometers. During Sun-oriented operation, calibration and solar measurements will be alternated 15 minutes each.

The final accuracy of the instrument depends upon the absolute accuracy of the available standards such as transfer sources and/or detectors. The precision of measurement depends only upon the design of the instrument for which each subsystem is designed to have an accuracy better than 0.1 percent. The proposed instrument is capable of accuracies better than that of the standards available at the present time.

Only a few spectral solar irradiation measurements ranging from the near ultraviolet to the near infrared have been performed. The most extensive measurements were obtained by means of a spectrometer onboard an aircraft or from high-altitude observatories. The full-disk irradiation flux was measured. Corrections for atmospheric absorption were applied in all of the measurements. Comparison of these data shows discrepancies mainly in the ultraviolet part of

the solar spectrum. Measurement outside the atmosphere over an extended period of time should improve the accuracy and the precision of such measurements, eliminating the absorption corrections needed by ground-based and aircraft experiments. The Space Shuttle seems adequate for such new measurements because it allows not only preflight and postflight calibration of the experiment but also inflight calibrations.

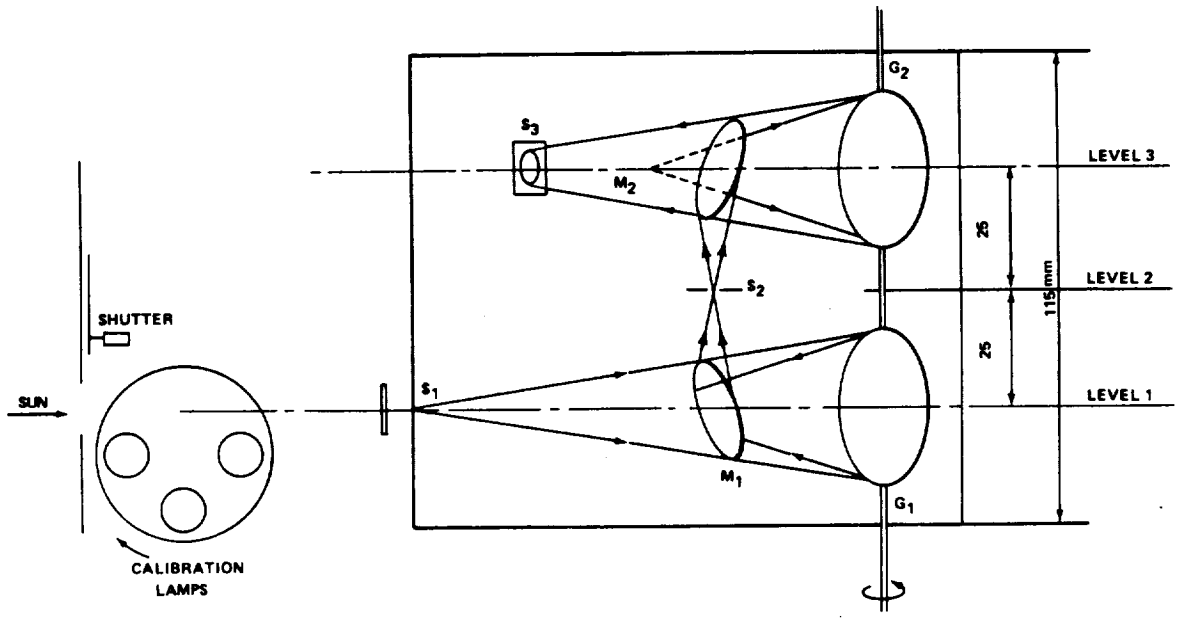


Figure IV-7. Solar spectrum instrument diagram.

SECTION V

LIFE SCIENCES





SPACE SLED VESTIBULAR FACILITY
(1ES200)

ESA Facility

Experiment 1ES201 was originally proposed by the principal investigator together with an accelerating platform (space sled). ESA later agreed to build and provide the "Space Sled Vestibular Facility" (ES200) which can be used in several Spacelab missions. It essentially consists of a plastic seat shell suspended on a gimbal system (Fig. V-1) which can be accelerated by an electromotor along two guiding rails from one end of Spacelab to the other. The acceleration profiles can be preselected between 0.001 and 0.2 g. Oscillating acceleration of the sled will also be possible (motion sickness studies). While one crewmember acts as a test subject in the chair, another, located at the sled control console, initiates each experiment run, monitors the equipment performance and, if necessary, actuates the emergency stop. Acceleration/deceleration is controlled by means of an automatic profile generator.

An important aspect of the facility design is that the test subject may not be able to detect acceleration changes through senses other than those of the balance organs. Visual perception is not possible because the head is enclosed, and noise and vibration levels are kept below the threshold perception level.

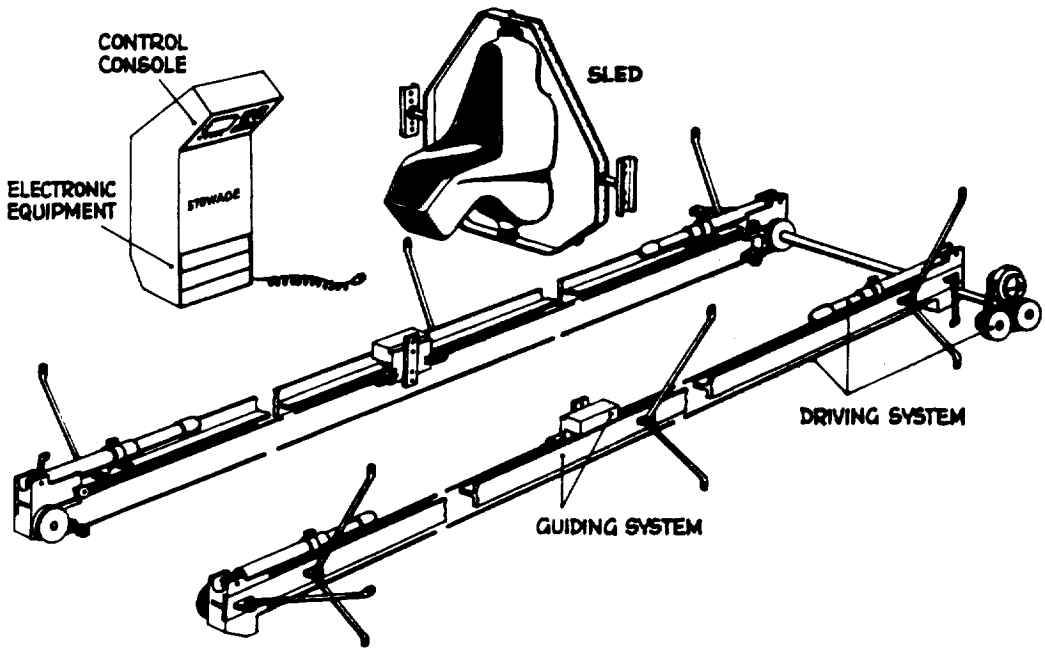


Figure V-1. Space sled facility — schematic perspective.

EFFECTS OF RECTILINEAR ACCELERATIONS, OPTOKINETIC, AND CALORIC STIMULATIONS IN SPACE (1ES201)

R. Von Baumgarten
Johannes Gutenberg Universität, Germany

The goal of this experiment is to increase our present knowledge of the human vestibular system in a weightless environment. In addition, new results concerning basic physiology of the vestibular apparatus and the functional organization of the human space orientation system can be expected when weightlessness is applied as a tool to vestibular research.

Specifically, the experiment is concerned with the study of the effect of linear acceleration of human subjects in orbital weightlessness. This mechanical stimulation will be combined with optokinetic (visual) stimulation to obtain information about visuo-vestibular coordination and about the integration of multisensory stimuli within the orientation centers of the brain. Caloric stimulation of the outer ear channels will be performed without and with simultaneous linear acceleration. The caloric part of the experiment would allow the investigation of whether or not density differences of fluid within the semicircular canal system are responsible for certain eye movements (caloric nystagmus). Caloric stimulation during linear acceleration of the sled would serve as a control and also permit the simultaneous stimulation of the otolith and canal systems.

Another important aim of the sled experiment is to investigate the pathogenesis of space sickness and possibly its prevention. For this purpose, oscillating linear acceleratory stimuli of known time course and force vectors will be applied to a crew member until the first signs of motion sickness occur. To measure vestibular adaptation to the space environment, the thresholds for self-motion detection will be measured using very weak acceleratory stimuli twice, once on the second day and once on the last day of the mission. Also, adaptation to motion sickness-provoking stimuli will be measured by comparing the results of the first with the second dynamic session. Various important physiological and psychological parameters (e.g., eye movements, illusory sensations, respiration, and blood volume pulse) will be recorded.

Between the "dynamic" sled sessions on the second and last day, four "static" sessions are foreseen during which the effects of moving visual (optokinetic) stimuli on the posture and of caloric stimuli on the eye movements will be explored without sled acceleration.

Each of the two dynamic sessions will start with a self-motion threshold determination, using very weak accelerations in the Z-axis (head to feet). The subject reports his sensations verbally and by "joystick" response. The next runs are performed in the Y-axis (side to side of the subject). Rotational eye movements are expected and are recorded by TV or charged coupled device (CCD) technique. The subject has to reset, by joystick operation, a movable target-cross on a TV screen in front of his right eye. The joystick movements indicate the amplitude of any illusory sensations relative to the position of the target-cross. These measurements are followed by optokinetic and caloric stimulations before and during sled runs in the Y- and the X-axis (nose-occiput) of the subject. The dynamic session will be concluded by continuously oscillating the subject back and forth in the X-axis for motion sickness research.

To achieve the overall objectives, five subsystems (or systems related to specific parts of the investigation) are needed in addition to those provided by the sled.

One subsystem is optokinetic stimulation. The test subject's right eye will be stimulated by optical patterns played back from a TV recorder via a small TV monitor. The subject's responses will be recorded through a joystick. The outputs of the joystick can also be used to move a target-cross within the TV picture.

Eye movements of the left eye (x, y, and roll) are measured in another subsystem. The movements will be measured by TV or CCD technique and transmitted to ground in real time or near real time.

In the caloric stimulation subsystem, both inner ears of the test subject can be stimulated by heated or cooled earplugs. Each earplug contains a Peltier element which allows control of ear temperatures between 0°C and 44°C.

During the posture experiment (a fourth subsystem), the test subject will be standing upright with his feet fastened to the floor. His right eye will be stimulated by optical patterns. The reaction of his body will be recorded by the Spacelab TV camera, by electromyographic sensors on his legs, and by a two-axis potentiometer (joystick) mounted to the floor.

The fifth subsystem provides the means for physiological measurements. Within the helmet worn by the test subject there is a miniaturized data acquisition system used to measure approximately 20 parameters such as electronystagmography, electromyography, blood pulse, respiration, linear acceleration, rotational acceleration, etc.

In addition to the parts of the investigation performed in orbit, measurements will be made on the ground. These measurements, some of which will be similar to those made in orbit, are needed to select parameters to be used in orbit and to obtain reference data on the test subjects. These ground-based measurements are to be made both premission and postmission.

The results of the wide variety of experiments using the sled during the first mission shall be used as a baseline for more specific sled experiments on later missions.

VESTIBULAR EXPERIMENTS
(1NS102)

L. R. Young
Massachusetts Institute of Technology, USA

This joint U.S./Canadian research program represents a group of closely related experiments designed to investigate space motion sickness, any associated changes in otolith-mediated responses occurring during weightlessness, and the carryover of any such changes to postflight conditions. The experiments aimed at assessing otolithic responses in space are intended to clarify presumed alterations in vestibular function during weightlessness. The underlying research question is one of environmental neurobiology: How does a fully developed sensory motor system, which receives partially redundant information from several sensory mechanisms, reorganize to account for the loss of usable information from one channel because of an environmental variation? All indications are that adaptation takes place over the course of several days and may carry over to postflight terrestrial conditions. This problem of basic importance can be studied only in an orbiting vehicle. Parabolic flights are too brief, and ground studies are contaminated by the influence of the Earth's gravitational field (i.e., a 1-g bias).

A second major objective relates to space motion sickness and man's well-being and productivity in space. The appearance of space motion sickness on Skylab, combined with earlier experiences on Apollo, Soyuz, Vostok, and Voskhod identified the problem as one of considerable concern for astronaut performance and well-being. Although Skylab experience indicates that adaptation to the zero-gravity environment occurs within 1 week, space sickness remains, from an operational standpoint, a problem for the inexperienced short-term space traveler.

The proposed research program will concentrate on experiments to bring out any change in vestibular function at several levels: vestibulo-ocular reflexes, vestibulo-spinal pathways, cortical functions involving perception of motion and spatial orientation, visual vestibular interaction, and motion sickness susceptibility.

Seven experiments are planned. Experiments 1 and 2 will be performed on the space sled and can be accomplished in the same experimental session. Experiment 1 involves the measurement of perceived velocity during linear acceleration of the body to gain information about linear acceleration thresholds

and zero-gravity motion perception. A joystick will be used to manually indicate subjective motion (direction and velocity). Experiment 2 involves the measurement of eye movements (horizontal, vertical, and rotational) associated with the body accelerations conducted as part of Experiment 1. The space sled will be used to provide the acceleration profiles needed for these two experiments. For Experiment 2, conventional electrooculogram equipment will be used to record horizontal and vertical eye movement. Ocular counter-rolling (OCR) will be recorded photographically.

Experiment 3 will investigate the perception of self-motion and OCR movements induced by a rotating visual field. The experiment will have its own station consisting of a deployable rotating visual field and head immobilization device, a joystick to signal perception of motion, and a camera for recording OCR.

Experiment 4 will investigate the astronaut's awareness of body position in the absence of visual cues. Skylab crews reported that with the eyes closed or the lights out, they eventually lost the sense of where objects were relative to their bodies. This experiment is designed to determine whether this phenomenon can be demonstrated objectively and accurately described and to test several different hypotheses concerning its mechanism. Subjects will be allowed to observe several different targets and will be asked, while blindfolded, to recall where the targets are, point to them, and describe their body image.

Experiment 5 will test the effects of alterations in otolith organ contributions to leg muscle activity in three specific experimental situations, each requiring a different motor control strategy on the part of the subject. Hopping, constant acceleration, and constant velocity tests will be conducted on-orbit as well as preflight and postflight. Spacelab tests will be conducted using elastic cords to provide the forces necessary to keep the subject in place while hopping, or to accelerate him toward the floor in the two types of "falls." Electromyographic activity will be measured in the calf muscle of one leg, and a linear accelerometer will be used to determine vertical accelerations. Subject floor contact will also be determined.

Experiment 6 involves objective measurements of motion sickness susceptibility in space using several methods. One method involves provocative testing using the space sled linear accelerations. The subjects will be stimulated until a standard malaise endpoint is reached or a fixed number of oscillations has been achieved. Motion sickness symptomatology will be graded by a trained payload specialist using the scale developed by Graybiel and used on the Skylab M131 experiment (Human Vestibular Function). The investigators also plan to modify an existing instrumentation technique to objectively measure pallor.

A second method for measuring motion sickness susceptibility involves passive monitoring of crew activity and motion sickness symptomatology without provocative testing. The objective is to determine whether any sickness symptoms which appear can be related to head movement and to investigate the type of head movements required. Head angular and linear accelerations will be monitored on several crew members by means of a very small head-mounted accelerometer package coupled to a multichannel belt tape recorder. Participating crew members will report motion sickness symptoms on a pocket voice recorder. The objective of the motion sickness experiments is to obtain accurate reports on motion sickness symptomatology by well-trained observers and thereby to determine if, in fact, space sickness is an extraterrestrial form of motion sickness and, if so, what types of head movements are particularly nauseogenic. The investigators plan to study and document the crew's increasing resistance to space sickness during the course of the mission.

Whereas the inflight tests described heretofore have as their focus the assessment of changes in otolith function and motion sickness susceptibility during weightlessness, the primary function of the preflight and postflight tests proposed as part of Experiment 7 is the evaluation of any residual effects of the 7-day weightless exposure on vestibulo-spinal and vestibulo-ocular pathways. The ground-based equivalent of almost all of the experimental protocols conducted during flight will be repeated at least twice preflight and postflight for each subject. As part of Experiment 6, motion sickness susceptibility to a variety of provocative tests will be evaluated on several occasions preflight and immediately postflight. The objective of these tests is to determine if they are of value in predicting space sickness susceptibility on-orbit. In addition, several of the ground-based tests will be used to assess vestibular and postural changes: OCR will be measured during a steady tilt as well as during transient linear acceleration and visually induced tilt.

In addition to preflight and postflight testing of the flight crew, tests will be conducted on normal and abnormal subjects not only to develop experimental protocols for the space experiments but also to provide normative, baseline data to which the results of the space testing can be compared.

VESTIBULO-SPINAL REFLEX MECHANISMS
(1NS104)

M. F. Reschke
NASA/Johnson Space Center, USA

Data and observations from previous manned space flights, particularly the Skylab missions, suggest that significant alterations occur in vestibular, neuromuscular, and related sensory system functions upon exposure to weightlessness. Of particular interest has been the observation of changes related to otolith input and vestibulo-spinal responses observed postflight. However, aside from the limited behavioral indications obtained during flight and immediately postflight, little is known about postural reflex behavior during sustained weightlessness. The proposed experiment is designed to yield information about this process.

The investigation has three basic objectives. The first is to investigate, during prolonged weightlessness with Hoffman response (H-reflex) measurement procedures, vestibulo-spinal reflexes associated with vestibular (otolith) responses evoked during an applied linear acceleration. This objective includes not only an evaluation of otolith-induced changes in a major postural muscle but also an investigation with this technique of the adaptive process of the vestibular system and spinal reflex mechanisms to this unique environment. The second objective is to relate space motion sickness to the results of this investigation. This does not imply that any attempt will be made to induce motion sickness symptoms during the experiment. However, the observed relationship between evoked vestibulo-spinal reflexes and any incidental occurrences of motion sickness during any part of the mission would supply valuable information. The third objective is to utilize the ESA-provided sled to obtain the necessary linear oscillations for otolith stimulation.

The proposed experiment involves activation of nerve tissue (tibial N.) with electrical shock and the recording of resulting muscle activity (soleus) with surface electrodes. Soleus/spinal H-reflex testing procedures will be used in conjunction with linear oscillation through the subject's mid-body or Z-axis. This method will allow the acquisition of extensive and highly descriptive quantitative data on the status of the H-reflex.

The experiment will utilize a small package of rack- and sled-mounted, low-power electronic equipment, including an experimental control panel, a stimulus isolation unit, physiological amplifiers, monitoring equipment, and a

dedicated microprocessor, located in the Spacelab. Experiment control will be accomplished with the microprocessor which has been programmed to sequence the stimuli necessary to elicit the H-reflex, collect data obtained from the soleus muscle, and store the responses while they are being averaged or analyzed prior to downlink through the onboard telemetry system.

All crew commands to the microprocessor will be issued through a switch panel. These commands will include sled frequency information, display commands, and system mode (i.e., test, static stimulate, and run).

The investigators' laboratory, using human subjects, recently has employed soleus/spinal H-reflex testing procedures in conjunction with an accelerative stimulus of approximately 1.8 g through zero-g (provided by NASA's KC-135 parabolic aircraft) to assess changes in postural muscles as a function of variable gravity load on the otoliths. Results indicate that weightlessness induces a potentiation of the H-response which may last throughout the period of zero-g, and that hyper-g results in an inhibition or, in some cases, a complete absence of this response. The investigators wish to expand these results to longer periods of weightlessness, with the expectation that long-term adaptations (7 days) will be evident in the results which reflect the crew members' increased ability to function effectively in space.

THE INFLUENCE OF SPACE FLIGHT ON ERYTHROKINETICS IN MAN (1NS103)

Stephen L. Kimzey
NASA/Johnson Space Center, USA

The most consistent finding relative to the influence of space flight on the hematologic system in man has been a significant reduction in the circulating red cell mass. This phenomenon has been observed in both the American (Gemini, Apollo, Skylab, and ASTP missions) and Russian (Soyuz-Salyut missions) manned programs. The exact mechanism and etiology of this loss is currently unknown, but the most recent data from the Skylab flights strongly implicate a suppression of normal erythropoiesis.

The flight duration of Spacelab 1 (7 days) will probably result in only minimal changes (5 to 8 percent) in the red cell mass compared to the longer Skylab flights. However, the changes in the erythrokinetics begin during the early phases of the mission (perhaps within the first 24 hours), and it is essential to document these early changes to establish the exact mechanism of the response.

The purpose of this experiment is to measure specific factors relative to the control of erythrokinetics, particularly erythropoiesis, in man which might be altered during the first 7 days of exposure to the weightless environment of space flight. It is anticipated that these data will provide new information relative to the mechanism by which the red cell mass is reduced during space flight. Such information is necessary to assess the overall impact of the observed red cell mass change on man's potential for participation in space flight missions of varying types and duration.

Blood samples will be collected from crew members during the preflight, inflight, and postflight periods. These samples and samples taken from control groups on the ground will be analyzed as described in this section. The choice of specific parameters for analysis in this study was based on the data previously collected, the restraints imposed by the use of human subjects, and the guidelines established for the first Spacelab mission. The experiment is designed to establish: (1) if there is a significant change in red cell mass and plasma volume during the initial period of exposure to weightlessness, (2) if the plasma concentration of erythropoietin is reduced, (3) if there is an increase in the plasma concentration of erythropoietin inhibitors, (4) if there is a change in the effectiveness of erythropoiesis, and (5) if the number and age distribution of reticulocytes are altered.

To meet these goals, an integrated test protocol has been designed to examine: (1) hemoconcentration and red cell morphology, (2) blood volume, (3) erythropoietin — activation and/or inhibition, (4) hemoglobin-oxygen affinity (indirect), (5) serum components related to the control of erythropoiesis, (6) iron kinetics, and (7) reticulocyte response.

A flow diagram for the control of erythropoiesis (Fig. V-2) has been constructed to identify those components most likely to influence the red cell mass during space flight. The blocks identified by numbers form the basis for this experiment protocol. Emphasis will be placed on evaluation of the end result (change in red cell mass) and the measurement of erythropoietin and rate of erythropoiesis. Although documentation of a change in the plasma concentration of erythropoietin will not necessarily reveal the mechanism of the "anemia of space flight," it will serve to identify the areas which need additional study to fully understand this process.

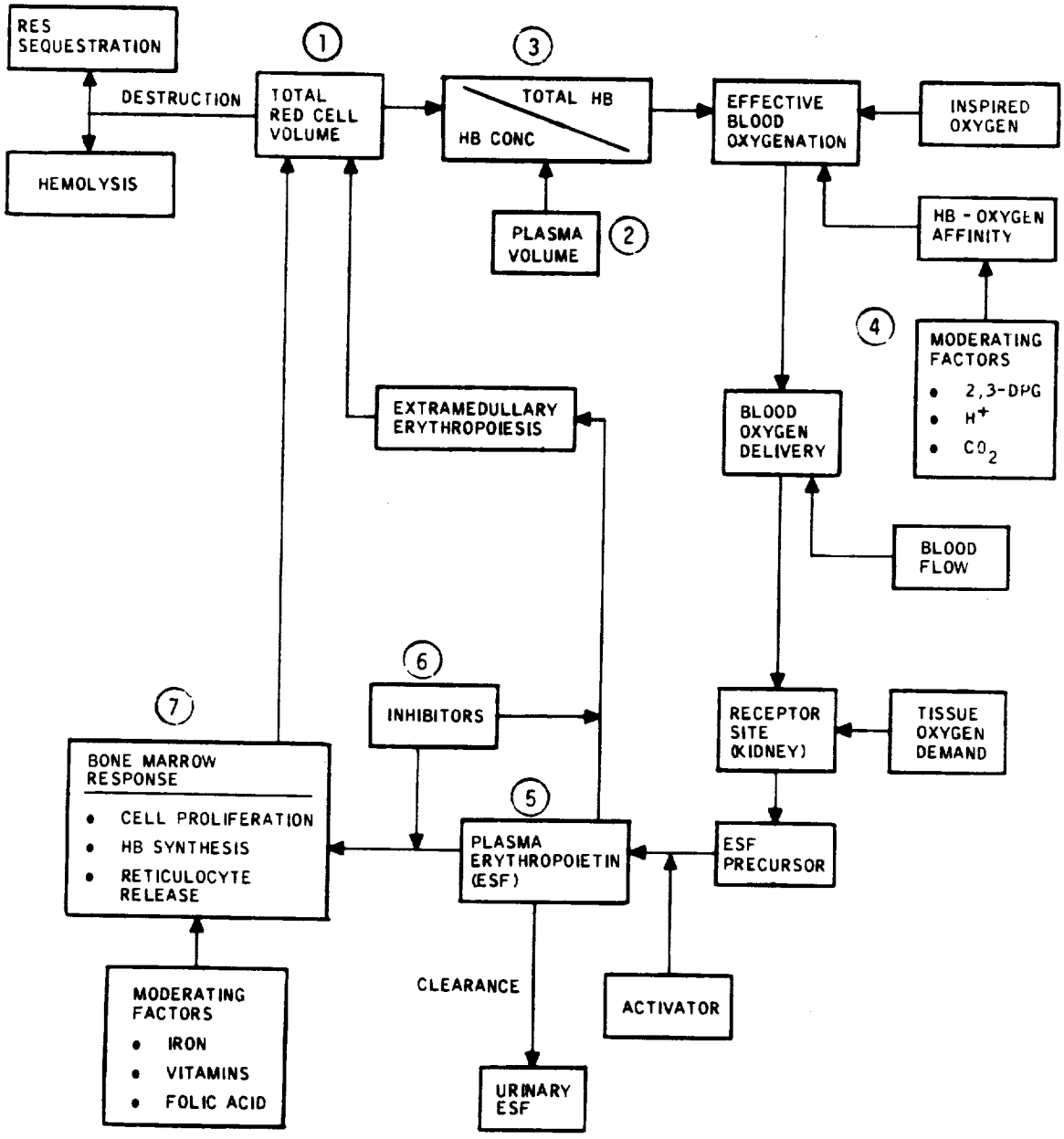


Figure V-2. Flow diagram for control of erythropoiesis.

1ES026
1ES032

MEASUREMENT OF CENTRAL VENOUS PRESSURE AND DETERMINATION OF HORMONES IN BLOOD SERUM DURING WEIGHTLESSNESS (1ES026 and 1ES032)

Otto H. Gauer
Physiologisches Institut der Freien Universität, Germany

Measurement of Central Venous Pressure from an Arm Vein (1ES026)

Upon entry into the weightless condition, the Skylab astronauts experienced a severe engorgement of the cephalad circulation characterized by distended neck veins, a puffy face, and nasal congestions. These findings were corroborated by the appearance of the astronauts' "chicken legs" resulting from a drastic loss of extracellular fluid (ECF) and blood volume from the thighs and calves of the order of 2 liters. The forces which caused these huge fluid shifts are not known. It is impossible to produce comparable effects by the elimination of hydrostatic pressures by a mere change of posture in the 1-g field. One may speculate that the compliance of the interstitial fluid spaces in the long axis of the body varies and is regulated by some factors related to gravity.

There can be little doubt that the major portion of the 2 liters of ECF displaced from the lower extremities is taken up by the intrathoracic circulation. Since this region is the origin of important reflex activity, it is proposed to record central venous pressure to obtain objective data on the degree of the engorgement. Of practical importance is the question of how close the astronauts are to pulmonary edema and whether the pressure falls toward normal during the time of the mission. Since hydrostatic pressure gradients are absent in zero-gravity and flow resistance is small in the distended veins, central venous pressure can be measured by simply puncturing an arm vein.

For this experiment, six sterilized needle-manometer (strain gage) assemblies, filled with heparin-saline will be taken aboard. The Shuttle crew will take turns, one as operator and the other as subject, to puncture an antecubital vein and record venous pressure for approximately 2 minutes. Afterwards, the manometer is removed from the needle, and blood samples are drawn through the same needle for hormone estimation (1ES032). The first pair of measurements is to be done as soon as possible, not later than 6 to 18 hours after entry into weightlessness. One measurement is planned as late as possible in the mission. A third measurement in the middle of the

mission is highly desirable. The measurements must be done on the same subject for the series of three measurements and preferably at the same subjective time of the day. The pressures will be recorded on a small battery-powered tape recorder and will be evaluated after the end of the mission.

Collection of Blood Samples for Hormone Estimations (1ES032)

Gross deviations from normal fluid and mineral metabolism have been observed in weightlessness. They are in all likelihood initiated by the central engorgement of the low pressure system (Gauer-Henry-reflex). Extensive analyses of hormones responsible for the control of water and mineral balance were performed in Skylab. However, many questions remain to be answered. For various reasons the following determinations could not be made at the time of the Skylab missions: (1) antidiuretic hormone (ADH) in plasma and (2) prostaglandins. ADH plays an important role in volume control. The determination of its presence in plasma is now feasible. The prostaglandins are possible candidates for a natriuretic principle which seems to contribute to the regulation of mineral metabolism in weightlessness.

After completion of venous pressure recording, the manometer is detached, and 50 milliliters of blood is drawn and centrifuged. The serum fraction is stored at below -20°C. After return to ground, assays will be made for the following hormones: vasopressin, catecholamines, renin, aldosterone, corticosteroids, and prostaglandin E_1.

As noted, a number of hitherto unknown problems related to the control of fluid volume and the physiology of the low pressure system of the circulation were discovered during the Skylab missions. If they can be solved (and that is the purpose of these experiments), our knowledge of the overall regulation of the circulation and fluid metabolism in health and disease may be greatly augmented.

EFFECTS OF PROLONGED WEIGHTLESSNESS ON THE HUMORAL IMMUNE RESPONSE OF HUMANS (1NS105)

E. W. Voss, Jr.
University of Illinois, USA

The objectives of the investigation are (1) to use the unique properties of the space environment to improve understanding of life processes on Earth and (2) to enhance man's well-being and productivity in space.

Despite the significant recent advances in our understanding of the immune response, several important aspects relevant to the first objective remain unexplored. Among these is the interrelationship of the various classes of immunoglobulins. Since it is becoming more apparent that various immunoglobulins represent separate and distinct systems, it has not been possible to clearly investigate their interrelationship. One possible mechanism to study these potential interrelationships is to use the effect of weightlessness as a stress factor and subsequently measure inhibitory, compensatory, or enhancing interrelationships. It is conceivable that the various systems will not respond to sustained weightlessness equivalently, and thereby a mechanism to study interrelationships between the various classes will be available. Knowledge relevant to interrelationships between the immunoglobulin classes may lead to future control and manipulation of the immune response for obvious medical benefits.

The second objective is of considerable practical significance to future manned space flights, since it is important to establish the state of immune competency under conditions of sustained weightlessness. This is important from at least two standpoints. First, knowledge relevant to the capability of humans in space to respond immunologically to potential foreign pathogens is of obvious importance. Second, a suppressed immune response may jeopardize the health of humans on prolonged space flights.

After obtaining baseline data on all flight personnel, the experimental approach will be to obtain blood samples from space personnel just prior to their entering the Orbiter, 24 hours prior to the return flight, and 15 days after the mission is complete. Those samples taken prior to entering the Orbiter will be considered preflight controls, and the levels of each immunoglobulin class will be determined for every individual. Antibody levels for certain common antigens will also be analyzed to determine preflight titers. The latter

will be correlated to the levels of immunoglobulin proteins. All values established will be used as reference values for comparison to the postflight sera analyses. Samples taken at the latter two times will be analyzed in a manner similar to the preflight sera.

The only equipment required onboard Spacelab 1 will be sterile plastic syringes containing anticoagulant (approximately 1.0 milliliter), hypodermic needles, and a plastic container to hold the tubes containing the blood samples in a refrigerator.

Analyses of all blood samples should reveal if weightlessness is a stress factor on the humoral immune response. If any effects are observed, the data should reveal if the effects are general or specific. Compensatory reactions between classes of immunoglobulins should be evident by the experimental design. Finally, recoverability will be determined if suppression effects are evident.

EFFECT OF WEIGHTLESSNESS ON LYMPHOCYTE PROLIFERATION (1ES031)

Augusto Cogoli
Eidgenosische Technische Hochschule, Switzerland

The in vitro mitogenic stimulation of lymphocytes represents a good model for the study of cell differentiation. Results of previous experiments strongly suggest that weightlessness may affect cell proliferation. When lymphocytes are constantly cultured in an environment with twice the Earth's gravitational force (g), cell activation by mitogens is remarkably accelerated compared to the activation of cells kept at 1-g.

The low-gravity environment of Spacelab provides a unique opportunity to perform investigations in cell and molecular biology. One of the most appealing features is the transformation of gravity, a physical entity always constant in our ground laboratory, into a variable parameter like temperature or concentration. Consequently, living organisms which underwent evolution and development in a constant gravitational environment are suddenly confronted with a new situation. Therefore, the survival and proliferation of mammalian cells is a challenging aspect of space biology. We not only face the possible effects of zero-gravity per se, but we must also master constraints arising from the limited facilities on board spaceships and from the safety requirements which apply to the hardware to be flown on manned spaceflights. Moreover, it is known that long duration spaceflights and space stations where men will spend a significant amount of time are actually planned. Consequently, it is important to investigate the behavior and the survival capacity of living systems in a "space environment."

In our approach to this problem we are studying the stimulation of lymphocytes by mitogens in vitro. Lymphocytes are the cells responsible for the immune response. Specific antigen receptors are localized on the cell surface. The interaction between antigen and receptor stimulates lymphocytes to proliferate and to produce antigen specific antibodies (the last limited to cells of the B-type). A similar reaction can be triggered in vitro when lymphocytes are exposed to a number of substances called mitogens. The transition from the status of "resting" to that of stimulated lymphocytes is an example of cell differentiation. Therefore, the in vitro activation of lymphocytes by mitogens at zero-gravity can be regarded as a suitable model for the study of (1) cell survival, (2) the triggering of the immune response, and (3) the mechanism of cell differentiation in weightlessness.

The objective of the experiment is the study of the effect of weightlessness on lymphocyte proliferation to detect possible alteration of the cells responsible for the immune response during long-duration spaceflights. As a consequence, further information is expected on the mechanism of cell differentiation.

Human lymphocytes in culture medium will be delivered shortly before launch in an incubator which will be kept at 37°C by batteries and stowed in the Orbiter mid-deck. When Spacelab is in orbit, the incubator will be transferred into the Spacelab module and fixed onto a rack. The incubator will then be connected to the dc power supplied by Spacelab. Mitogen is added to the culture by the payload specialist. A control without mitogen is run in parallel. After 70 hours of incubation, radioactive thymidine is added. Thymidine is a constituent of DNA and will be incorporated into dividing (stimulated) cells at a higher rate than into resting (control) cells. After 2 hours, cellular activity will be stopped by fixation with glutaraldehyde and the incubator power will be switched off.

After landing of the spacecraft, the amount of thymidine incorporated into the cells will be determined in the ground laboratory. The cell morphology and the distribution of cell organelles will be investigated by electron microscopy. A parallel experiment will be run with an aliquote of the same cell batch in the ground laboratory at Cape Canaveral.

The hardware for this experiment includes culture flasks and an incubator. The tissue culture flasks consist of four cubic culture chambers made of aluminum and fixed together to form a block which fits in the incubator. The inner culture chamber is cylindrical and can contain up to 15 milliliters of culture. Holes for three syringes are drilled in the exposed sides of each chamber. By means of a piston, a solution of the volume of 0.2 milliliters can be added to the culture. The culture chamber is provided with a stirrer which can be turned manually from the outside. Cell viability is satisfactory in this system.

The incubator has the following characteristics: external dimensions — 19 × 16 × 7 centimeters, weight with the culture chambers — 5.5 kilograms. The temperature can be kept at 37°C for up to 24 hours by batteries during the prelaunch and the launch phases. During the experiment the incubator will be heated by the 28 volt dc supplied by Spacelab.

There are well-substantiated reasons for expecting spaceflight to produce effects on lymphocyte activation:

1) Lymphocytes from crew members of Soyuz 6, 7, and 8 showed a different reactivity toward phytohemagglutinin (a widely used mitogen) after flight. A delay in blastogenesis and mitosis was observed. It has not yet been established whether this effect is due to weightlessness per se or to metabolic impairments (e.g., metabolism of calcium or chlorides) occurring during spaceflights.

2) A number of relevant observations were made during the experiments of Biosatellite II. Weightlessness alone interferred with the mitotic spindle mechanism in microspores, megaspores, and root tip cells of the wild flower Tradescantia. In addition, a lowered mitotic rate, increased cell length, and enlarged nuclear volume were observed in wheat seedling root tip cells in the absence of gravity.

3) Cell organelles such as nuclei or ribosomes have different densities. It is conceivable that weightlessness and gravity have an influence on the intracellular distribution of cell organelles, particularly in lymphocytes which differentiate into larger blast cells with uropods. This assumption is sustained by the application of the Boltzmann equation to the distribution of cell organelles in the cell.

4) Recent work in our laboratory has shown that high-gravity levels have a dramatic effect on lymphocyte activation.

THREE-DIMENSIONAL BALLISTOCARDIOGRAPHY IN WEIGHTLESSNESS (1ES028)

A. Scano
University of Rome, Italy

Ballistocardiography is a method of physiological investigation consisting of the recording of periodic motions of the human body which result from heart activity and blood ejection into the aorta and its main branches. These small displacements or the correlated accelerations (mainly along Z-axis) can be recorded as a ballistocardiogram by means of photo or electronic devices as a series of waves in temporal relationship to the events in the cardiac cycle. The terrestrial gravitational field interferes in any technique of supporting the subject's weight; in particular, it makes it difficult to record a three-dimensional ballistocardiogram. Gravity also affects the blood circulation through hydrostatic phenomena and correlated orthostatic regulations. Nevertheless, ballistocardiography remains an interesting method for simple, rapid, noninvasive cardiovascular performance evaluation, and recent experimental contributions support this view.

The primary aim of the proposed research is to record a three-dimensional ballistocardiogram under a unique condition, peculiar to space flight (that is, on man freely levitating in weightlessness), and to compare it with tracings recorded on the same subject on the ground. The investigators hope to obtain a recording that is unaffected by any artifact and that will be useful for clarifying the meaning of ballistocardiogram waves in different physiological and perhaps pathological conditions. Another purpose is to investigate cardiovascular and possibly fluid adaptations to weightlessness from data collected almost simultaneously on the same subjects during the other cardiovascular and metabolic experiments. Other objectives are to gather biomechanical data on man's respiratory movements, body accelerations, and vibrations in relation to head, limbs, and trunk motions.

At present it appears that the more reliable and simple technique is to secure to the subject's back suitable miniaccelerometers in triaxial arrangement by means of a very light and rigid frame fastened with belts (Fig. V-3 and V-4). The output of these transducers and a peripheral electrocardiogram lead will be recorded on tape by means of a four-track miniature recorder connected by wire (total weight no more than 1.5 kilograms). The unit is self-contained with no connections to Spacelab systems. Recordings will be analyzed postflight.

A standard experimental sequence in flight will consist of 30 seconds recording during normal breathing (body stretched out and muscles relaxed); 30 seconds recording during breathholding; 30 seconds recording during normal breathing (body in crouching posture); 30 seconds breathing through respiratory resistance; 3 minutes of physical exercise and 60 seconds recording immediately after stopping; 2 minutes rest; 30 seconds normal breathing; 30 seconds breath holding; 30 seconds with upper limbs in strong isometric muscle contraction. Altogether, approximately 12 minutes for each sequence would be required. This pattern should be repeated (at about the same circadian time) every day, or at least every second day the subjects remain in space, on two persons — ideally, the youngest and the oldest scientists onboard.

Prior to and after the flight, the subjects will receive cardiovascular examinations, including ballistocardiography recordings and stroke volume determinations (i.e., a determination of the volume of blood ejected during systole from the left ventricle into the aorta), physical exercise tests with metabolic measurements, and a basic anthropometric survey.

In conclusion, this investigation aims at improving our knowledge of heart functioning and efficiency in various physiological conditions. Weightlessness will be used as a unique tool to help solve some clinical and space cardiovascular problems.

ORIGINAL PAGE
BLACK AND WHITE PHOTOGRAPH

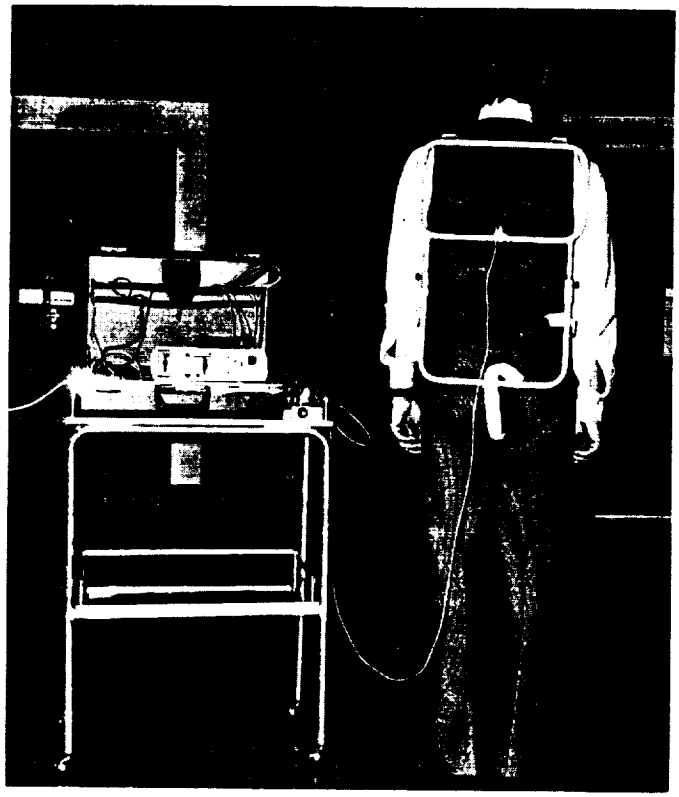


Figure V-3. Back view of ballistocardiographic apparatus.

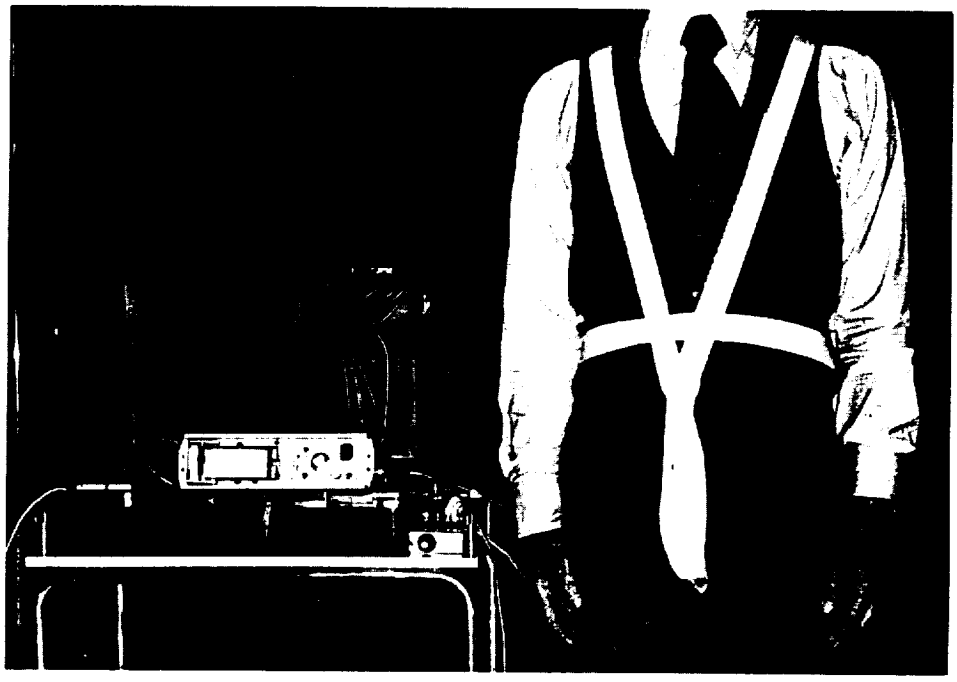


Figure V-4. Front view of ballistocardiographic apparatus.

PERSONAL MINIATURE ELECTROPHYSIOLOGICAL TAPE RECORDER (1ES030)

H. Green
Clinical Research Center, United Kingdom

In all previous space flights the personnel exposed to zero-gravity conditions have been highly selected astronauts, many of them with test pilot experience. We are now entering an age in which not only many more people will experience space flight but also, in terms of age, fitness, and previous stress exposure, they will be much more representative of the normal population.

Nothing is known about the physiological reactions of such a population to the overall stress profile of a mission. Such information is not only of scientific interest, but it should also have a bearing on personnel selection and the determination of behavioral guidelines for various stages of the flight. Therefore, the objectives of this experiment are to collect general physiological data on normal man in an abnormal environment to form the basis of future physiological studies; to collect continuous electroencephalogram (EEG) and electrooculogram (EOG) data to study sleep levels (the Skylab EEG studies were of very limited duration); to collect EEG, EOG, and electrocardiogram (EKG) data during ascent into and descent from orbit; and to flight test the miniature tape recorder for future use.

It is proposed to use a standard Oxford Instruments Medilog recorder (Fig. V-5), of which some thousands are in service, as the data capture instrument. It is a battery-powered, four-channel cassette tape recorder with a 24 hour endurance, weighing 400 grams, and with dimensions of 130 × 120 × 50 millimeters. It is carried on the person, usually attached to a belt, and together with its electrode leads imposes virtually no restrictions on the wearer. For EOG's/EEG's, a small preamplifier is required (10 × 6 × 12 millimeters) which is worn on a light neck band.

The signals to be recorded are the EKG, EOG, EEG, and a timing and event marker. The data will give information about heart rate (interval histogram and its derivatives) and morphology changes (frequency range 0.1 to 100 hertz), and document adaptation to zero-gravity by using the EOG and EEG signals for sleep staging. Ideally, the subject should be studied for 3 or 4 days before launch, throughout the mission, and for a few days in the postflight period.

In addition to the recorder, spare batteries, tape cassettes, and an electrode reapplication outfit will be required. A very small battery-powered monitor would be used to check the electrodes and to permit short sections of tape to be played back for quality control. The overall weight of all the equipment is of the order of 3 kilograms. All replay and analysis would be accomplished on existing equipment after the end of the mission. With the exception of the monitor box, all the equipment and techniques described are in daily use in clinical medicine.

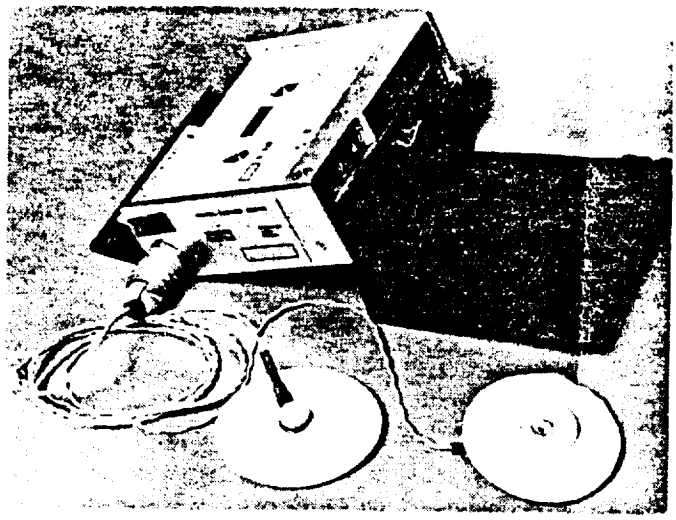


Figure V-5. General view of the recorder showing the foam-backed electrodes.

MASS DISCRIMINATION DURING WEIGHTLESSNESS (1ES025)

Helen Ross
University of Stirling, United Kingdom

This experiment is concerned with the ability of the astronaut to distinguish between the mass of objects, when both he and the objects are in the weightless state. The situation differs in at least two ways from a comparable experiment on weight-discrimination on Earth: (1) the test objects differ only in mass, and not in weight, and (2) the astronaut himself is also weightless, and the changed weight of his arm may interfere with his ability to discriminate.

In previous experiments, weightless conditions have been partially simulated by supporting the test objects on an air-bearing table. The experimental subjects estimated the mass of the objects by pushing them over the cushion of air. Under these conditions, the threshold of discrimination was approximately twice as large as under normal conditions. However, the subject's arm retained its normal weight during the experiment. Other experiments involving an increase or decrease in the weight of the arm have shown that this is an important variable. In general, subjects perform poorly when the arm weight is first increased or decreased, but their performance returns to approximately the normal level when time is allowed for adaptation to the change in weight.

The main object of this experiment is to compare the threshold for weight-discrimination on Earth with that for mass-discrimination in orbit. We can predict that the threshold for mass-discrimination will be higher than for weight-discrimination due to the loss of sensory information concerning weight. However, once the astronaut has adapted to the weightless state, his mass-discrimination will probably be finer than simulations with air-bearing tables have suggested.

Tests will be conducted premission and postmission and early and late during the mission while the crew is experiencing weightlessness. The object of the premission test is to obtain baseline data on weight discrimination under normal gravitational conditions. The object of the early weightless test is to obtain data on mass-discrimination shortly after entering orbit, before the astronaut has become fully adapted to the weightless state. The late weightless test will be conducted to obtain similar data after a few days of weightlessness, when the astronaut should be fully adapted. The postmission test objective is to obtain data on weight-discrimination on return to Earth.

The reason for the premission test is to obtain baseline data on weight-discrimination for comparison with the data on mass-discrimination during the weightlessness.

The early and late weightless tests will provide the data on mass-discrimination, and any difference between the two will show the effects of adaptation or other changes.

The postmission test will show whether there is any after-effect of space flight on weight-discrimination on Earth. It is probable that the astronauts will initially be maladapted to Earth's gravity. This may result in a raised threshold for weight-discrimination in comparison with the premission test.

The apparatus consists of a mass discrimination box (Fig. V-6), which measures 30 × 20 × 14 centimeters when closed. The box opens in half and unfolds to reveal 24 balls, each of 3 centimeters diameter. The balls are fastened in position by cords, held under tension, which can be released when the balls are in use. The balls are of different masses, and each ball is labeled with a letter. A drawer containing a pencil and record cards can be pulled out from one side of the box.

The box is stowed in a rack in the module when not in use. The astronaut who is performing the test takes the box from the rack and clamps it in an open position on a work surface. He opens the drawer containing the record cards. The record cards contain a list of paired comparisons (e.g., BG, FD, CA, etc.). The astronaut releases the cords for the weights labeled B and G, then throws each ball from hand to hand in turn and decides which of the balls has the greater mass. He underlines the letter corresponding to that ball on the record card. He secures the cords and balls in their correct places in the box and then proceeds to make a comparison for the next pair in the same way. When he has completed all the comparisons listed on the record card, he places the card at the bottom of the pile of cards in the drawer, closes the drawer, fastens the box together, unclamps the box, and stows the box back in the rack.

The various paired comparisons vary in the number of grams difference in mass between the two balls, though many of the pairs are actually repeats of other pairs. The results will show which intervals can be correctly discriminated on a better-than-chance basis and allow the "threshold" interval to be determined. Performance under 1 g and zero-g can thus be compared in a quantified manner.

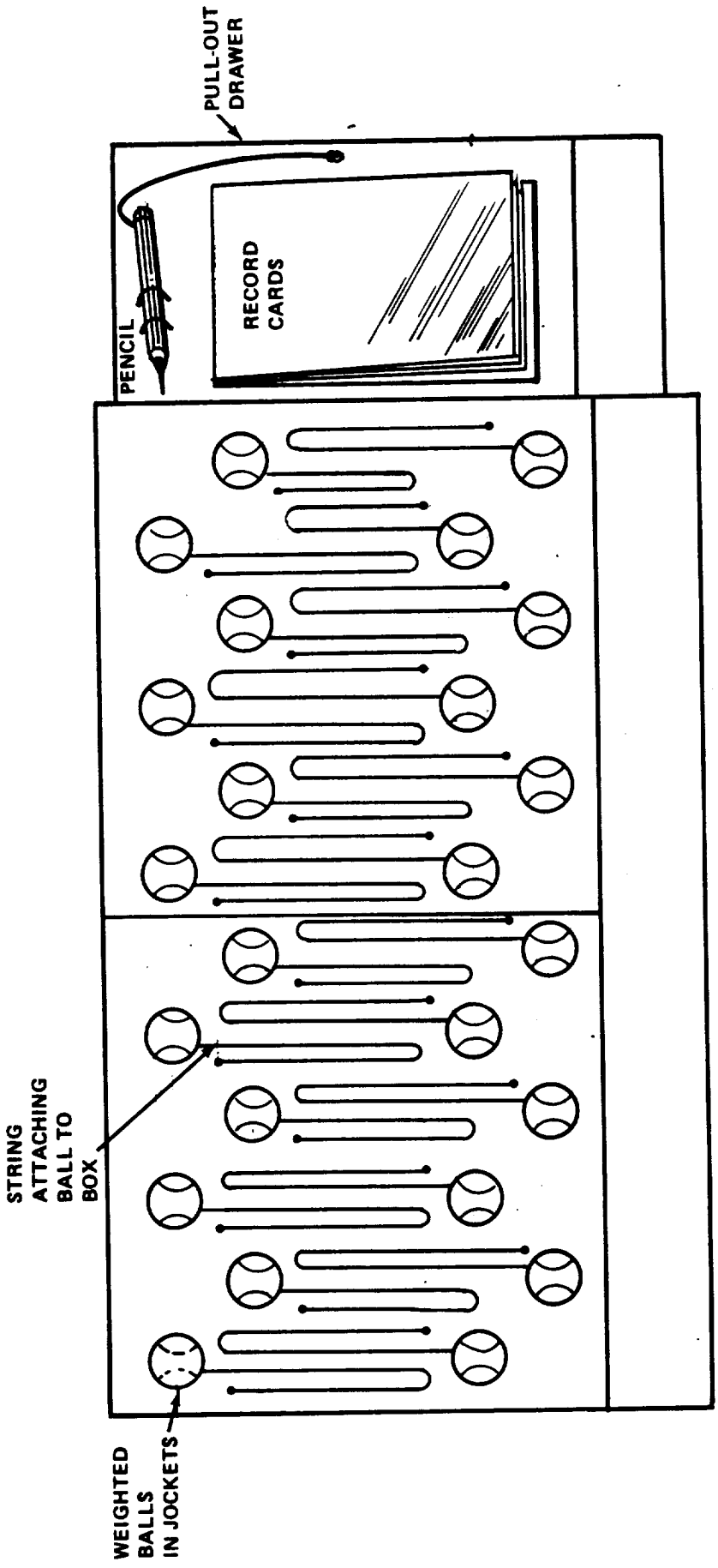


Figure V-6. Mass-discrimination box.

NUTATION OF HELIANTHUS ANNUUS IN A MICROGRAVITY ENVIRONMENT (1NS101)

Allan H. Brown
University of Pennsylvania, USA

Interest in nutation and in the kind of biophysical mechanism that can account for it is at least partly due to the fact that we do not understand how a plant senses the Earth's gravitational force or other accelerating forces, how it processes the information and transduces it into chemical form, and how the hormonally transmitted signals from sensor to responding tissue are capable of ordering an appropriate differential growth response. If something of basic importance concerning nutation can be learned, such knowledge might have application to the even broader and still vexing question: How does a plant know which way is up?

Nutations of plant organs have been studied by plant physiologists for more than a century. Roots, tendrils, shoot tips, hypocotyls, pedicels, etc., usually exhibit growth movements in which the structure describes elliptical (often circular) patterns (Fig. V-7). Because the organ is growing, the locus is actually a helix which is often irregular. The period of oscillation usually is in the range $10^{1.5}$ to $10^{2.5}$ minutes and is temperature dependent.

Nutation is affected by gravity and can be altered by various kinds of geotropic stimuli. It even has been suggested that nutation is completely dependent on gravity and that it can be explained simply as a succession of geotropic responses whereby the plant organ "seeks" a preferred orientation such as the plumb line but continuously overcompensates to generate a hunting pattern. Modern proponents of the geotropic-response-with-overshoot view of nutation have used that concept as the basis for a mathematical model. Within the past decade the model has been tested by plant experimentation and by computer simulation. However, that excellent biophysical work has not swayed modern adherents to the Darwinian view that nutations are endogenously driven.

The only way we can marshal critical experimental evidence to decide between the Darwinian concept of endogenously motivated nutation and the more mechanistic concept of gravity-dependent nutation will be to determine if nutation proceeds in the absence of a gravitational force. Space laboratories were invented for answering just that kind of question, and that is the objective of this experiment. If nutation persists in weightlessness, parameters describing the motion will be measured.

Simulation tests of the weightless condition (e.g., on horizontal clinostats) have been attempted; but, as everyone knows, any Earth-bound simulation of the state of free fall must be imperfect at best. Tests using simulated weightlessness have been inconclusive chiefly because one cannot be sure how effective the simulation may be. The adequacy of simulations can be determined only if results obtained on the simulator can be compared with those obtained in a space experiment.

In the present experiment [Helianthus Flight Experiment (HEFLEX)] the test subject is a dwarf sunflower seedling, Helianthus annuus. Nutation will be measured by recording in time lapse mode the video images of a population of seedlings that were grown at 1-g but will be observed at virtual zero-gravity (Fig. V-8). Only infrared illumination and an infrared-sensitive video camera will be used (to avoid certain complications caused by the plants' responses to visible light). Images will be recorded at 10-minute intervals on video tape.

Prior to launch, a set of plant specimens at a succession of growth stages will be placed onboard the Orbiter. Some plants will be ready to go on camera the first day of the Spacelab 1 mission. Others will be installed in a rotor that can impose a 1-g centripetal force until it is their turn to be placed before the camera. Toward the end of the mission some plants that were brought onboard as dry seeds and, after planting by a payload specialist to initiate germination, were grown only on the rotor for 4 days will be put on camera.

Four plants will be in view of the camera at any one time. The payload specialist will change plants once each day. He will select from a set of eight plants at the proper age the four best for surveillance by the camera.

After the mission, the video tape will be recovered and the plant images will be displayed on a video monitor in the laboratory, photographed on 16 millimeter film, and analyzed frame by frame to determine the kinetics of nutation for each specimen tested.

If nutational oscillations in the HEFLEX data can be identified, the concept of a gravity-driven movement cannot apply to Helianthus seedlings without some modification. On the other hand, if the investigators do not identify nutations, they will be justified in concluding that the endogenous concept is not supported by HEFLEX results.

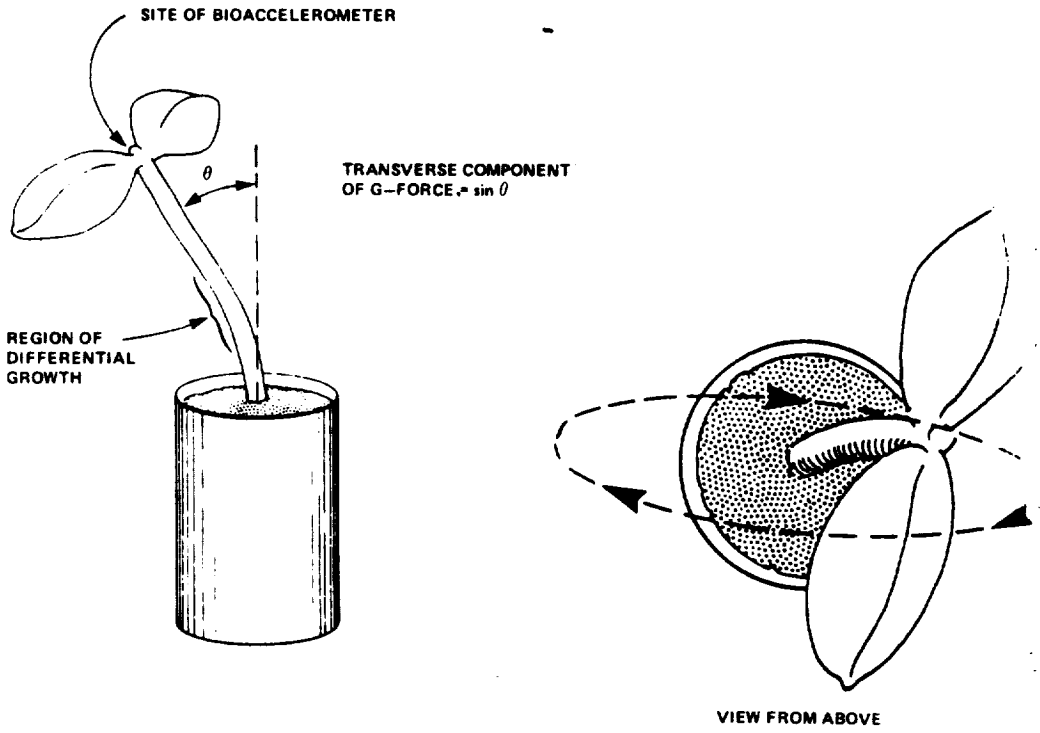


Figure V-7. Pattern of plant movement.

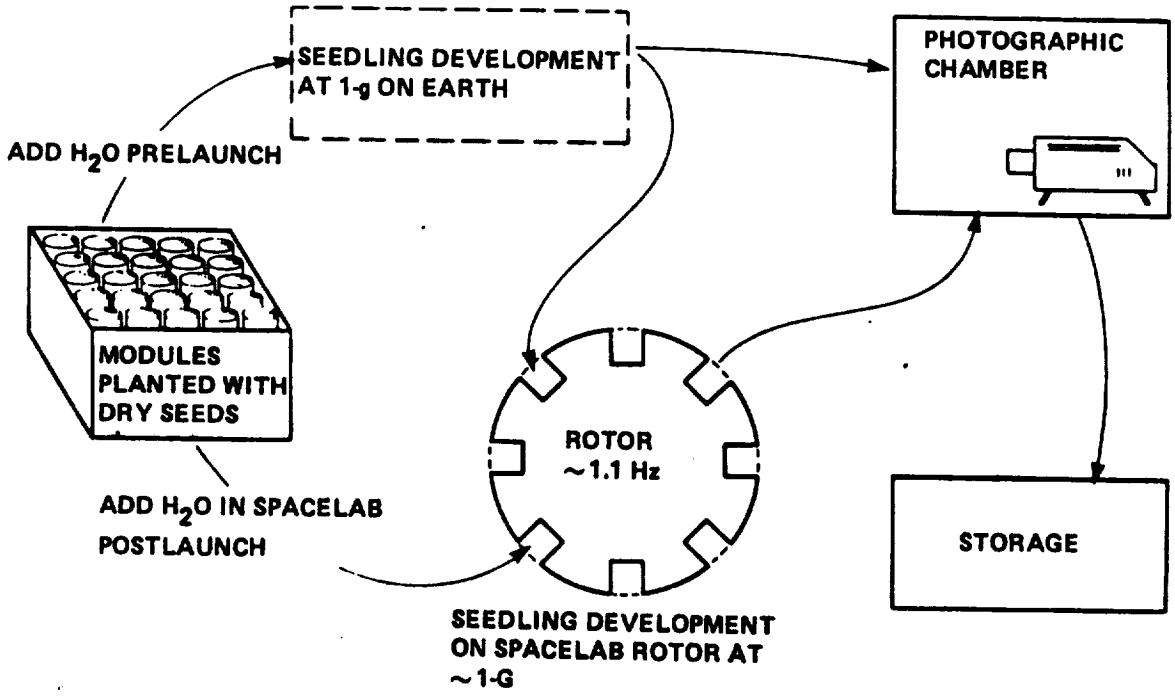


Figure V-8. HEFLEX experiment flow.

PRELIMINARY CHARACTERIZATION OF PERSISTING CIRCADIAN RHYTHMS DURING SPACEFLIGHT: NEUROSPORA AS A MODEL SYSTEM (1NS007)

Frank M. Sulzman
Harvard Medical School, USA

For many years it has been known that numerous physiological variables are not constant during the 24 hour day but, rather, exhibit diurnal variations. Because these circadian rhythms can persist in conditions of constant temperature and constant light or darkness, they have been regarded by most investigators to be manifestations of an endogenous timekeeping system. Additional evidence often cited as supporting the endogenous clock hypothesis is the fact that while the period lengths in constant conditions are approximately 24 hours, only rarely are they exactly 24.0 hours, and, in fact, these periods need not match any known geophysical periodicity. Thus, this biological clock which provides the organism with temporal information is capable of measuring time in the absence of environmental signals.

An alternative explanation for these persisting circadian rhythms which has been argued for many years proposes that subtle changes in geophysical variables provide temporal information to organisms in otherwise constant conditions; i.e., the timing system is exogenous, and organisms perceive daily timing signals such as periodic fluctuations in air pressure or slight fluctuations in gravity associated with the rotation of the Earth in relation to the Sun and the Moon. It has been shown that geophysical variables (e.g., atmoshperic pressure and electromagnetic radiation) can affect circadian rhythms. An obvious test of this exogenous clock hypothesis would be to determine if circadian rhythms persist outside of the Earth's environment.

Initial examination of the effects of the Spacelab environment on the temporal organization of living systems can best be undertaken by following circadian rhythms in microorganisms. Many eukaryotic microorganisms exhibit circadian rhythms whose formal properties (entrainment, persistence, period length, and the effects of light and temperature) are very similar to those of more complex living systems, viz., mammals.

The common fungus Neurospora crassa provides an excellent experimental model for this study because of its well-characterized circadian rhythm of growth. The band strain of Neurospora produces patches of extensive growth

approximately once each day (Fig. V-9). These growth patterns are due to a circadian rhythm of conidiation (asexual spore formation) which is expressed in a culture maintained in constant darkness as patches of dense growth at approximately 22-hour intervals. Thus, a record of the functioning of the biological clock which is responsible for timing these events is readily available. In the present investigation, experiments will be performed by innoculating Neurospora at one end of a growth tube containing a nutrient-agar medium and, after several days of growth in constant darkness, determining the growth rate, banding patterns, and circadian period and phase information.

The simplicity of this experimental system is such that it can be conducted in a small, light-tight, carry-on package (approximately 0.5 cubic meters) requiring no power or inflight maintenance (Fig. V-10). Identical control cultures will be grown on the ground during Spacelab 1, and at the completion of the mission the growth patterns of the experimental and control cultures will be measured.

This investigation will serve as a preliminary test of both the macroenvironment of space and the microenvironment of Spacelab for effects on the temporal organization of living systems. The results of this project will improve our understanding of the circadian timekeeping mechanism which is so ubiquitous on Earth.

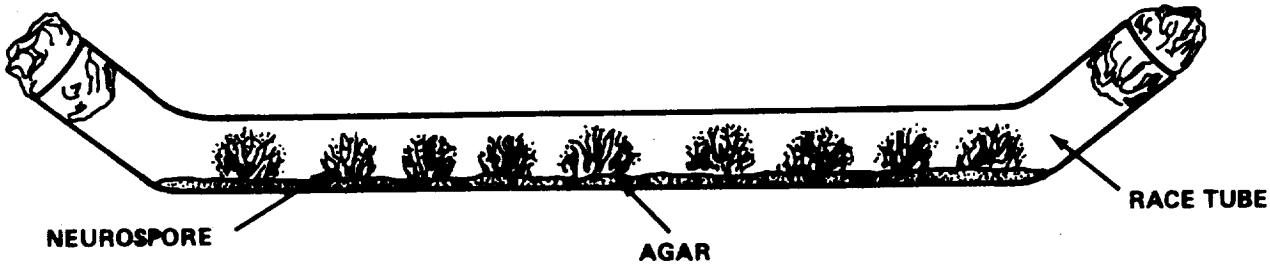


Figure V-9. Stylized representation of the circadian rhythm of Neurospora conidiation.

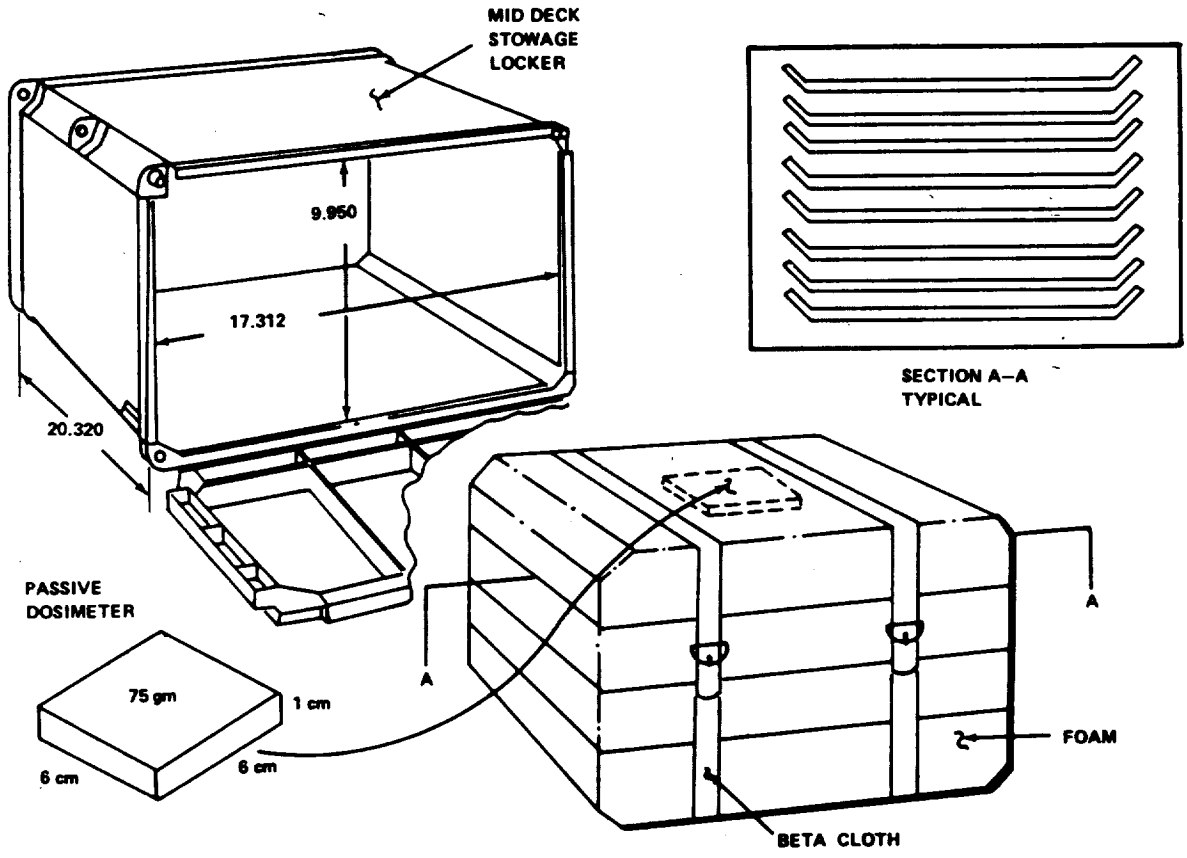


Figure V-10. Spacelab 1 carry-on package for Neurospora.

MICROORGANISMS AND BIOMOLECULES IN HARD SPACE ENVIRONMENT (1ES029)

G. Horneck
Institut für Flugmedizin/Abteilung Biophysik, Germany

Exposure to hard space environment may influence living matter at the cellular level (inactivation, mutation induction, growth disturbances), at the subcellular level (membrane damage, genome alteration, enzymatic disorganization), and at the molecular level (comformation alteration of macromolecules, radiation products in DNA, and protein).

The objective of this experiment is to expose, during a complete spaceflight mission, microorganisms and biomolecules to space vacuum and selected wavelengths and intensities of solar ultraviolet radiation and to measure quantitatively the influence of these factors, applied singly or simultaneously, on the integrity of microbial systems and biomolecules. Specifically, this experiment will be used to study (1) disturbances in development, inactivation of germination, outgrowth, colony formation, and induction of mutations in bacterial spores of Bacillus subtilis; (2) disturbances in cell growth and division, inactivation of colony formation, and induction of mutations in vegetative cells of Bacillus subtilis; and (3) alteration of biological activity and of molecular structure in enzymes and nucleic acids. For that purpose, more than 300 dry samples of the different test systems, which are accommodated in four square-shaped, quartz-covered containers will be exposed to selected combinations of space vacuum and of solar irradiation of different wavelengths and intensities (Fig. V-11). The wavelengths will be selected by a filter system, while a shutter will be used to determine the total exposure time.

The data from postflight evaluation of the biological flight and the ground control samples will be compared with the findings of simulation experiments on the ground (Table V-1). Precise information on the effects of space factors on living matter is expected which may contribute to the solution of several problems of space biology (e.g., the contamination problem, hazards to man by microbial mutants, and the interplanetary transfer of biological matter). Contributions to problems in basic research (e.g., the role of water in biological systems, primary processes of radiation, and the function of the cell envelope) are also expected.

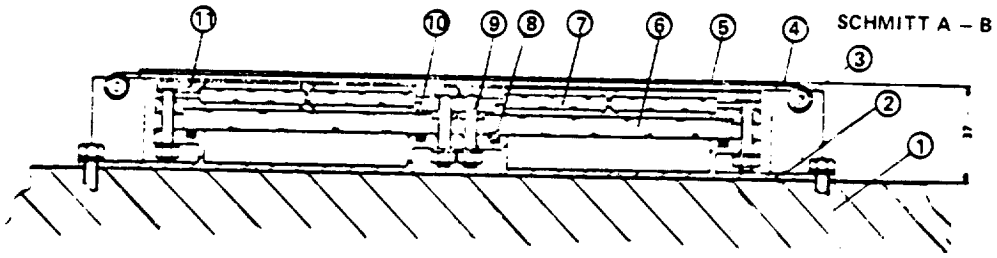
TABLE V-1. VACUUM EFFECTS ON BACTERIA

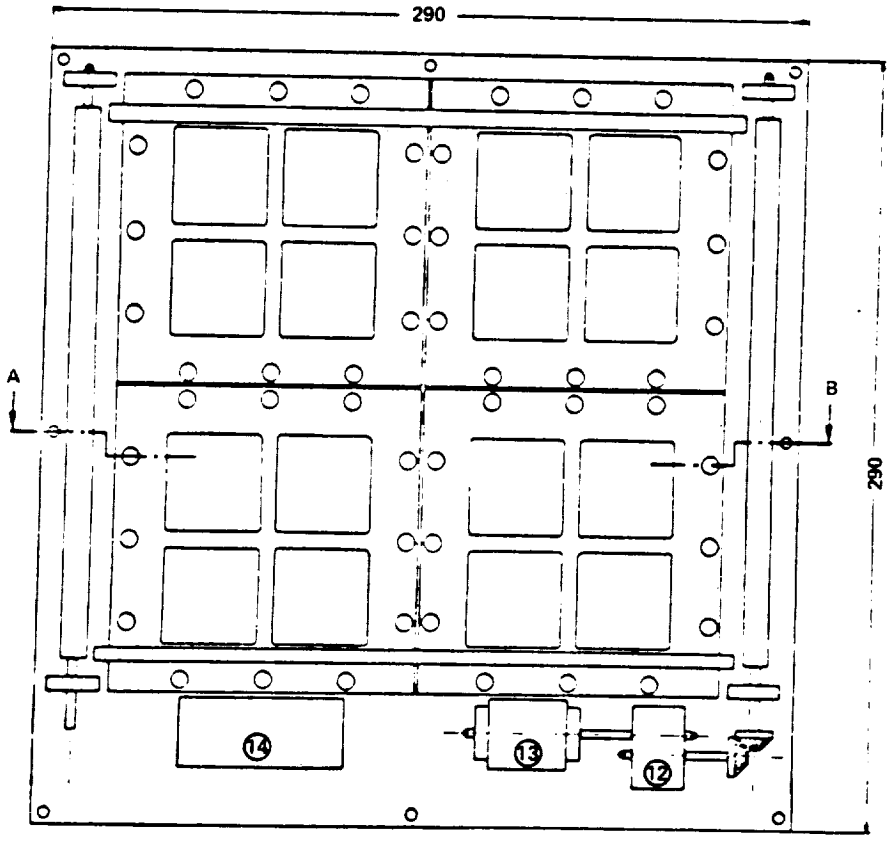
Effects of Colony Formers

- Prolonged lag-phase of subsequent growth
- Repair of cell membrane damage during lag-phase
- Increased sensitivity to X-rays
- Increased sensitivity to UV radiation
  - No photoenzymatic repair
  - Little or no excision repair
  - DNA-protein cross-links
  - Spore type photoproduct
  - R_f 0.4 photoproduct
- Decreased sensitivity to heat

Effects of Noncolony Formers

- No cellular elongation
- No phage production
- No respiration
- Damage to the cell envelope





1	COLD PLATE	8	VITON O–RING
2	BASE	9	V4A SCREWS
3	SHUTTER TAKE–UP SPOOL	10	LOWER FRAME
4	SHUTTER FOIL	11	UPPER FRAME
5	SHUTTER GUIDE SLOT	12	GEAR BOX
6	QUARTZ PLATE	13	MOTOR
7	FILTER SYSTEM	14	ELECTRONICS

Figure V-11. Sketch of the exposure box assembly.

ADVANCED BIOSTACK EXPERIMENT
(1ES027)

H. Bucker
Institut für Flugmedizin/Abteilung Biophysik, Germany

This experiment, which will be conducted in a multidiscipline and mutinational (Germany, France, USA) collaboration of scientists, is part of a biophysical program the main purpose of which is to determine the radiobiological importance of cosmic radiation particles of high atomic number and high energy (HZE). To accomplish this, it is necessary to perform microdosimetry of HZE particle irradiation.

Previous biostack experiments on Apollo 16 and 17 and Apollo-Soyuz Test Project clearly demonstrated that the very high local concentration of absorbed energy produced by single HZE particles can have serious biological effects upon an organism since complete cells can be damaged or destroyed. The ultimate consequences of such damage is dependent upon the organism's ability to repair or replace the affected cell.

The specific objectives of the advanced biostack experiment are (1) to confirm, complement, and enlarge the information obtained from the previous experiments by applying improved and advanced methods of localization and physical and biological evaluation, performing advanced experiments based on these data, and including additional biological specimens and additional radiation detectors; (2) to determine the biological importance of nuclear disintegration stars; (3) to determine the interference of HZE-particle-induced effects with those of other space flight factors (e.g., weightlessness); and (4) to determine the distribution of HZE particles and of stars at different locations inside the module and on the pallet.

Variations of the typical biostack concept are planned for exposure at different locations inside the module and on the pallet (three biostacks in the module and one on the pallet). The experimental packages consist of layers of different biological objects sandwiched between different types of detectors (e.g., plastic detectors and AgCl crystals) of heavy particles and cosmic radiation. This method permits the localization of the trajectory of each HZE particle in the biological layer and the correlation of biological impairment or injury with the characteristics of the responsible HZE particle. Two types of detector stacks will be used. One is completely passive, the other is active. The active package (Fig. V-12) contains detectors made of AgCl and thus

requires power to drive the lights needed to stabilize the images. The passive package contains no AgCl and is similar to the lower part of the active package. One of the active packages will be located on the pallet.

The experiment results will contribute to the solution of the problems of potential hazards to man from HZE particles of cosmic radiation during long-duration or repeated space flights, the establishment of radiation protection guidelines for man and biological experiments during future flights, and the understanding of the nature of the action of single particles on biological matter — which represents a base problem of radiation biology.

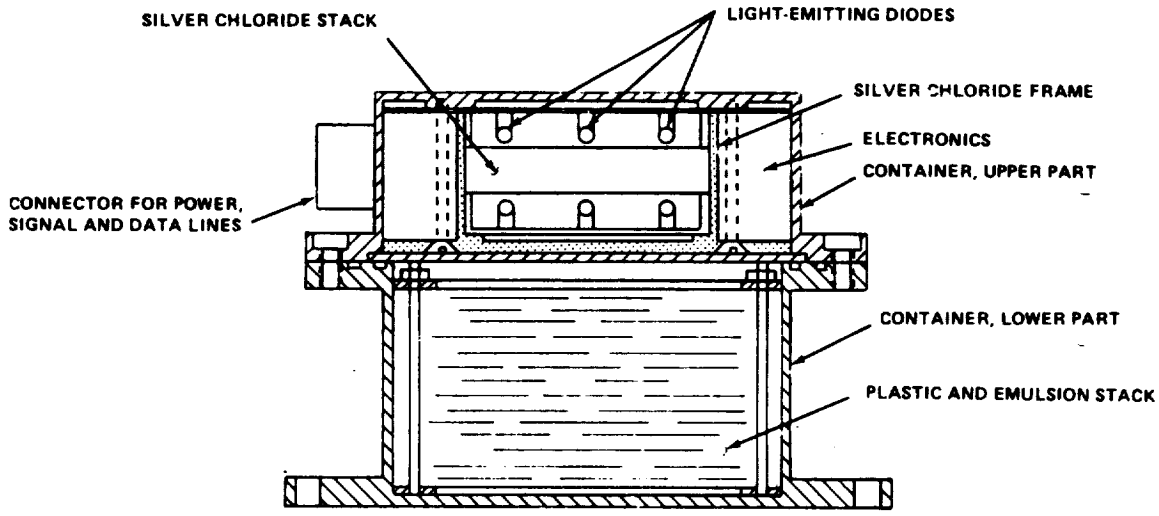


Figure V-12. Advanced biostack.

RADIATION ENVIRONMENT MAPPING
(1NS006)

E. V. Benton
University of San Francisco, USA

The proposed investigation stems from concern over the potential biological hazard from exposure to cosmic radiation. Documentation of the nature of cosmic radiation inside spacecraft is vital to the protection of man in space. The prime experiment objective is to map the cosmic radiation field inside the Spacelab vehicle. In addition to the integral LET spectrum of protons and HZE particles, the parameters to be determined include the total radiation dose; fluence of neutrons, protons, and high charge and energy (HZE) particles. These results are to be derived from measurements made in passive dosimeters.

Twelve small, lightweight, passive dosimeter packets and three thick, multilayered stacks of plastic detector films will be attached to the spacecraft at sites which will reflect a wide range of spacecraft shielding. Postflight analysis of the passive dosimeter packets and the thick plastic stacks will be carried out in the laboratory. Standardized data reduction techniques developed through the investigators' experience in the analysis of passive dosimeters from previous manned spaceflight missions (U.S. and U.S.S.R.) will be utilized.

The materials to be used in the passive dosimeter packets include cellulose nitrate (CN) and Lexan polycarbonate plastics, AgCl crystals, and thermoluminescent detectors. The following listing briefly describes the operation of these materials.

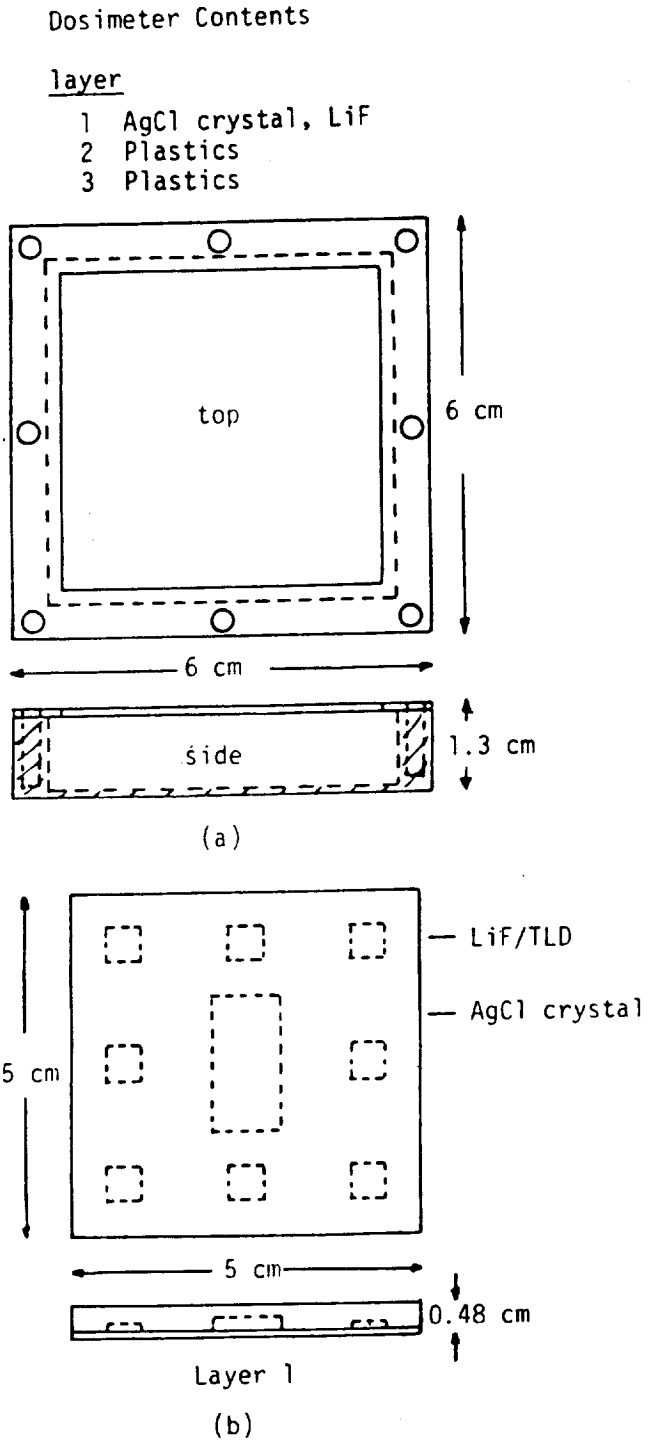
1) Plastic nuclear track detectors — HZE particles produce microscopic damage along their paths in plastics. This damage can be developed into the form of a track by the use of a chemical etching technique. The result of this process is an etch pit whose dimensions are a function of the etching time and etchant temperature as well as the magnitude of radiation damage at the etching site. The magnitude of damage is satisfactorily represented by the restricted energy loss of the particle.

2) AgCl crystal detectors — Single crystals of silver chloride doped with cadmium, AgCl(Cd), register tracks of penetrating ionizing particles. Particle tracks in AgCl(Cd) are initially stabilized with yellow light to prevent fading and subsequently developed by exposure to ultraviolet light. The developed track is similar in appearance to particle tracks in photographic emulsions.

3) Thermoluminescent detectors — Thermoluminescent detectors (i.e., TLD chips) record total radiation dose down to a few millirads. Heating of exposed chips causes light emission in a certain temperature range (approximately 150°C). The amount of light emitted is directly proportional to the radiation dose received by the TLD chip.

Figure V-13 shows some details of the arrangement of the small passive dosimeter packet. The thick stacks of plastic films each contain 200 Lexan polycarbonate films. Each film is 0.0019 centimeters thick with a 10 × 10 centimeter surface. The stack of films is sandwiched between top and bottom aluminum plates, and the assembly is held together with bolts. The overall thickness is 4.5 centimeter and the weight is approximately 700 grams.

The value of the knowledge to be gained from the investigation is that (1) it will provide baseline data for evaluation of radiation risk to man on this and future Spacelab missions, (2) it will provide radiation baseline data for experiments which may be affected by radiation, and (3) it will be a continuation of the program of documentation of radiation inside manned spacecraft which has included measurements onboard Gemini VI, Apollo missions 8 through 17, all Skylab missions, Apollo-Soyuz Test Project, and Kosmos 782 and 936. The expected results to be derived from this investigation will be a valuable part of the overall information required to determine man's long-term capability to function in space.



Dosimeter properties: dimensions — L = 6 cm, W = 6 cm, H = 1.3 cm
mass — ∿100 g
materials — Aℓ holder

Figure V-13. Passive dosimeter packet.